University of Stavanger

Faculty of Science and Technology

MASTER'S THESIS

Study program/Specialization: MSc. in Petroleum Engineering, Reservoir Engineering	Spring semester, 2021 Open
Writer: Siren Tjensvoll Kverme	………………………………………… (Writer's signature)
Faculty supervisor: Andrianifaliana Herimonja Rabenjafimanantsoa, Rune Wiggo Time	
Thesis title: Application of Fiber Optic Technology in Reservoir Monitoring	
Credits (ECTS): 30	
Key words: Reservoir Monitoring Completion Fiber Optics PRM EOR Weatherford Equinor	Pages: 84 + enclosure: 18 Stavanger, 15.06.2021

Application of Fiber Optic Technology in Reservoir Monitoring

Master Thesis in Cooperation with Weatherford Norge AS

Submitted 15.06.2021

Graduate Student:

Siren Tjensvoll Kverme

MSc. Petroleum Engineering – Reservoir Engineering Student

Faculty of Energy Resources

University Supervision:

Andrianifaliana Herimonja Rabenjafimanantsoa

Senior Engineer

Rune Wiggo Time

Professor

Abstract

The purpose of this thesis was to gain an overview of fields of application of fiber optic technology in reservoir monitoring, how such a measurement system is operated, and challenges that can occur.

For automated and integrated processes in the exploration and production of hydrocarbons, the information available before, during, and after operations is of great value. Where to place wells and templates, at which rate and when production and injection is to take place are just a few of the decisions in such processes. Fiber optic technology which is common in reservoir monitoring tools in a production well, is also used for seismic and monitoring of the subsurface and pipelines along the seabed. Fiber optic measurement systems are of great value thanks to real-time data, which are an advantage in decisions to be made on short notice.

By implementing fiber optic sensing elements along a wellbore, from the reservoir section and up to the surface, well intervention operations, testing of downhole safety equipment, well integrity assurance, and an active reservoir management on drainage and injection strategies can be optimized and profitability maximized. With in-well fiber optics already in place, they can be used for various operations. From cementing a liner, reservoir monitoring, and fluid characterization, to measuring strain and conditions of downhole equipment.

Published papers, course material and equipment from Weatherford, discussion with field specialists, and personal experience have been the basis of the thesis. It was successfully demonstrated how a bad splice affects the optical power transmitted through a fiber optic cable, that attenuation on the emitted light has a boundary, and how important a test of an entire measurement system before operations is.

The installations by Equinor at the Johan Sverdrup field are a good example of benefiting from implementation of technology from the start of development. The digitalization of the green field is part of their high ambition of a 70 % recovery.

Fiber optics are a great choice of measurement systems for reservoir monitoring with many sensing elements already available in today’s market, and will most likely be a preferred choice for monitoring many wells and reservoirs in the years to come.

Acknowledgements

This thesis marks the end of my Master's degree within Reservoir Engineering under the Department of Energy Resources at the University of Stavanger. I chose to write my thesis for the Department of Energy and Petroleum Engineering which covers the relevant subjects of instrumentation, measurement systems, flow and well engineering, the phases of a well's life, and completion, which are areas central in projects I am involved in, in my daily work in the Production Optimization Department at Weatherford.

I would like to thank my supervisors, Andrianifaliana Herimonja Rabenjafimanantsoa and Rune Wiggo Time for their guidance and support through each stage of the process. Your valuable expertise in formulating the research questions and methodology, brought my work to a higher level. Thank you for good discussions and valuable advice.

I am grateful for my team at Weatherford, for their insightful feedback and for their significant experience and skill level, especially within completion and reservoir monitoring.

I acknowledge the support of Weatherford, for allowing me the opportunity to write my thesis in collaboration with them, and in providing the technology and expertise needed during my thesis work.

My sincerest thanks go to my family and friends for believing in me, and for their unconditional support throughout my studies.

Contents

List of Figures

List of Tables

Abbreviations

Bbl – Barrel

BOE – Barrels of Oil Equivalents

Bopd – Barrels of oil per day

DAS – Distributed acoustic sensing

DTS – Distributed temperature sensing

EM waves – Electromagnetic waves

ICD – Inflow Control Device

NCS – Norwegian Continental Shelf

NORSOK – Norsk Sokkels Konkuranseposisjon

OTDR – Optical Time Domain Reflectometer

OWHO – Optical Wellhead Outlet

PLT – Production Logging Tools

PRM – Permanent Reservoir Monitoring

PT – Pressure and Temperature

RFID – Radio Frequency Identification

RIH – Run In Hole

RMS – Reservoir Monitoring System

SAGD – Steam Assisted Gravity Drainage

TAT-1 – Transatlantic No. 1

TAT-8 – Transatlantic No. 8

UK – United Kingdom

VSP – Vertical Seismic Profile

1. Introduction

The exploitation of fiber optic measurement systems for reservoir monitoring has grown for over 30 years and has been a great aid in production optimization within the oil and gas industry. Fiber optic instruments can measure acoustic signals, flow, pressure, and temperature in wells in the subsurface and along pipelines on the seabed. Implementing several sensing elements in a well completion can provide valuable real-time data on changes in the subsurface and wellbore environment during operations [1].

Through gathering real-time data early in field life, decisions regarding drainage strategies, and production and injection profiles can be made in advance of operations. Also, more complex fields will be developed, and wells installed, relying on reservoir monitoring technology for profitability assurance. With this knowledge an earlier confirmation on recoverable reserves can be obtained, leading to an optimization of hydrocarbon recovery and reservoir management, and a reduction in necessary well interventions Thus, permanent downhole monitoring can lead to a reduction in operational costs altogether [1, 2].

1.1. Background

On the Norwegian Continental Shelf, NCS, the expected remaining resources of oil equivalents are 8 billion Sm^3, where approximately 50 % are proven. For comparison the amount of remaining resources is 19 times the equivalents that will be produced from the Johan Sverdrup field alone. The total of proven and not proven resources on the NCS is around 15.8 billion Sm^3 [3]. The oil and gas industry in Norway, is classified as one of the country's major industries and will be profitable for many years to come [3].

Improved recovery is part of the increased reserves on the NCS over the last 20 years. As stated in the Norwegian Petroleum Directorate Resource Report in 2019 [4], the reason for the increased reserves "is that decisions have been taken on a number of different measures for improved recovery from the fields". By having a better understanding of the sub-surface and a well thought-out placement of wells, together with measures for improved recovery and operational efficiency, the resulting increased reserves will lead to a larger creation of value. One way of obtaining this information is by using fiber optic technology in a measurement system [4].

1.2. Measurement system

A process is defined as “a system which generates information” [5]. The information from a process is desired by an observer, where the measured variable can be used in i.e. analytical predicting models or judgement of physical performance. Measured variables can be movement in time and space, compositional and displacing properties of gases and liquids, or with regards to transmitting energy or power. A measurement system can be explained by the input variable being the true variable, and output as the measured variable. By comparing input and output, a quantification of the system’s accuracy can be obtained [5].

A general structure of a measurement system, presented in Figure 1.1 below, can contain several elements, but vary for which information it is desired to evaluate. There are four elements in the general structure, a sensing element, a signal conditioning element, a signal processing element, and a data presentation element [5]. The true value enters the system through the sensing element, which is in contact with the process and is dependent on the measured variable. A sensing element can be an electric pressure and temperature gauge, an acoustic fiber optic cable, or an orifice plate measuring flow rate. The signal conditioning element conditions the output of the sensing element for further processing, i.e. an amplifier of millivolts to volts, an attenuator of light signal when its intensity is too high, or an oscillator converting power from a direct current to an alternating current. The third element, the signal processing element, also conditions the output from the previous element but provides an output that is more suitable for presentation in the last element. The signal can be converted from analog to digital, or it can be calculations done by a computer or instrument. Lastly, the data presentation element, display the measured values as a final product, in a familiar presentation to the observer. This can be temperature or pressure on point scale indicators, a chart recorder presenting data over time, or an alphanumerical display [5].

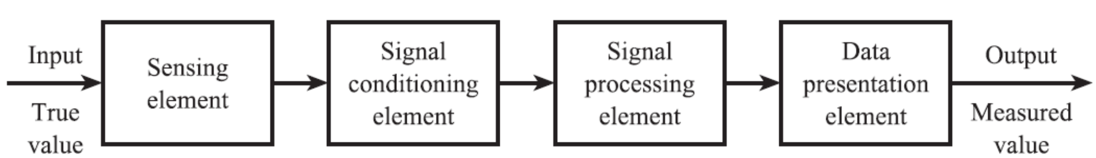

Figure 1.1: General Structure of a measurement system, with four basic elements [5].

1.2.1. Reservoir monitoring

In the primary, secondary, and tertiary recovery of hydrocarbons there are properties that need assessing to decide the most feasible recovery mechanisms. Properties of the reservoir are key factors for the recovery, and quantifying these are crucial before production starts, and beneficial throughout the process. The motivation for recovery mechanisms and drainage strategies are often economical, as the process of oil and gas recovery is tied to the net present value of a field. Thus, it is important to optimize the process as much as possible, which can be supported by i.e. reservoir monitoring instruments. In the choice of measurement systems, key factors are reliability with regards to failure rate, and initial and operational costs throughout its lifetime [5, 6].

Measurement systems used in the context of the production of hydrocarbons include sensing elements for i.e. fluid characterization, formation evaluation, flow rate, reservoir characterization, and other chemical and physical factors influencing the production. The output values of these sensing elements are reservoir data, mapping of the different formation layers, and the number of hydrocarbons and water present in the layers. Specialized systems generating data for this information can be flow measurement systems, gas chromatography, intrinsically safe measurement systems, and optical measurement systems. Optical measurement systems used in reservoir monitoring will be further investigated and presented in this thesis [6].

1.3. Objective and Scope

To understand how fiber optic measurements are carried out and how they can be implemented in reservoir monitoring, an investigation of this type of measurement system was carried out. Hands-on work with fiber optic cables and sensing elements provided a practical point of view for operating and installing such measurement systems. The various field applications elaborate on the several fields of application, and the great value fiber optic technology can bring to the oil and gas industry. Thus, the objective of this thesis is how fiber optic technology is applied in reservoir monitoring.

The thesis is organized with an introduction to measurement systems, the theory behind fiber optic measurement systems, fields of application, and experimental work and case studies. The theory in Chapter 2 explains the basic principles of light propagation, the construction of a fiber optic cable, and fiber optic sensing elements. Chapter 3 includes experimental work on fiber optic sensing elements and measurement systems, field implementation in the Johan Sverdrup field, and a presentation of Weatherford's equipment and delivery within reservoir monitoring systems in Norway. In Chapter 4 the results and discussion of the results are presented, followed by a conclusion in Chapter 5. Appendix I covers a well's elements and barriers, and Appendix II present data tables from Chapter 3.1.1 and 3.1.2.

2. Theory of Fiber Optics

How can transferred light signals through an optical fiber lead to a better understanding of the reservoir's geology and behavior? Timing the different oil recovery processes and applying methods of enhancements is critical for the resulting recovery. Production optimization is all about methods, and operational phases applied to obtain the most hydrocarbons from a reservoir in the most efficient and economically feasible way. The recent years growing focus on environmental challenges, has also forced the industry to focus on clean production, and i.e. their carbon footprint. Besides the chemical aspects in the production processes, there is a technology that can support and guide the several phases in a well's lifetime, such as fiber optics. To investigate the number of possibilities by using fiber optics, a deeper understanding of the technology is needed.

2.1. History

Communication by light can be traced back to earlier times with signal fires and is comparatively found in our everyday activities such as driving vehicles or boats using light signals for communication and navigation, or in a control panel when operating several types of machines. It is also thanks to the fiber optic telecommunication technology that one can communicate from one side of the earth to the other, through the communicating network all around us [7].

The first glass is traced back to 2500 B.C., and glass was drawn into fibers in Roman times around 25 B.C. In the 1790s an optical telegraph system was invented in France by Claude Chappe. In 15 minutes, information could be transmitted 200 km through a chain of towers. In the middle of the 1800's a way to guide light through a water jet and bent glass rods was reported. At 100 years after Chappe's invention, American Alexander Graham Bell replaced it with an electrical photophone, which transmitted voice signals through light. Although, the photophone was far too sensitive to the surrounding conditions, such as weather and visibility. The resulting transmitted light was of poor quality. Thus, the invention was not applicable from a practical point of view. At the same time, William Wheeler invents a system using an electric arc lamp to illuminate houses with light pipes, and Dr. Roth and Professor Reuss of Vienna light up body cavities during surgery and dentistry with the help og bent glass rods [7, 8].

At the beginning of the 1900's Clarence W. Hansell proposed a way to transfer images by fiber optics and received American and British patents for it. Although the English physicist John Tyndall found a solution to Bell's invention before it was developed, it was not until 1934 American Norman R. French turned Bell and Tyndall's experiments into an optical telephone system using quartz rods and patented it. His system could transmit voice signals through a network of optical cables, made of glass or similar material, considering both the *attenuation coefficient* for operating wavelengths, as well as the principle of *total internal reflection*. At this point the process of flame hydrolysis to make fused silica was also developed by American chemist Frank Hyde [7, 8].

The first transatlantic telephone cable came into operation as TAT-1 in 1956, through a cooperation between the UK, the United States, and Canada, capable of transmitting 36 voice circuits at 4 kHz. From 1951 to 1956 transparent cladding for fiber was suggested, and Lawrence Curtiss introduced both glass and plastic cladding. A year later Basil Hirschowitz tested a fiber optic endoscope on a patient, and he also licensed gastroscope technology together with fellow American scientists Curtiss and Wilbur Peters [8].

Single-mode waveguides were patented in 1960 by Elias Snitzer and Will Hicks, creating a fiber so fine that it only transmitted one mode of light. For transmitting the light signals, the laser was developed in 1958 by Schawlow and Townes and demonstrated in 1960 by Theodore Maiman. A receiver was in place a couple of years later, leaving only a suitable transmission medium to be found. Simultaneously AT&T starts its conversion to the digital telephone transmission system, the first semi-conductor diode laser is made. This decade was also the time an optical amplifier was described, and Stewart Miller patented the graded index waveguides and millimeter waves [7, 8].

Within the next decade Corning Glass Works had manufactured a step-index fiber with satisfying properties. Attenuation was at the time not to surpass 20 dB/km, unlike today's glass fibers with attenuation as low as 0.2 dB/km. Both the picturephone and digital video transmission were introduced, and a multi-mode fiber doped with germanium made. The lasers had improved their lifetime from 10 to 100 years, and the telephone system was implemented in cities across the world in the late 1970s, creating the network we use daily 50 years later [7, 8].

The coming 20 years of fiber technology, improved distances of fiber cables, and at which speed light was transmitted. The fiber optic transmission window was set at 850 nm, 1300nm, and at 1550nm, which are still relevant. The eighth transatlantic communication cable was set in service, and TAT-8 was a single-mode fiber optic cable carrying 40 000 telephone circuits between the United States, France, and The UK [7, 8].

2.2. Wave Fundamentals

Light or also known as electromagnetic waves (EM waves) can travel at the speed of light in a vacuum. According to Einstein's Theory, the energy is proportional to the frequency of the EM wave [9]. Compared to mechanical waves and sound waves, EM waves are not in the need of a medium to propagate and can travel through anything. EM waves are defined as "waves that are created as a result of vibrations between an electric field and a magnetic field. In other words, EM waves are composed of oscillating magnetic and electric fields." [10]. They have movement perpendicular to their direction, with the electric and magnetic field moving in phase, illustrated in Figure 2.1 below. Vector Z is the direction of propagation, vector E is the electric field direction, and vector H is the magnetic field direction. Waves are described and measured by wavelength, frequency, and amplitude [9-11].

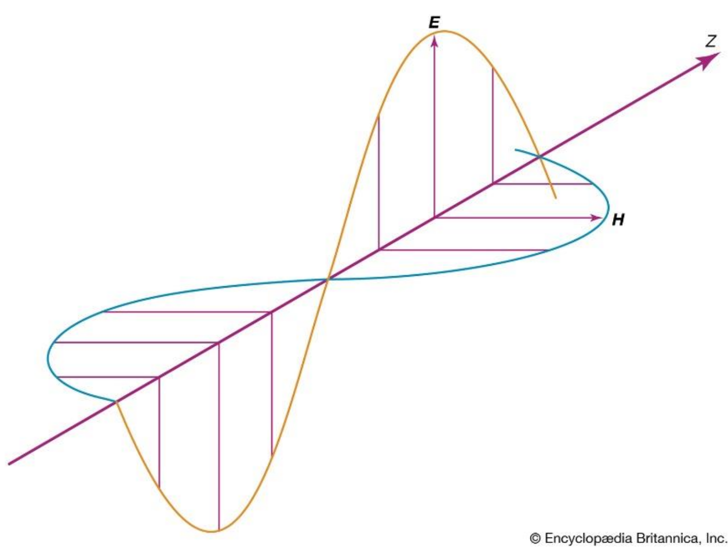

Figure 2.1: Electromagnetic Wave [11]

To describe the propagation of a plane wave, the displacement a can be written as a function of sine, equation 2-1. An elaboration of the different elements of the equation and their units of measure will follow.

$$a = A\sin(\omega t - kz) = A\sin 2\pi \left(\frac{t}{T} - \frac{z}{\lambda}\right) \qquad \text{2-1}$$

Where:

a displacement; electric or magnetic

A amplitude [units of displacement]

ω angular frequency [s^{-1}]

t time [s]

k wave number [m^{-1}]

z length in direction z [m]

T period of oscillation [s]

λ wavelength [m]

When an EM wave is emitted and falls on an interface between media of different optical densities, the speed, and angle of the wave change. The change of direction of travel is called *refraction*. Light also travel at different velocities in the same material, due to differences in wavelengths. The variation in velocity is called *dispersion* and is together with refraction an important aspect in fiber optics. The speed at which light travels varies with the material it is in, although it will never travel faster than it would in a vacuum. Thus, the ratio between speeds in vacuum and medium is called the index of refraction, *n* [9, 12].

Figure 2.2 below illustrates the angles of rays passing through the material of different indices of refraction, n_1 and n_2. As an incident ray with angle θ_1, measured from an imaginary normal line, travels through an interface between the materials, it results in a reflected wave and a refracted wave with angle θ_2. The reflected wave is of the same angle as the incident ray, according to the law of reflection [9]. *T*he ratio of angles in Figure 2.2 can be written as equation 2-2 below.

$$\frac{sin\theta_1}{sin\theta_2} = \frac{n_1}{n_2} \qquad \text{2-2}$$

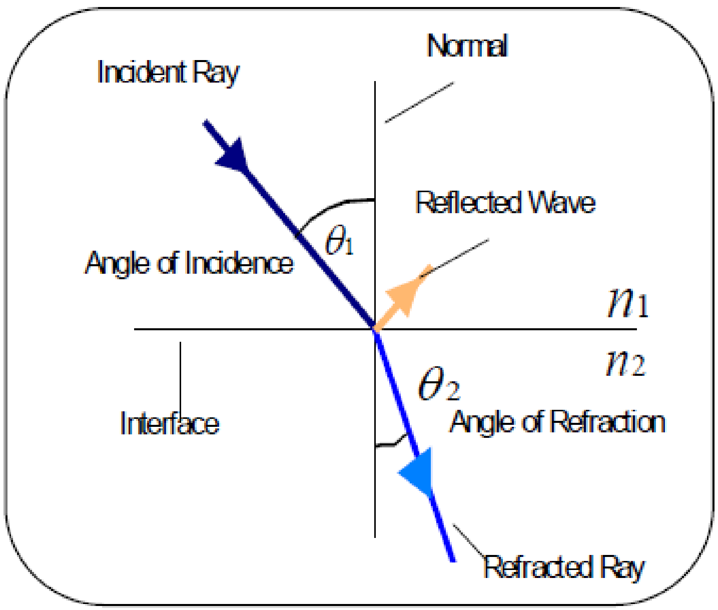

Figure 2.2: Ratio of angles from incident ray and refracted ray [12].

In a continuous spectrum of different wavelengths and frequencies, electromagnetic energy exists from the form of invisible radio waves and microwaves to visible light and gamma rays. Visible light, which one can physically see, is within the range of approximately 400nm – 750nm. In comparison, the operational wavelengths for fiber optics are from 800nm – 1600nm, presented in Figure 2.3 below.

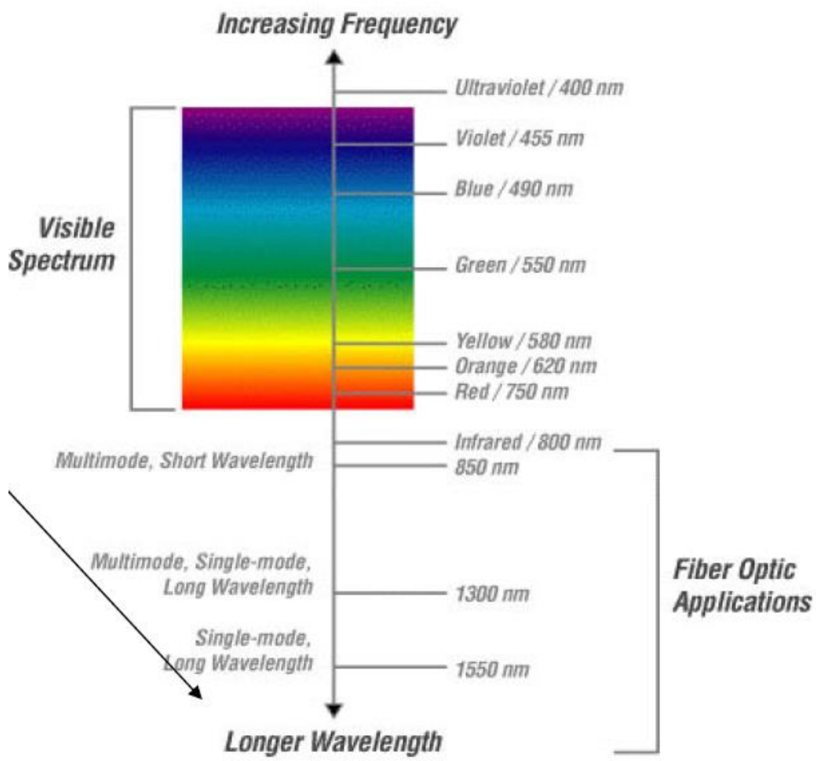

Figure 2.3: Visible spectrum vs. Fiber Optic applications [12].

For a practical comparison of which frequency interval fiber optics are applicable, one can look at the wi-fi our computers and phones connect to. The latest within telecom is the 5G networks, which transmit information at a frequency of $5x10^9$ Hz (GHz). Fiber optic application work within the interval of 100 THz to 1 PHz [$1x10^{14}$ – $1x10^{15}$ Hz] [7].

2.2.1. Total Internal Reflection

As light propagates through a fiber, at the interface of two layers of different media, there can be partly reflected light or total internal reflection. Figure 2.4(a) below shows two layers of different refractive indices, n_1 and n_2, where $n_1 > n_2$. The red line is the incident ray, the blue is the refracted ray, and the green is the reflected ray. Concerning the incident angle, θ, and refraction indices, the refraction angle, θ', is given by *Snell's Law* in equation 2-3.

$$n_1 \cdot \sin(\theta) = n_2 \cdot \sin(\theta') \qquad \text{2-3}$$

In Figure 2.4(b) the angle of incident is equal to the critical angle, θ_c. Thus, the angle of refraction becomes $\frac{\pi}{2}$,when incident angle $\theta = \theta_c$. The critical angle is given by equation 2-4.

$$\theta_c = sin^{-1}\left(\frac{n_2}{n_1}\right) \qquad \text{2-4}$$

At the point when $\theta > \theta_c$, Figure 2.4(c), the refracted ray is superseded, and the phenomenon of total internal reflection occurs. Hence, the incident angle of light in a fiber optic cable is crucial [13].

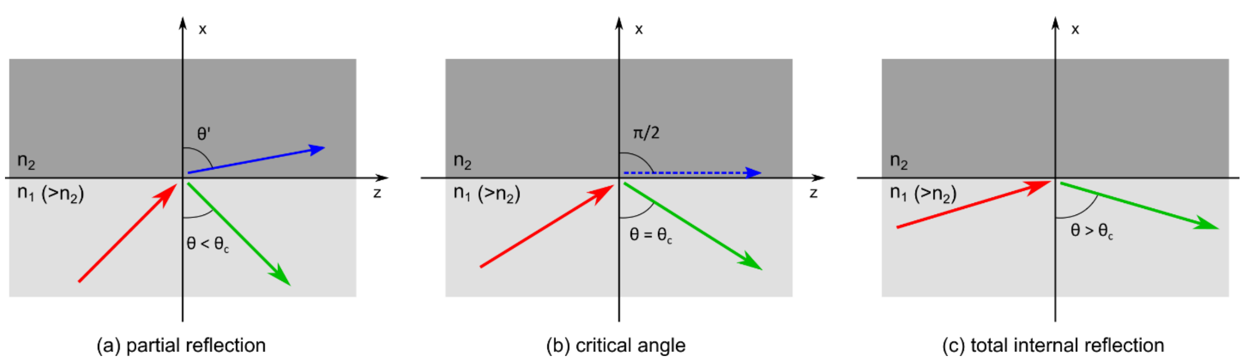

Figure 2.4: Snell's Law & Total Internal Reflection [13].

2.3. Construction & Design

As mentioned in the previous sub chapter, the properties of the transmission medium for fiber optics affects the way light propagates. From a chemical point of view, there are favorable properties, and from a physical point of view, there are necessary ones. When constructing a fiber optic cable there are different versions, regarding modes, capabilities, and environmental restrictions one must consider. Depending on the final area of use, some properties are changeable. Breaking down the construction of a fiber optic cable step by step will emphasize the importance of different aspects in relation to the use.

The inner core of an optical fiber is made of glass or silicon dioxide, SiO_2, with a diameter from 8 to 63 µm. When producing the silica core, it is done by the process of chemical vapor deposition. Involving high temperature oxidation, thermophoretic deposition, and sintering and consolidation, the glass is made. In addition to producing ultra-pure fused silica, the process also gives off chlorine gas. The chemical reaction equation for the process is given by equation 2-5.

$$SiCl_4 + O_2 \rightarrow SiO_2 + 2\, Cl_2 \qquad \text{2-5}$$

For producing a core with a high refractive index, which is essential in the propagation of light within the cable, a dopant is added. Dopant materials can either give a higher or lower refractive index. For a higher refractive index, one can add i.e. germanium dioxide, GeO_2, of phosphorous pentoxide, P_2O_5. These two dopants do not include instability between phases and are mostly defined by a resulting composition of the glass with desired properties. Other properties which can be affected by dopants are thermal and thermomechanical properties, viscosity, and stress state. GeO_2 increases both linear and nonlinear refractive index while at the same time enhancing photosensitivity and Raman gain. Whilst P_2O_5 increase the refractive index together with reducing the viscosity, thermo-optic coefficient, and photo-darkening. Another outcome of adding a dopant of foreign molecules to the silica is that the light scattering is increased. Hence, the attenuation is increased [7, 14].

Surrounding the core, where most of the light is transmitted, there is a layer with similar properties as the core. The cladding has a lower index of refraction, namely, to create a difference between it and the core to obtain total internal reflection. Total internal reflection is principally keeping all the light within the core. On the outside, the glass center is a coating, with a surrounding gel solution as resistant to anything leaking into the optical fibers.

A mechanical and environmental protector, a buffer, is the next layer surrounding the inner part of the cable. The buffer can be of many different materials and layers, depending on what it will be used for, and in which surrounding conditions. When fiber optic cables are used on the surface or downhole the buffer must be resistant to liquids such as different compositions of water or hydrocarbons. This layer can i.e. be silicone, Teflon, acrylate, or a type of metal, and can also provide a temperature limit for the fiber. The outermost layer is called the outer jacket and is typically a plastic tube that also provides mechanical protection. An example of the construction of a surface patch cable, with the different layers, is illustrated in Figure 2.5 below. Figure 2.5 also gives an impression of the dimensions fiber optic cables are constructed with.

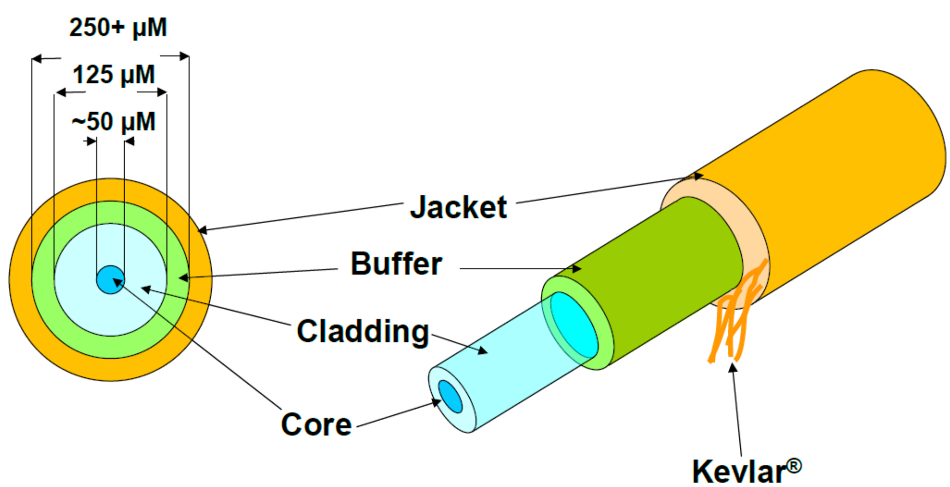

Figure 2.5: Standard Weatherford MM Patch-cord construction [12].

2.4. Optical Fiber Profiles

When creating an optical fiber with the desired refractive index, the shape of the fiber, will define how many modes can be guided through it. As a function of the radius, the profile describes the radial change in refractive index, from the core axis towards the cladding. This is called the refractive index profile, and how light propagates through the fiber is dependent on the shape of the profile.

There are two types of index profiles that are suitable for different types of optical fibers, with regards to modes transmitted through the cable. For a single mode fiber, a step index profile is used, which maintains a constant refractive index at the interface between core and cladding. Thus, the cladding has a lower refractive index. Light propagates as meridional rays in a step index profile, as they propagate each reflection across the axis of the fiber, illustrated in the top of Figure 2.6 below. A step index profile has a low bandwidth, no signal distortion, and very little attenuation.

For multi-mode fibers, a graded index profile is used. In a graded profile the core has a uniform refractive index, which decreases toward the interface between core and cladding, while the cladding has a constant refractive index. Light propagates as skew or helical rays, which never cross the fiber axis, bottom of Fig. below. As several modes propagate in multi-mode fibers, the path of each mode is different. Although the speed of the rays is the same, the ones closer to the core axis travel at a slower speed due to the refractive index being higher in the center than at the interface. As the path of travel is shorter for the rays closest to the axis, the several modes' arrival at the end of the fiber still takes place at the same time. Compared to the single-mode with a step index profile, the multi-mode graded index profile has some signal distortion, a higher bandwidth, and some attenuation. An illustration of the propagation of meridional rays and skew rays is shown in Figure 2.6 below. The figure also illustrates how single-mode waves (meridional) propagates in an optical fiber compared to the multi-mode (skew) [15, 16].

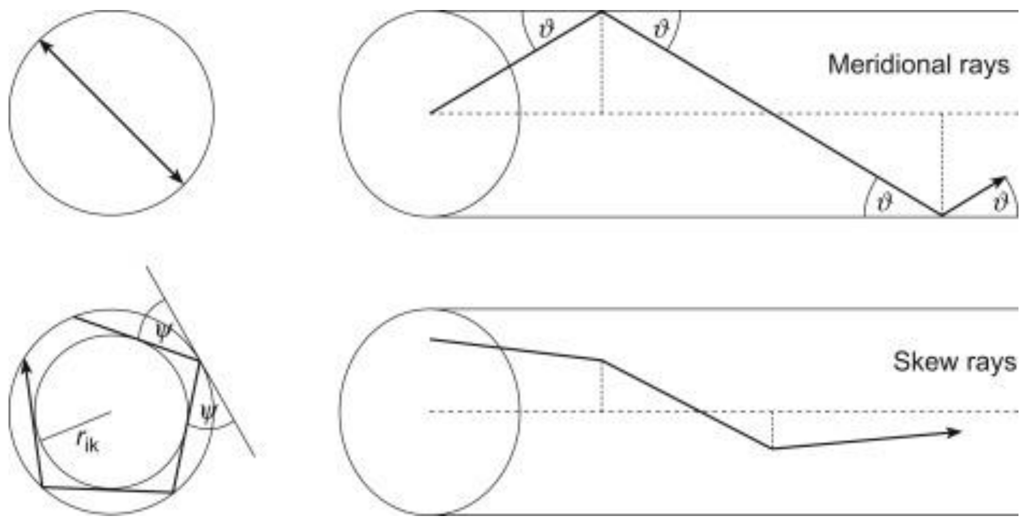

Figure 2.6: Propagation of meridional rays vs. Skew rays [16].

2.5. Fiber Optic Sensors

During formation evaluation and drilling there are several parameters that are obtained by different logging tools. In a petroleum engineering context well logs are used to provide a detailed record of acoustic, electrical, and physical properties of the formation rock. Well logging also provide information on the fluids in place and their contacts, along with changes that occur through exploration, development, and production. Typical well logs include acoustic, electrical, radioactive, pressure, and nuclear. Some logging methods are also applied during other phases of a well, either while running completion, during production, intervention, or abandonment. For measuring downhole data, such as flow, pressures, and temperatures, there are fiber optic sensors, which is a growing technology for providing real-time data at high accuracy. Fiber optic sensors include pressure and temperature (PT) gauges, flow meters, Bragg gratings, distributed temperature sensing, DTS, distributed acoustic sensing, DAS, and seismic [12, 17].

Compared to the previous methods mentioned, there are many advantages of fiber optic technology, especially with regards to copper wire. Bandwidth is increased by up to x1000, there is no radiation, sparks, or shorts, no electromagnetic or radio frequency interference, and it is much harder to tap into concerning the security. Fiber optic cables have lower attenuation, and they are much smaller in diameter and cost. Besides the oil and gas industry, which is estimated to make up the biggest part of the fiber optic sensor market, it is also used in pipelines, geothermal, infrastructure, wind energy turbines, military, and security systems [18, 19].

The sensors are of two broad classifications, extrinsic and intrinsic sensors. An extrinsic sensor is within the concept of photonics, where light is guided out of the fiber to a medium within the desired sensing area. From there the light is modified according to the variable of interest before it is gathered back into a fiber, and further processed. Whereas with an intrinsic sensor, the variable of interest modifies the light externally, while the light is propagated and kept within the fiber. Extrinsic sensors are often used for chemical or biomedical measurements, and intrinsic for physical [20].

2.6. Parameters & Applications

Properties fiber optic sensors can provide information on can be mechanical; stress, strain and pressure; geometrical; distance, thickness and liquid level; dynamical; velocity, flow rate and vibrations; physical; acoustics, electric current and temperatures; chemical/biochemical; flammable or toxic gasses, and compositions; and others such as signal loss, broken fibers or leakage. The information carried by the parameters of light waves comprises amplitude, frequency, intensity, phase, and polarization. Based on which type of parameter a sensor is applied for, they are further divided into intensity- and phase-modulated sensors. Phase-modulated sensors have a higher sensitivity and precision than intensity-modulated ones. Hence, they are at a higher price than the latter [21].

Producing a fiber optic cable, designed for reading measurements in a well, requires certain criteria to be met. Checking the quality requires preset parameters and standards for both the cable and the chosen method of measurement. How light is launched in a multi- and single-mode fiber, and attenuation of the propagating light, are important factors in measurements. In a multi-mode fiber, energy is launched and distributed over all the fibers, while for single-mode energy is partly launched and partly radiated. The launched energy decreases as the light propagates, which is called attenuation, and is measured in decibels.

2.6.1. Measurement methods

An optical measurement system consists of three basic elements, a light source, a transmission medium, and a detector. Besides these, there are also conditioning, processing, and presentation elements. Optical measurement systems are divided into two types, variable source and fixed transmission medium, or fixed source and variable transmission medium which is mainly presented in this thesis, Figure 2.7 [5].

From the source, the amount of power emitted is a function of wavelength, $S(\lambda)$. The efficiency of the transmission medium, $T(\lambda, I)$, varies with the wavelength and value of the measured variable. For optical fibers, there are efficiency constants to be taken into account, for the coupling between the source-medium, and medium-detector, K_{SM} and K_{MD} respectively. Sensitivity of optical signal conversion to an electrical signal in the detector is given by K_D, and the response of the detector to varying wavelengths, by $D(\lambda)$ [5].

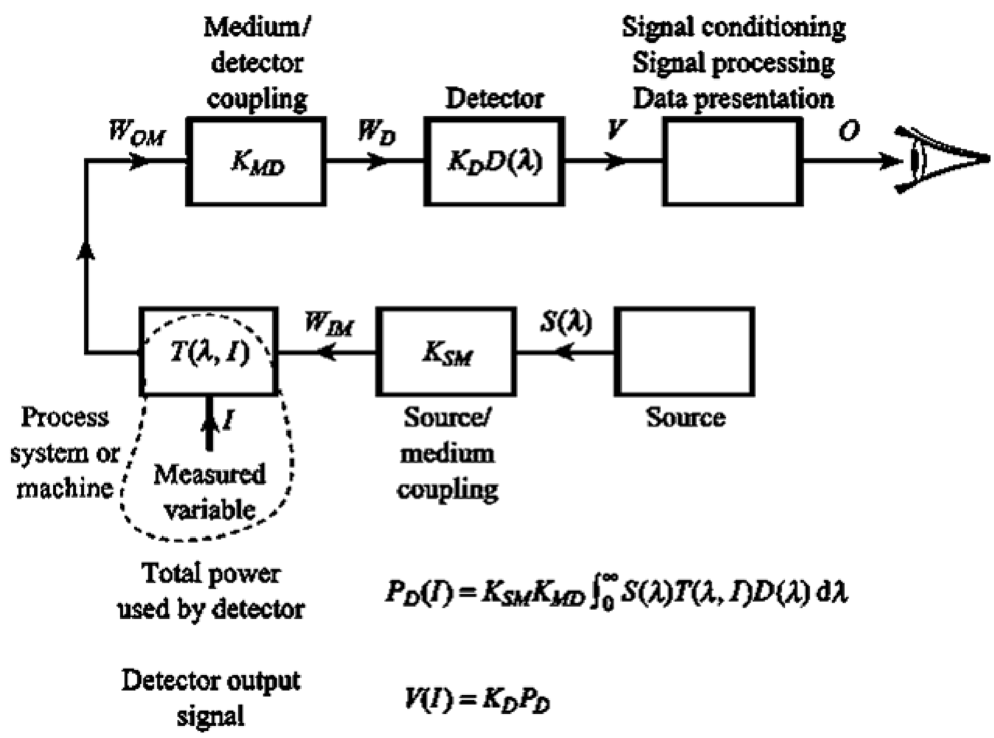

Figure 2.7: Fixed source, variable transmission medium system illustration [5].

Power propagates through the system, entering the medium, W_{IM}, leaving the medium, W_{OM}, entering the detector, W_D, which generates an output signal, V. The detector output signal given by equation 2-6, is a function of the measured variable, from multiplying the total power used by the detector, P_D, and its sensitivity constant [5].

$$V(I) = K_D P_D \tag{2-6}$$

The main parts of a fiber optic measurements system are the fiber optic cable, the interrogators on the surface, and software used to process and present data. An example of the structure of a measurement system for reservoir monitoring in a well, with regards to components and data transfer, is presented in Figure 2.8 below. The elements include a fixed source located in an instrument room on an offshore rig, which is connected to an optical wellhead outlet (OWHO) in the wellhead area through a surface cable and junction box. The function of a wellhead is mentioned in the appendix Completion. From the OWHO a downhole PT gauge is connected to the system by a downhole fiber optic cable. In comparison to Figure 2.7 above, the source, the reservoir monitoring system (RMS) unit or interrogator, is a laser but also contains the detecting and processing elements. The light is generated from the laser, through a variable transmission medium, the fiber optic cable, and back to the RMS unit.

According to the general structure of a measurement system, Figure 1.1, the sensing element in this type of setup is the PT gauge and the fiber optic cable. The signal conditioning and processing element is the RMS unit in the instrument room, and the data presentation element is both on monitors located in the central control room and onshore, and on a physical or virtual server that can be remotely accessed. Remote access is used for configurations of different fiber optic instruments in one well, and several wellhead systems on one rig, as well as for fault finding if there is a problem with readings on the monitors.

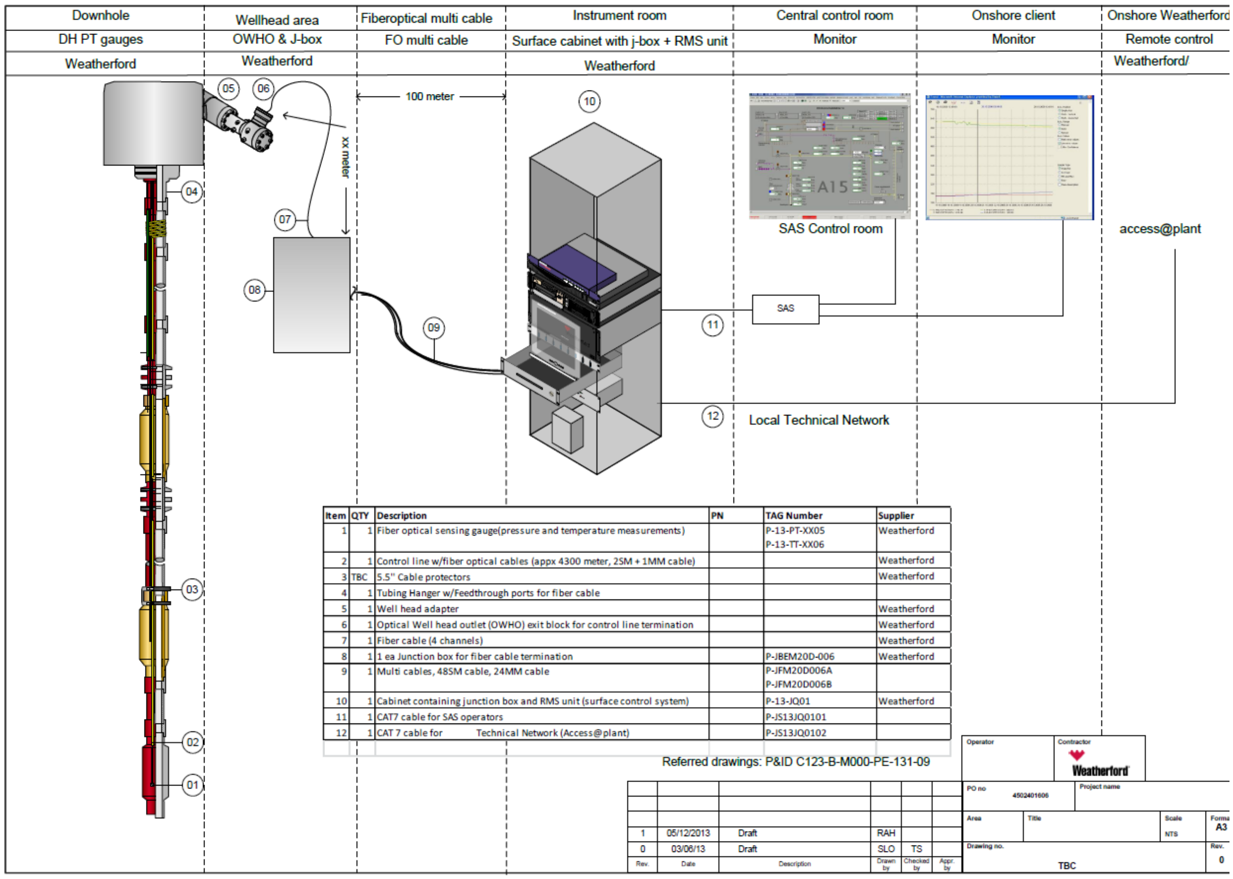

Figure 2.8: FO Configuration for an entire downhole measurements system [12].

Attenuation

Measuring attenuation can be carried out by two techniques. The Through Power Technique requires two measurement points, one at the transmitter and the other at the receiver. As attenuation occurs along with the optical fiber, and one end is some kilometers down into the subsurface in a well, the through power technique is not achievable in this type of operation. The method Backscattering Technique on the other hand only uses one measurement point. Light is launched in one end, measured as it is received at the same point, and attenuation and changes along the fiber can be observed and quantified [7].

Attenuation can be quantified by comparing the amount of optical power entering a device to the optical power leaving it, or as a reduction in power between two cross sections. The change in optical power for fiber optics and electronics is measured in decibel and is given by equation 2-7 below. Although, in fiber optics there is mostly attenuation or loss to be measured. A loss of 0.1

dB is equivalent to 98 % transmission of light, 1.0 dB to 80 % transmission, and 3.0 dB to as little as 50 % transmission. By plotting optical loss [dB] versus transmitted light [%] and extrapolating a trendline (below the thick line), the transmitted light will go to 0 % when the optical loss reaches 6.00 dB, illustrated in Table 2.1. The magnitude of attenuation is dependent on the wavelength of the launched light and occurs due to scattering, absorption, and light loss in connectors or splices. The wavelength dependency is beneficial in finding the optimum operating wavelengths. Due to inhomogeneities in density at very small magnitudes, scattering occurs, and as a result, there is light loss at all wavelengths. Optical communication and optic measurements in wells both operate at the wavelengths 1310 nm and 1550 nm, which are advantageous with regard to scattering loss [7, 12].

$$dB = -10 \cdot log_{10}({}^{P_{out}}/_{P_{in}}) \tag{2-7}$$

Table 2.1: Optical Loss vs. Transmitted light, actual data above the black line, and trending data below [12].

Optical Loss [dB]	Transmitted light [%]
0.10	98
1.00	80
3.00	50
4.00	34
5.00	17
6.00	0

Rayleigh Scattering

There are three classifications of scattering processes for light with a change in direction and frequency. The first is Rayleigh scattering, defined as “when the light is scattered without frequency shift” [22]. Rayleigh’s scattering can also be explained by how one observes the color of the sky. Light from the sun hits air molecules, and scatter in all directions. Due to being in the shorter wavelength end of the visible spectrum, in Figure 2.3, the sky appears blue.

When taking scattering in the perspective of fiber optic cables, light is scattered in the core due to unconformities in the glass, which results in attenuation. Rayleigh scattering is considered to be elastic and linear because there is no change in frequency and the photon energies are unchanged as they are scattered. With a dependency on wavelength, the *Rayleigh scattering law* describes the scattering as being directly proportional to $\frac{1}{\lambda^4}$. Thus, a higher operational wavelength means lower scattering, and is crucial for fiber optic measurements [7, 23].

The principle of the Backscattering Technique is Rayleigh scattering. As light propagates through the glass, it is attenuated when reflected backward due to Rayleigh scattering. A mirror couples out the reflected power and variations in the backscattered light are measured. By deriving the attenuation coefficient with respect to the time and length light has traveled, optical faults and events can be detected. The calculation is done by calculating the length of the fiber and from this the attenuation coefficient between known lengths can be found. The length, L, is calculated by equation 2-8.

$$L = \frac{\Delta t}{2}\frac{c_0}{n_g} \qquad \text{2-8}$$

Where Δt is the difference in time between the peaks of initial and end pulses, c_0 is the speed of light in a vacuum, and n_g is the effective group refractive index in the core glass. From known lengths, i.e. at two given points (depths), the attenuation coefficient, α, can be calculated by equation 2-9, where $P(L_1)$ and $P(L_2)$ is light power at Length 1 and Length 2.

$$\alpha = \frac{5}{L_2 - L_1}\log\frac{P(L_1)}{P(L_2)} \qquad \text{2-9}$$

For this equation to apply, the fiber core diameter, the numerical aperture, and the backscattering factor had to remain constant throughout the fiber [7].

Raman Scattering

The second classification is Raman scattering, which is defined as "when the light is scattered with a relatively large frequency shift that is independent of scattering angle" [22]. Raman scattering measures electromagnetic radiation when the kinetic energy of a photon changes. Thus, the reaction is inelastic and there occurs an increase or decrease in photon energy. When the incident radiation is less than the scattered radiation it is called Stokes Raman scattering, while an increase from incident to scattered radiation gives anti-Stokes Raman Scattering. By measuring the difference in the incident and scattered radiation, one obtains information on the frequency and vibrational energy, which can i.e. provide temperature measurements. Figure 2.9 below illustrates how intensity and wavelengths are read for Rayleigh and Raman scattering. The Rayleigh scatter in the middle of Figure 2.9(b) illustrate no difference in energy, while Stokes in red and anti-Stokes in blue had a change in energy (intensity). Raman scattering is often associated with Raman spectroscopy, which is used for creating detailed images for analyzing chemical compositions of biological matter [24, 25].

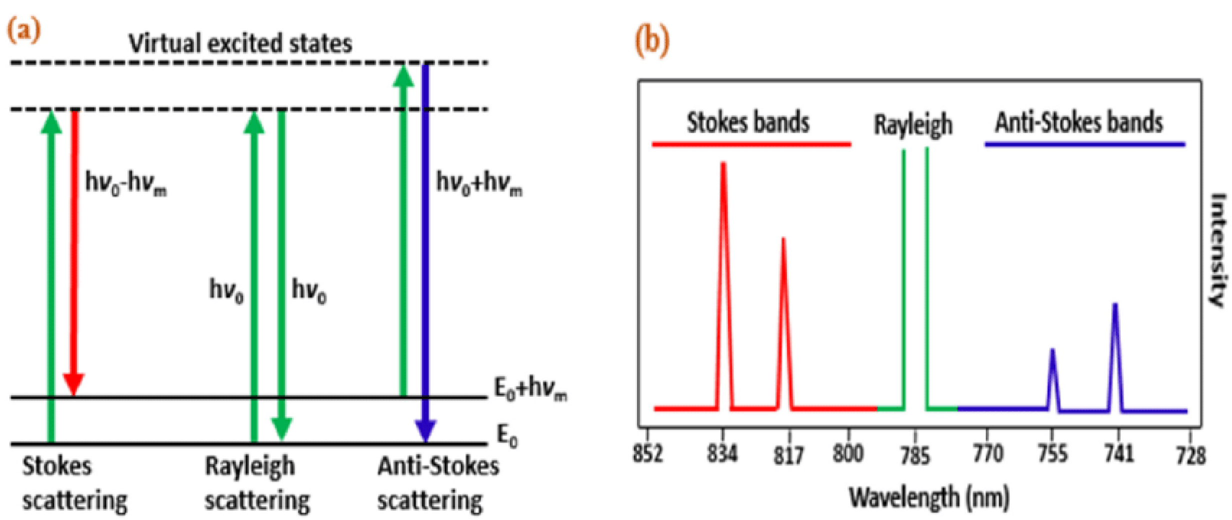

Figure 2.9: Schematic representation of Rayleigh and Raman scattering, and the Raman spectrum [25].

Brillouin Scattering

The third type of light scattering, Brillouin scattering is defined as “when the light is scattered with a small frequency shift that varies continuously with scattering angle” [22]. As for the Raman scattering, Brillouin scattering is an inelastic effect, due to the photon losing energy. The loss of energy leads to the light being scattered at a longer wavelength. Acoustic phonons exchange energy with the photons, resulting in backscattered Stokes light. For Brillouin scattering, an acoustic wave traveling along with the fiber, apply periodic strain to the fiber. The strain produces a change in the refractive index, which moves at the velocity of sound. The result of this effect is vibrations which shift the frequency, in the backscattered energy. Acoustics can be used in sensors to locate events, such as a valve opening or closing in a well, and also give information on flow through distributed sensing [16, 21].

Optical Time Domain Reflectometer

Instrumentation operating on the principle of the Backscattering Technique, namely an Optical Time Domain Reflectometer (OTDR), can give a visual graph of the fiber cable, illustrated in Figure 2.10 and Figure 2.11 below for single-mode and multi-mode fibers respectively. The graph is presented with dB on the y-axis, and position on the x-axis. One can observe events such as where different parts of a fiber cable have been spliced together, and how much loss there is between these parts. If there are fractures on the fiber cable, these would be visible, and the depth of the event located.

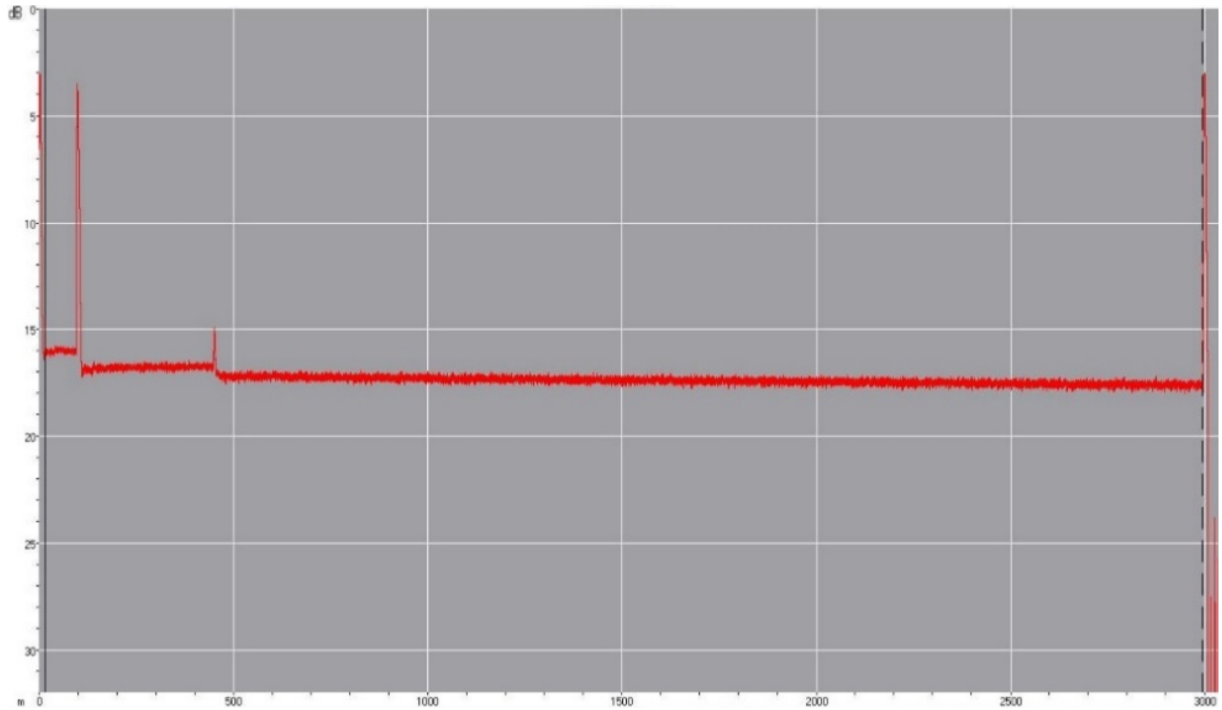

Figure 2.10: OTDR trace of SM fiber cable in a well [12].

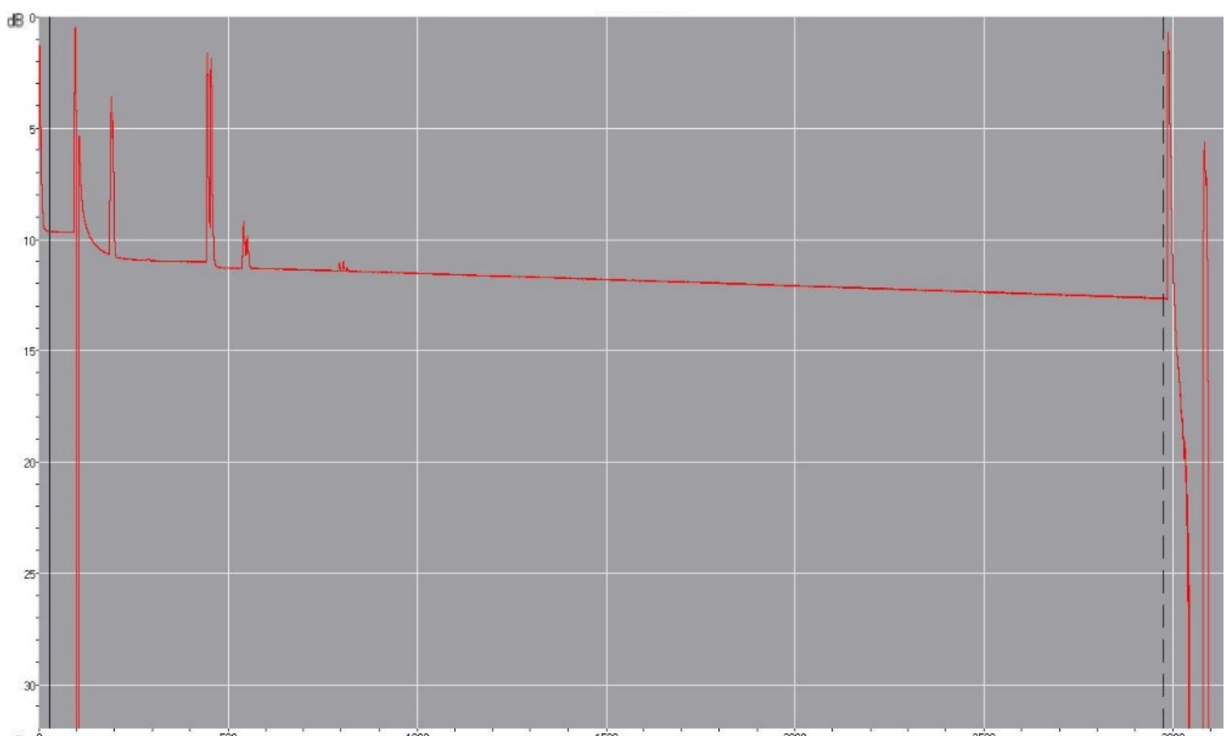

Figure 2.11: OTDR trace of MM fiber cable in a well [12].

The peaks shown in Figure 2.10 and Figure 2.11 above, are different parts of an optical system in a well. There will always be a high peak at the start and end of the cable, due to the sudden change in refractive index, which causes light to be backscattered. For the second and third peaks in Figure 2.10, there can also be observed a shift in dB level. The curve will fall as there is energy loss, attenuation, over connections in the optical system. Starting from the bottom of the well and up, there can be gauge reading temperatures and pressures at several places, and the fiber cable continues out of the well through a wellhead outlet at the Christmas tree at the top. A brief explanation of the well and the Completion, is presented in The Well under Completion. To get a connection to topside instruments located on i.e. a drilling platform, the downhole fiber cable is connected to a surface cable through a junction box, and lastly connected to a topside interrogator. An interrogator can act as both an optical transmitter and receiver, and a processing element.

Bragg gratings

Fiber Bragg gratings are characterized as intrinsic sensors. “The fiber Bragg grating is very simply a periodic structure printed along the propagation axis of an optical fiber.” [20]. A fiber Bragg grating acts as a filter inside the core of the fiber optic cable, providing a reference point or reflection spectrum for the receiver processing the signal. The reflected spectrum is specific wavelengths and is dependent on index and distance. Fiber Bragg gratings can provide parameters for temperature, pressure, strain, acoustics, and displacement.

Bragg gratings functions as point sensors, with a reference point at a given location on the fiber cable, i.e. as pressure and temperature reading at the top of the reservoir section in a well. When light propagating through a fiber optic cable reaches a Bragg grating, the narrow spectrum of wavelengths is reflected towards the source, while the rest of the signal travels the entire length of the cable. Although, the reflection spectrum is precise, if a Bragg grating is subjected to strain it can cause a shift in reflected wavelengths. Strain can be a result of temperature changes or poor packaging of the fiber Bragg grating. Thus, readings from the bragg grating can deviate from expected values and will need to be taken into consideration and adjusted in the calibration. A shift in reflected wavelengths can also be used as a reference when the value of interest is how much strain is acting on the optical fiber. There can be placed several Bragg gratings in one optical fiber, in a distributed configuration. The wavelength spectrum to be reflected must be different for each of the Bragg gratings, such that the reflections do not overlap [2, 20, 26].

Flowmeters

Fluid flow is a process within many industries, such as chemical engineering, chemical engineering, and petroleum. In the petroleum industry measuring fluid flow is present in both pipeline monitoring and well monitoring systems. Drilling processes involve several different fluids, and production with the multiphase flow containing oil, gas, water, and sand, which vary throughout the production phases. For maintaining well control, safety, and production efficiency, a measurement system providing information on flow rates, composition, and changes is crucial. Instead of determining the said information when fluids reach the surface, i.e. by time-consuming, conventional topside separators, in-well sensing elements were introduced [27, 28].

For harsh environments, with high pressures and temperatures, and corrosive fluids, fiber optic flowmeters are well-suited. There are two variations of fiber optic flowmeters, one based on fiber interferometry, and the other on optical hot-wire anemometry [27]. Hot-wire anemometry is temperature-based and can be implemented with the previously mentioned fiber Bragg grating sensors, granting several sensing elements in one fiber optic cable. By placing flowmeters in multilateral wells, one can also obtain information on production in every lateral. Thus, flowmeters are advantageous for production optimization in both single, and multilateral wells [27, 29]

Distributed Sensing

From early work in fiber optic sensing intrinsic sensors aimed for measurements at certain points. Although, investigation of the possibility of influencing the transmitting properties of an intrinsic sensor through measuring the parameter field as a function of position, was slowly developing with time, providing a distributed measurement. The ability to do measurements along the fiber has been of great significance for the oil and gas industry and fiber technology in general. Distributed sensing contributes to well lifetime optimization through monitoring, for operating companies and reservoir engineers. The fiber technology itself is exclusive due to these types of measurements over very long distances, and are beneficial in i.e. a production or injection wells [20, 30].

Distributed sensing is different from optical point sensors, as it utilizes the fiber itself as the sensing element. A series of pulses is sent down the fiber, and the interrogator processes the returning signal with a reference to time, providing distributed measurements at several points at a predetermined length interval along with the fiber. As a cost-effective solution, excluding several sensing elements, one can obtain temperatures, strain, and acoustics [30].

DTS

Distributed temperature sensing systems use Raman backscattered light to localize temperatures. Anti-Stokes and Stokes light's amplitudes are strongly and weakly dependent on temperature, respectively. From the ratio of amplitudes detected, a temperature profile along the fiber can be calculated. Accurate data is based on temperature resolution from time and signal launch rate and on a spatial resolution from the distance between points of measurements [30].

DAS

Distributed acoustic sensing systems use backscattered light and strain from acoustic energy. Each light pulse injected into the fiber, samples points on the entire length of the cable, with a predetermined distance of typically 1 meter between each point. To process the acoustic measurements, which hand off an enormous amount of data for a several thousand meters well, the interrogator and software to process the information are crucial. Distributed sensing has been a major part of Equinor's project on the Johan Sverdrup field, presented in Chapter 3.2.1 [30, 31].

Hydrophones and Seismic

Today acoustic sensors also include fiber optic hydrophones and seismometers, which can be applied to oil and gas exploration, earthquake inspection, and military applications. This type of underwater sensor gives several advantages with regards to sensitivity, size, and weight, no EM interference, and a large dynamic range. Interferometers are used to create an interface between light in the fiber cable and acoustic field, sensors transfer pressure fields to fiber strains, and an interrogator processes the data [20, 21, 32].

2.7. Optical Budget

As energy is transmitted through an optical cable, which can be several kilometers long, the quality and strength of the signal reaching its destination are crucial. A fiber optic system installed in a well, has several elements implemented to it before and during installation. These are instruments for measurements, safety barriers, and section-specific equipment with regards to the completion. When the equipment is installed there will often occur an integration of equipment to the fiber optic cable, which leads to the fiber cable being cut and rejoined, spliced. Other reasons which require splicing fiber cables are to obtain the desired length or to repair a broken cable.

In the planning phase, one creates what is called an optical budget, which takes the entire system into account with regard to how much the total optical loss is expected to be. An example of a complete system is given in Figure 2.8. Expected and actual loss might differ, as there are numerous factors when installing instruments offshore, but it does provide an anticipated loss. Thus, the theoretical loss is often considered a maximum, and the actual loss should not exceed this value. For an operator, the optical budget will be the base for what a supplier can deliver, and an overview of the setup. Hence, it is a decisive factor when choosing the supplier, and which components to install.

2.7.1. Fusion Splicing

There are two principal ways to splice fiber cables together, fusion splicing and mechanical splicing. Although the mechanical splice provides a solution for working in an environment where open sparks are prohibited, it creates too much insertion loss and back reflection to be practical and for it to meet the optical budget and other criteria. Some parts of the cable will be located below the surface and placed in fluids or gas, while another part will be above surface level. For the signal quality and strength to be within given standards, there can be no leaks and losses cannot be too high.

There are two types of fusion splicing which are categorized by the conditions to be met. A high strength fusion splice uses a high voltage arc to weld the individual fibers together and is used for downhole operations, i.e. for installing a PT gauge for downhole measurements. A low strength fusion splice is used on the surface because it does not require to be pressure tested nor will it be run through different fluids. A low strength fusion splice does not meet the criteria for downhole environmental conditions but is used for i.e. connecting the downhole cable to the optical wellhead outlet, on the high-pressure side (downhole), or for connecting a surface cable to topside instrumentation. It is important to mention that this is one of Weatherford's criteria, and is not the same for all companies delivering fiber optic systems in the petroleum industry.

A fusion splice's quality is defined by the insertion loss and the tensile strength of the splice. Losses can be due to a mismatch between SM and MM fibers, misalignment, high cleave angles, and contamination. The process of fusion splicing requires stripping and cleaning the fiber. The moment the fiber is most exposed to i.e. contamination is when it has been stripped of its protective layers during preparation. Thus, this is a critical part of the process of splicing and requires caution. The several protective layers, Figure 2.5, can either be removed mechanically, thermo-mechanically or by chemical stripping, depending on the material. A high strength splice often requires chemicals for removal of the coating due to the material used in downhole cables, while for a low strength splice of a surface cable the coating can be removed mechanically with i.e. a wire stripper.

Before splicing the two ends together they have to be cut at precise angles, with a precision of a maximum $\pm 2^{o}$ to be approved by the fusion splicer. This is known as the cleave angle. If the angles are not within criteria, misalignment can occur leading to loss, and will also affect the tensile strength of the splice. When the cleave angle is off, it can be due to a crack in the glass, a lip on one end, or one end having a too sharp angle or corner for the ends to align, Figure 2.12. The fusion process itself can also create discharge in the form of bubbles, separation, or the splice being too thin or too fat, Figure 2.13. "A slightly fat splice is not unusual and there is no problem with loss or reliability." [12]. Estimated loss is displayed on the screen of the splicing apparatus, where a maximum accepted loss is 0.5 dB. When the quality of the splice is too poor according to the splicer apparatus, a new splice is recommended [12].

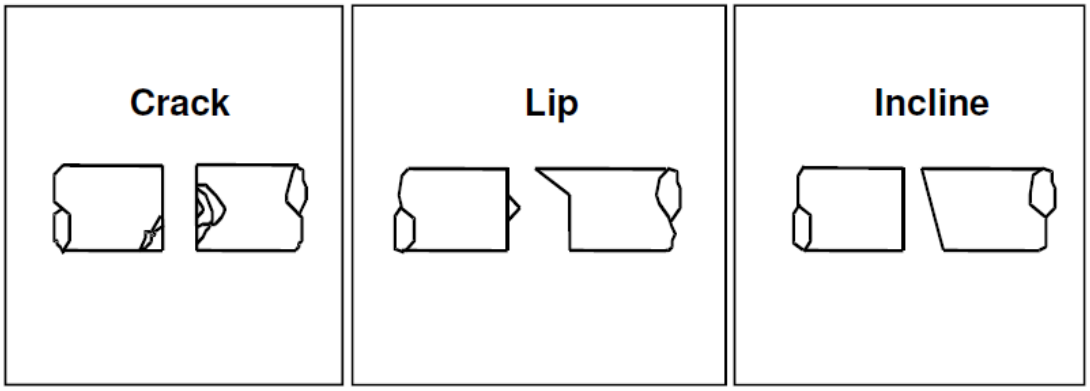

Figure 2.12: Bad cleave angles for splicing fibers [12].

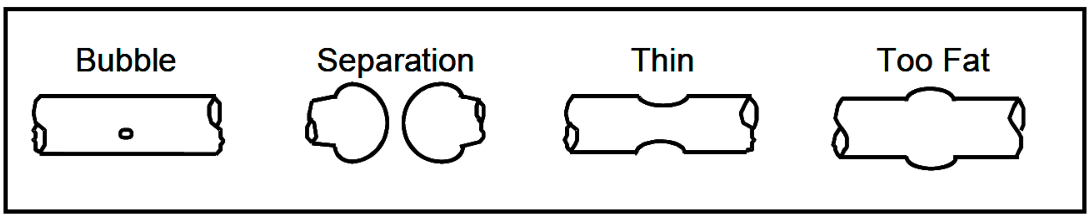

Figure 2.13: Bubble, separation, thin, or fat splice from fusion splicing [12].

After splicing, the exposed fibers need to be recoated, which is done by applying a protective layer in the form of a sleeve, and heat to seal around both sides of the splice. Checking the tensile strength of a fusion splice, by proof testing, is done on high-strength splices. This is also one of Weatherford's criteria for downhole fiber cables, with the intention of a long lifetime in a well under harsh conditions with regards to both exposures to fluids, and vibrations or movement. If one end of a fiber cable is cut, and not to be spliced, a process of cable end termination will be performed. This is to make sure nothing contaminates or enters the fibers, and for providing mechanical and environmental protection of the fibers [12].

3. Experimental and Field Applications

To have a first-hand experience with working with fiber optic technology, experimental work including splicing and testing of equipment was carried out at Weatherford's workshop. For investigating the fields of application for fiber optic measurement systems, the Johan Sverdrup installations, and other case studies are presented.

3.1. Experimental part

3.1.1. In house splicing

A 10 m downhole cable with a PT gauge installed in one end, which has been pulled from a previous completion, was used for the experiment. A low strength splice was used to connect patch cables to two SM pigtails, and a high strength splice to connect to the SM's from the downhole cable. Patch cables were needed to connect the fiber optic cables to an OTDR and a light source which has a specific type of connection of angled physical contact (APC). The light source was a "Run-in-hole" box (RIH), often used in offshore operations for checking signals on i.e. a downhole gauge during installation of the completion. The OTDR was used to check/test the optical loss through the splices, to investigate the quality of the splice. For a downhole cable to cable splice, the maximum accepted loss is 0.2 dB, which was the aim of the splices performed in this experiment. Simultaneously a difference in splice quality was attempted, for comparison of a good and bad splice in the results.

The RIH box functioned as a laser, shooting light through the fibers in the cable. A computer was used to investigate the strength of the light, through Weatherford's software called RMS, which reads and processes data from downhole instruments which in this case was the PT gauge. The gauge is connected to one of the SM fibers, and RMS will only see readings on this single fiber. These procedures of quality checking reflect what is used in an installation, and can be performed before, during, and after running completion in a well. Through the instruments, one will be able to check the signal strength and live pressure and temperature data throughout the operation. For this experiment, the amplitude and wavelengths were recorded, plotted, and investigated for checking the gauge functionality and signal strength. The quality of the splice was investigated through a comparison of the OTDR trace and RMS data. All equipment and instrumentation used in the experiment were borrowed from Weatherford.

Perform 50F Splice

Two APC patch cables (yellow) were to be spliced into two SM fiber cables (light blue) of approximately 30 cm. The patch cables were stripped down by mechanically removing the protective jacket and Kevlar threads, before stripping the bare fibers of coating. The glass fibers were cleaned with alcohol and cleaved before becoming spliced together using a 50-fusion splicer, which is a low strength splicer. The splicer gave an estimated fiber optic loss for cable 1 and 2, of 0.02 dB and 0.04 dB respectively.

Perform 40F Splice

Two single mode fiber cables (light blue) were to be spliced to SM1 and SM2 fiber cables (white and light blue respectively) in the downhole cable. Several layers of protective metal on the downhole cable had to be mechanically removed before exposing the fiber cables, which for this cable were 2SM and 1MM. For removing the jacket and coating, a thermal mechanical stripper was used, leaving only the glass fiber. A high strength splice requires a much more precise cleaning and cleaving. Hence, the fibers were cleaned by ultrasonic cleaning with a reactive solvent, which afterward was neutralized by de-ionized water. The fusion splice also required all water to be evaporated before splicing, which was done by using alcohol. It was used both an older and a newer reactive solvent for cleaning. Several attempts were required to obtain a precise cleave angle, by using an apparatus that utilizes vibration to cleave the glass fiber.

The cable to cable splice of SM-SM fiber cables was done with a 40-fusion splicer, which is a high strength splicer. SM1 was aimed to become the “best” splice, which gave an estimated fiber optic loss of 0.16 dB. SM2 was firstly cleaned with a poor solvent, which was not approved by the splicer. Using a better solvent gave a good splice and estimated fiber optic loss of 0.18 dB, but with a warning of a bad cleave angle, shown in Figure 3.1.

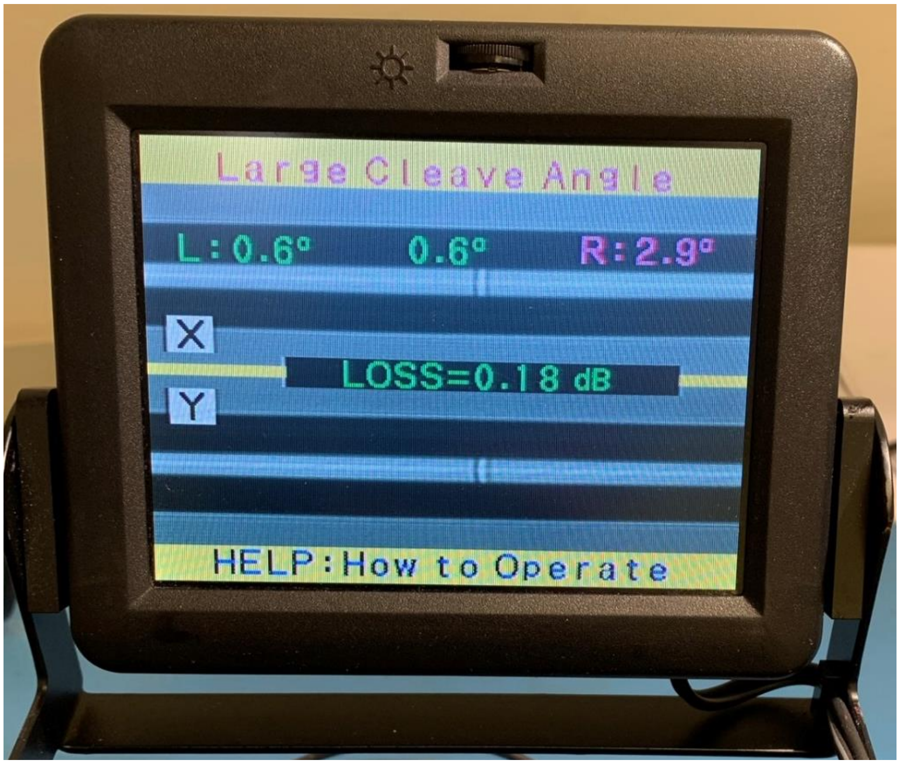

Figure 3.1: 40F Splicer giving a warning of a large cleave angle and estimated loss of 0.18 dB for the SM2 splice.

Proof Test

The SM1 high strength splice was mechanically proof tested with 85 kPsi tension for more than 3 seconds. SM2 was not proof tested, due to the bad cleave angle indicating a bad splice.

Gauge Functionality with RMS

The SM1 fiber was connected to the RIH box, and RIH box to a computer with RMS, as in Figure 3.2 below. When switching in the light source, the amplitude and wavelengths could be recorded. At the same time, pressure and temperature data were shown in RMS. The pressure data would not be correctly presented as the gauge's sensitivity is calibrated for higher pressures in a well. Thus, the atmospheric pressure in the workshop could not be measured accurately by the gauge with this setup. The RIH box has two ports, A and B, where both ports were used. Due to the RIH box "blinding" itself, an attenuator of 2 dB was added to the configuration. SM2 was also connected according to Figure 3.2, with both ports and a 2 dB attenuator. Signals were checked by running the RMS software.

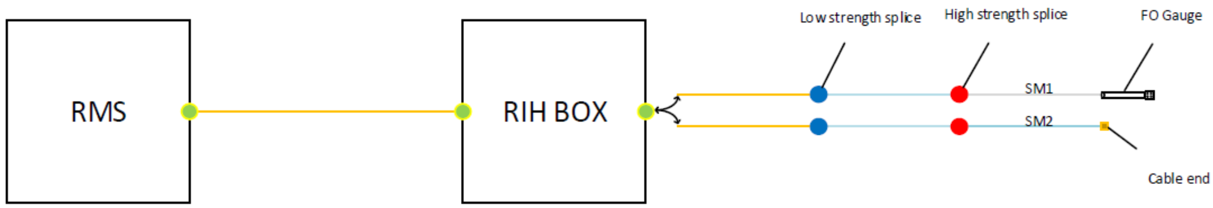

Figure 3.2: Configuration of fibers and instruments, for running RMS software.

OTDR

SM1 was connected to the OTDR, according to the setup in Figure 3.3, and a 30 seconds optical trace was performed at wavelengths 1310 nm and 1550 nm, and at 10, 50, and 100 averaging time. The shorter averaging time provides more details, and the longer less noise. The same traces were collected for the SM2 fiber, and all traces were transferred to a computer with a trace viewer application, for investigation and comparison.

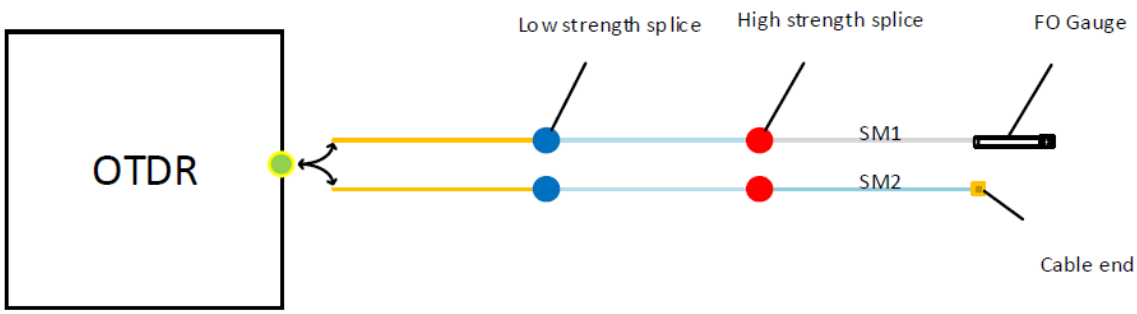

Figure 3.3: Configuration of fibers and instruments, for shooting optical traces with an OTDR.

3.1.2. Effect of strain on Bragg grating readings

When a fiber Bragg grating is implemented in a fiber optic measurements system it is produced with a specific pattern, which will reflect wavelengths within a given spectrum. For an upcoming offshore installation, a fiber Bragg grating was to be installed as a temperature reference point, called an ATS sensor. The fiber was spliced into a splice block, where several fibers were wrapped in a pattern for minimal strain and protection while RIH with a completion string.

The calibration file which reads the ATS sensor through RMS, correlates the reflected wavelengths to a temperature gradient calibrated for each ATS sensor. As mentioned in the subchapter Bragg gratings, the strain on the optical fiber will cause a shift in reflected wavelengths. To check whether strain was affecting the ATS sensor, RMS readings were recorded from the ATS sensor in the splice block.

ATS sensor in splice block

The ATS sensor was already spliced in a splice block, with one of the two fiber ends being free. An APC patch cable was spliced to the free end of the ATS sensor, such that a RIH box could be connected to the fiber. A computer with RMS software was connected to the RIH box, and wavelengths were recorded. The configuration of the system is shown in Figure 3.4.

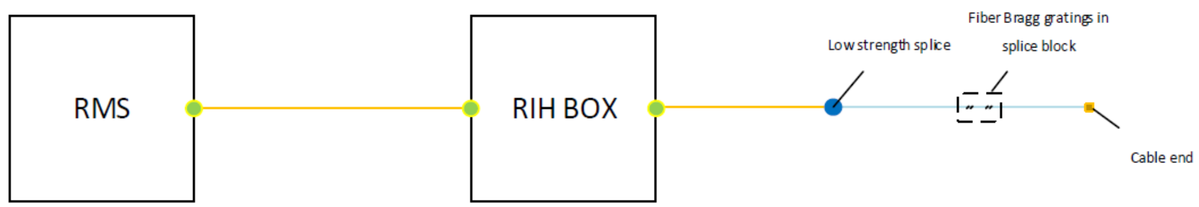

Figure 3.4: Configuration of fiber and instrumentation, for recording wavelengths from fiber Bragg grating (ATS) sensor.

Wavelengths recorded

The wavelengths recorded from the ATS sensor were investigated. A comparison of expected wavelengths versus actual wavelengths recorded was noted. If a shift in wavelengths was to be observed, the calibration file correlating temperatures to wavelengths would have to be adjusted, to account for consequent strain.

3.1.3. System Integration Test

The first part of the optical budget, 2.7, from Weatherford's operational point of view, is the total losses obtained when performing a SIT of all elements in a measurement system. Several splices must be done to connect necessary equipment, in the same manner as when the system is connected on surface and downhole for a well. From the SIT an estimate of the actual losses through all components can be obtained. Performing the connections and splicing does not necessarily give the same results onshore in the workshop, compared to on an offshore rig with entirely different conditions. After all elements have been connected, optical traces can be recorded to verify no critical errors in the system with regards to optical losses, noise, and reflection. Afterward, instruments can be integrated into downhole assemblies and pressure tested to check seals and i.e. a gauge's functionality.

A full SIT was simulated according to what would be done before an offshore installation on the NCS, according to Weatherford procedure. Two identical optical systems consisting of an OWHO, a fiber optic surface cable, and downhole cable, of approximately 100 m and 6000 m respectively, a downhole, optical PT gauge, and a gauge mandrel to protect and hold the gauge. Weatherford's gauge mandrel and optical PT gauge are shown in Figure 3.5: Weatherford gauge mandrel (left) and PT gauge (right) [33].Figure 3.5. The PT gauge measures pressure and temperature with an accuracy of ± 3 psi and ± 0.1 ^{o}C. The fiber optic configuration was of 2SM fibers and 1MM, and the measurement system to endure a maximum pressure of 20,000 psi and 200 ^{o}C.

Firstly, temporary pigtails were spliced to the fibers connected to the OWHOs, to have APC connectors in all fiber ends for the system testing. OTDR traces were recorded for all fibers, at 1310 nm and 1550 nm for SM, and 850 nm and 1310 nm for MM. A RIH box was used for checking the gauge functionalities and signal strength, through RMS software. Afterward, the gauges were mounted to the gauge mandrel assemblies. Pressure tests of a typical criteria for a well were performed, for checking seals and integration between mandrel and gauge.

Figure 3.5: Weatherford gauge mandrel (left) and PT gauge (right) [33].

3.2. Field Application

Across the world, fiber optics have been used in several industries for quite some time. Especially within the petroleum industry, it has been a long-term investment for exploration and production, providing valuable information on the subsurface. As Chapter 2.5 mentions, there are several advantages when using fiber optic sensors for measurements. The technology itself is reliable and flexible for integration of the measurement systems, which reduces risks and costs before and after installation. One of the major oilfields on the NCS to use fiber optics for PRM and well monitoring is the Johan Sverdrup field. Johan Sverdrup is referred to as Equinor's "Digital Flagship" [34], by means of using technology for optimizing safety, production, carbon efficiency, and daily work tasks [34, 35].

3.2.1. Johan Sverdrup Field

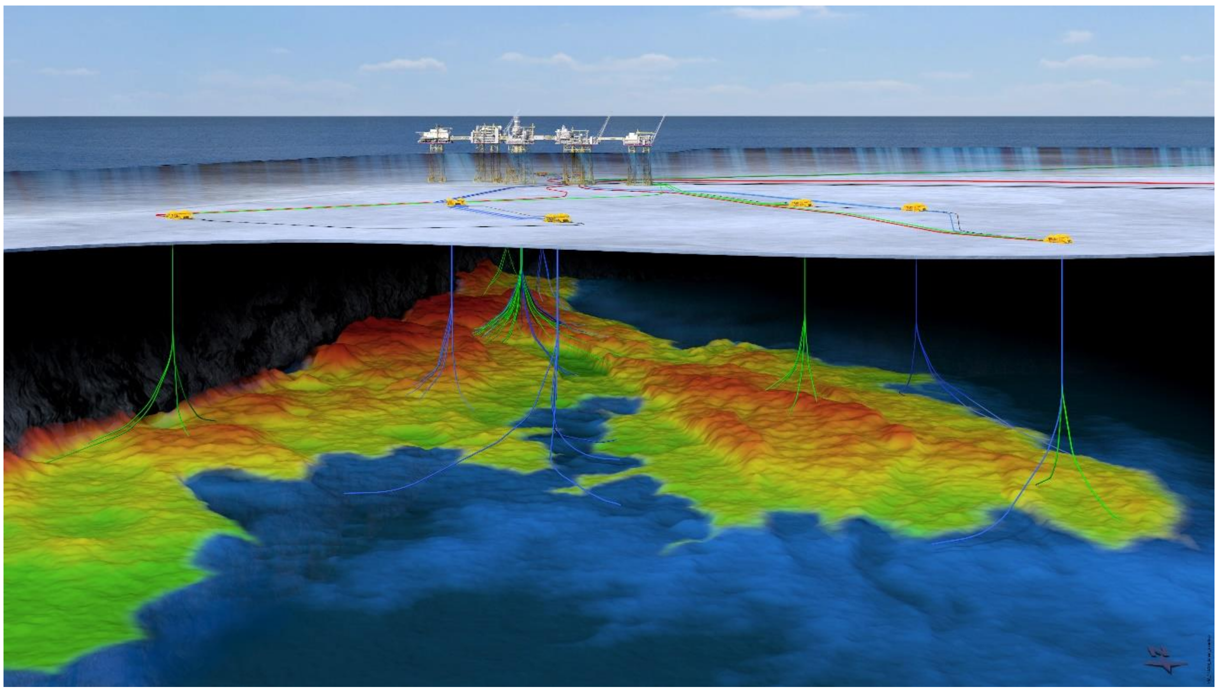

Figure 3.6: Johan Sverdrup field Overview [36]

11 years ago, one of the largest oilfields on the NCS was discovered in Utsira High, Figure 3.6. Named after a former Norwegian prime minister in the late 1880s, Johan Sverdrup has been developed and operated by Equinor Energy AS, with partners Lundin Energy Norway AS, Aker

BP ASA, Petoro AS, and Total E&P Norge AS. Percentages of the Johan Sverdrup license shareholders are presented in Figure 3.7. With its 2.7 billion barrels of oil equivalents, BOE, it is the third largest field on the NCS behind Ekofisk and Statfjord. Expectations were high from the day it was discovered, and the partners agreed on the goal of recovering more than 70% of its BOE, before production had started. The field is considered a major project in Norway for the next 50 years, with regards to the economy, digitalization, and carbon footprint in Norway's oil and gas industry [36-39].

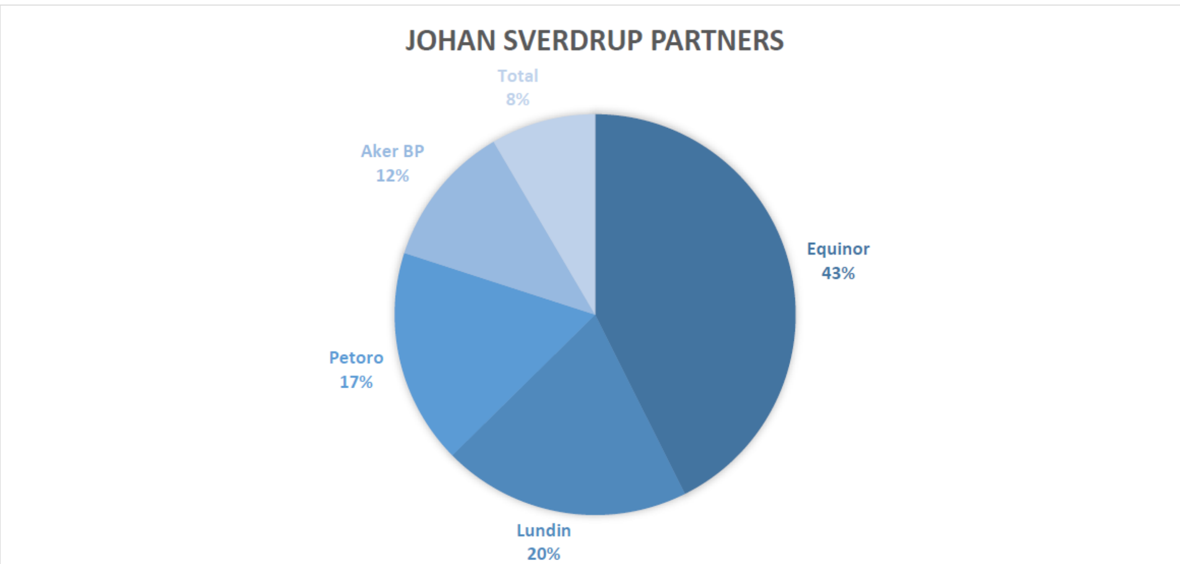

Figure 3.7: Shares in Johan Sverdrup [36]

After the first year of being on stream, Johan Sverdrup has produced approximately 130 million BOE. At first, the anticipated time for reaching the plateau production was in the middle of 2020 but was reached a few months ahead, in April 2020. With operating costs of less than $2.00 per bbl and a capacity of 470,000 bopd, numbers are strong for the break-even of $20.00 per bbl for full field development, when achieving 30,000 bopd above expected [36].

As a result of renewable hydropower from shore the field's CO_2 emissions are extremely low. The average CO_2 emission on the NCS is 10 kg CO_2/bbl produced, whereas Johan Sverdrup emits as little as 0.67 kg CO_2/bbl, which is equivalent to 3.7% of global average emissions. Electrification of major Norwegian fields and platforms is part of replacing polluting energy sources commonly used. Utsira High will have a power from shore solution, illustrated in Figure 3.8 below, covering Johan Sverdrup, Edvard Grieg, Ivar Aasen, Gina Krog, Gudrun, and Sleipner fields. Power from shore will lead to reducing CO_2 emissions by more than 620,000 tons a year [31, 40].

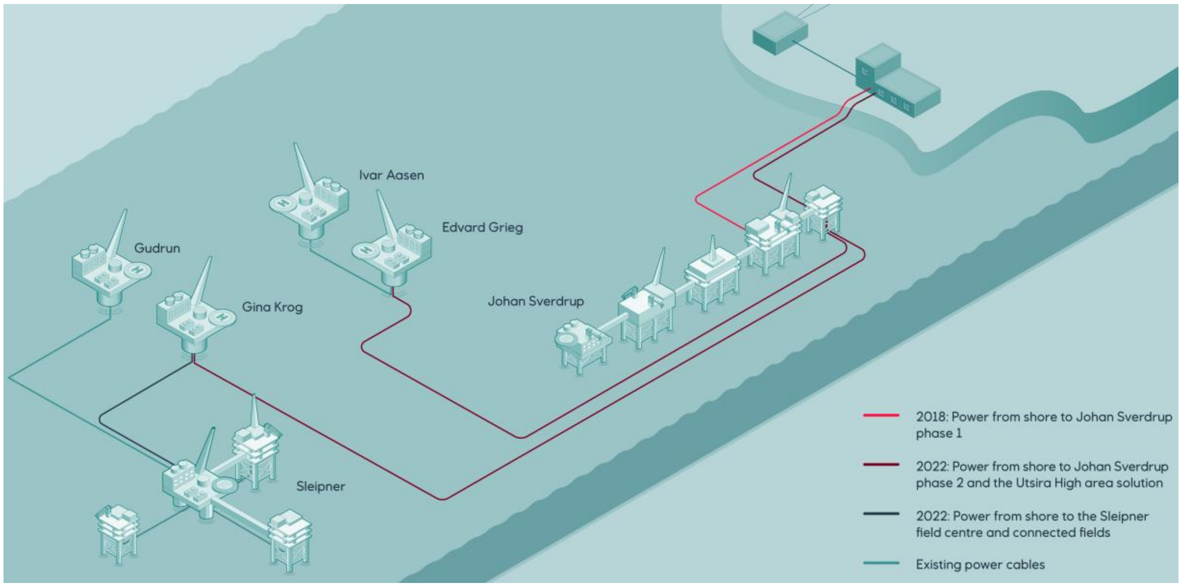

Figure 3.8: Hydropower supply from shore [31]

Phase 1 and 2

Phase 1 of development and production was approved in June 2015, and Equinor started the production in October 2019. Phase 1 included 4 platforms, 3 injection templates, and a power supply from shore. There is one processing platform, P1, one drilling platform, DP, one riser platform, RP, and living quarters, LQ, shown in Figure 3.9. Oil is exported to the Mongstad terminal through pipes, and gas to Kårstø processing plant through Statpipe.

Phase 2 was approved for development in May 2019, which will add a processing platform, P2, to the installation. The additional processing platform is part of increasing the overall production capacity of the field. With P2 capacity will be at 660,000 bopd, towards the target plateau rate of 720,000 bopd. At such high production rates, production from the Johan Sverdrup field contributes to 30% of Norwegian oil production alone.

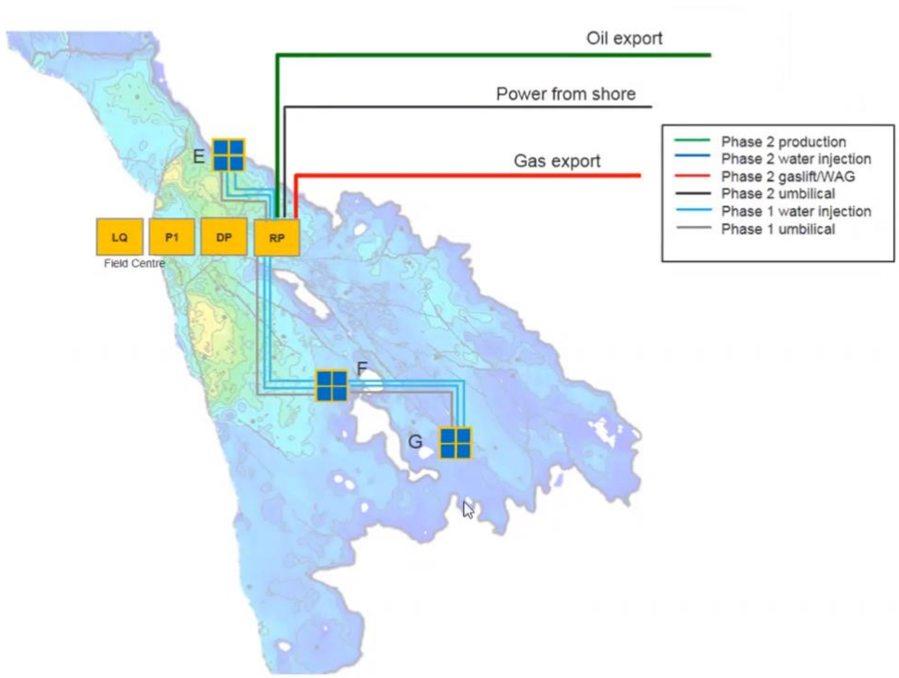

Figure 3.9: Phase 1 [31].

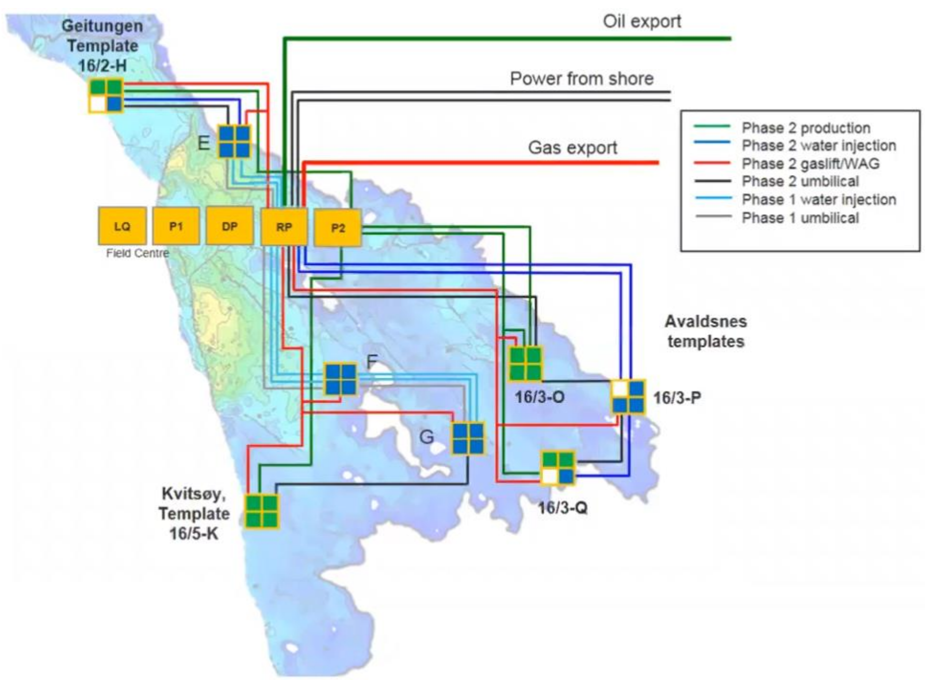

Figure 3.10: Phase 2 [31].

Development of Phase 2 is to take place at the end of 2022, and at this stage, the Utsira High power supply will be distributing power to the adjacent fields through Johan Sverdrup P2. Phase 2 includes a new module on the riser, 5 new templates, and 29 new wells altogether. The final templates and platforms are illustrated in Figure 3.10 [31, 37, 40].

Reservoir Description

The field's main reservoir lies is in the Upper Jurassic Intra-Draupne Formation sandstone at a depth of 1900 m, with average porosity of 28 % and an average net-to-gross of 97 %. The giant field of over 200 km^2 is known for its extraordinarily good qualities, with high permeability and porosity, hydrostatic pressure, and low gas-oil-ratio under-saturated oil. "The coarse grain size, lack of fines, scarcity of cementation, and extensive sheet-like distribution of siliciclastic sediments make the Intra-Draupne Formation sandstone an ideal reservoir" [41]. With this Olsen et al. [41] concluded the Upper Jurassic sandstone to be one of the best reservoirs the North Sea has come across. The remaining resources at Johan Sverdrup are located in the Upper Triassic Statfjord Group and Middle to Upper Jurassic Vestland Group sandstones [37, 39, 41].

Well design

Johan Sverdrup will mainly be produced with water injection and gas lift for pressure support. With the injection and production rates planned at Johan Sverdrup, the wells are designed for sustaining high rates, with the target production plateau of 720,000 bopd and re-injection of produced water at rates exceeding 100,000 Sm^3/day. Such high re-injection rates have never been reached on the NCS previously. For injectors, a deep injection point was important to avoid exposing the cap rock to high injection pressures. Additionally, the alignment of well paths has been optimized to ensure the injection pressures are as low as possible [31, 37].

The production wells in Phase 1 are mainly of three different well completion designs. There are screen completions of standalone inflow control device (ICD) screens and open hole gravel packs. The standalone screens are placed in shallow formations where net-to-gross sand is very high. The open hole gravel packs and cased and perforated completions are placed in the lowermost formations because of the possibility of encountering shales [31].

Digitalization

Over the years digitalization has been a big topic within the oil and gas industry. From development and exploration of fields through gathering and processing data, safety with respect to operations and personnel, and cyber security, to production optimization. Digitalization is important to avoid consequential production losses from operator errors and serious incidents to take place. Thus, the implementation of today's technology can aid the reduction of costs and improve maintenance operations on platforms. Several operating companies on the NCS has utilized integrated operations on older fields, such as Ekofisk (ConocoPhillips), Valhall (BP), and Ormen Lange (Shell), while Equinor's newly developed fields Johan Sverdrup and Aasta Hansteen applied the solutions from the beginning of operations [42].

The plan for development and operations Phase 1 at Johan Sverdrup included technology investments for reaching their high recovery target. Investments included "an observation well, permanent reservoir monitoring (PRM) across the field and well instrumentation and fiber optics through the well paths" [39]. Together with acquiring and analyzing data to make accurate and well-informed decisions, automatic production optimization, and using digital and online tools for everyday work tasks, the Johan Sverdrup field is undoubtedly well on its way as a digital frontrunner within the industry [34, 39].

3.2.2. Weatherford International Inc.

Weatherford is an international oilfield service company, specializing in wellbore and production solutions. Operating in over 80 countries all over the world, Figure 3.11, they provide equipment and services for oil and gas exploration and production. Within their portfolio, there are formation evaluation and drilling services, liner and cementations systems, as well as completions and safety systems. a more detailed definition of the products and services will follow in the following sub chapters.

Figure 3.11: Weatherford locations worldwide [33]

History

Weatherford Spring Company was founded in Weatherford, Texas in the 1940s, by Jess Hall, Sr. Its main products were drilling equipment and services. With its headquarters in Houston, expansion to Europe, and growth in provided services, the company was known for its casing cleaning, directional-drilling control, and fishing services. Together with the oil industry's rapid growth, Weatherford also had growth from the 1970s to the 1980s. Unfortunately, regardless of their comprehensive and varied services globally, the 1980s were tough as they were for many oil service companies. The domestic and international workforce was reduced remarkably, for the company to survive.

After several years of acquisitions and mergers, Weatherford International Inc. was founded by combining EVI Inc. and Weatherford Enterra Inc. in 1998. EVI Inc. came from several unions, starting with Energy Ventures which was founded in 1972, as a gas and oil exploration and production company. Acquiring CRC Evans in 1988, Grant Oil Country Tubular in 1990, purchasing Prideco in 1995, and with the growth and addition of a manufacturing plant in Canada, the name was changed to EVI in 1997. Simultaneously Weatherford International merged with Enterra and became Weatherford Enterra Inc. in 1995. The final merger in 1998 combining the three companies Energy Ventures, Enterra, and Weatherford, was first named Weatherford EVI Inc., but later they were renamed to Weatherford International Inc. At this point, they were the fourth largest oilfield service company in the world, in competition with Baker Hughes Inc., Haliburton Company, BJ Services Company, Schlumberger Limited, and Smith International Inc. [43, 44].

Weatherford Portfolio

Besides the main product which was drilling equipment and services, Weatherford Drilling and Intervention Services, additional principal divisions were formed, namely Weatherford Artificial Lift Systems, and Weatherford Completion Systems. Today the portfolio includes several services and products within these divisions, which are presented below.

Formation Evaluation Services

An essential part of the development of a reservoir is formation evaluation, described as “a key analytical process contributing to the identification of economically productive reservoirs” [45]. Parameters and properties must be investigated, defined, and evaluated, before further decisions and actions with regards to drilling, completion, stimulation, and production can be taken.

Reservoir characterization through laboratory evaluation, wireline services, and real-time logging from the surface or while drilling are services provided by the company [45].

Drilling

Weatherford delivers technology, tools, and services for drilling, including directional control and pressure management. When drilling with a managed pressure system, there are options for fundamental well control and critical situations. Working proactively to minimize hazard risks, drilling cost-effective wells, and enabling maximum reservoir exposure, are all important elements for operating companies. The drilling portfolio also includes cementing products.

Completion Systems

The completion systems include many products and services, crucial for optimal production. With a portfolio including safety systems, production packers, reservoir monitoring, flow control, sand control, fracturing products, and liner hanger systems, there are many products to create the ideal completion design. A completion setup varies with regards to the type of formation rock, i.e. a homogeneous sandstone or heterogeneous carbonate rock; reservoir characterization; oil, gas, high/low permeability or viscosity; and type of well; producer or injector. Different zones can be isolated with packer elements, monitoring systems can measure flow and provide pressure and temperature data, while sand control elements are important in sandstone reservoirs.

One of the noteworthy completion systems in the company's portfolio is their Single-TR1P solution, which enables the installation of lower and upper completion sections in one trip. Technology making this possible is a combination of radio-frequency identification (RFID) technology and the other completion elements available. RFID makes it possible to remotely activate downhole tools, such as downhole barriers or flow control elements, before or during production. An illustration of a TR1P system is presented in Figure 3.12. Weatherford completion systems are particularly an important part of deliveries on the NCS, which are presented in this thesis.

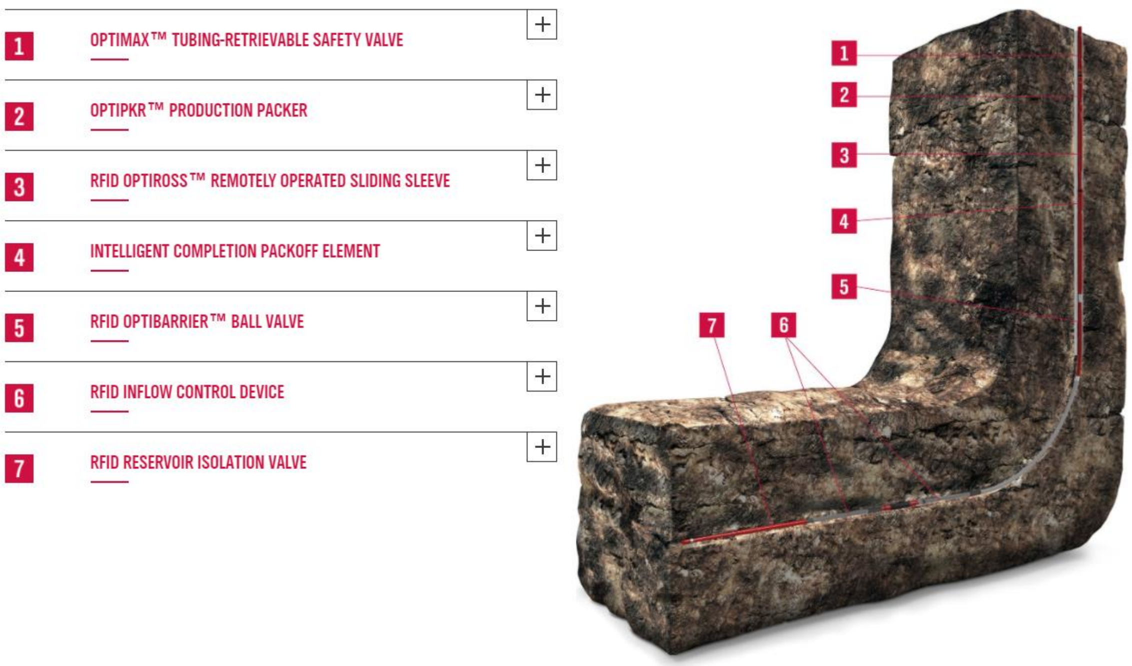

Figure 3.12: Single-TR1P completion setup [33].

Production systems

Integrated production systems together with the completion systems, provide flow measurements and well data in software solutions, presenting Weatherford's production optimization platform. There can be several measurement instruments in one well, collecting data throughout the well's lifetime, which need to be received, processed, or stored in topside instrumentation, and handed off to the client. Real-time systems help reduce operating expenses, as well as providing information for when i.e. injection should take place for optimum recovery or desired reservoir performance.

Tubular Running Services

On drilling or productions platforms, there are always risks of personnel working in hazardous zones, and this is something that needs to be kept at a minimum. Mechanized rig systems and automation of tasks reduce personnel's exposure to work in hazardous zones. Rig services, drilling with casing, and tubular management offline provide support to drilling and completion operations, increased efficiency, and supports easier handling of tubing on rig site by the make-up of several joints from shore.

Intervention and abandonment

Well intervention is important from the start of a well's lifetime until the abandonment is to take place. During drilling or production operations fishing services might be needed, i.e. when some object is lost-in-hole. Weatherford delivers expandable liners and casing patches for repairing casing or isolating zones. When a well is to be abandoned specialists, management and tools are supplied, and the finished product is ensured to meet a high compliance standard.

Weatherford Norway

On the NCS Weatherford's branch plant located in Sandnes, Rogaland delivers completion and production systems along with liner, casing, tubular running services. Within the reservoir monitoring discipline, fiber optics have been installed in several fields. Among the installations, the Johan Sverdrup field has been an important part of the portfolio with regards to new applications of the reservoir monitoring systems as PRM together with standalone screens and zone isolation packers. Implementing a fiber optic cable from the bottom of the well, in the reservoir section, required modifications from regular tools, and thorough planning and execution with cooperation between operator and contractors. Another field where fiber optics for monitoring has been installed is the high pressure-high temperature field Gudrun [12, 46].

Reservoir monitoring measurement elements mostly installed on the NCS include fiber optic PT gauges, downhole cables, surface cables, OWHO, and topside instrumentation and software. Not all installations include all the mentioned elements, as completions differ from each field and the client's needs. Weatherford's ForeSite Sense Optical solution can be applied in the subsea, platform, and land installations, for measuring in-well flow and reservoir pressure. It can gather data for pressure transient analysis, which is important in reservoir management and is applied to extreme high-pressure and high-temperature wells [33].

3.2.3. Case Studies

To bring forth fields of application for fiber optic technology, several case studies are presented in the following section. The dominating utilization within different types of measurement systems and gathering of information, is the distributed sensing of temperature og acoustics along the fiber optic cable.

Permanent Reservoir Monitoring

The world's largest permanent reservoir monitoring, PRM, system was installed at the Ekofisk field on the NCS, in 2010 by ConocoPhillips. The system of multicomponent sensors on the seabed was placed for seismic operations. The Jubarte Field in Brazil had a PRM system installed in 2012, to validate the detection of 4D elastic changes in the deep-water reservoir. A PRM system gives advantages for mapping reservoirs in the subsurface, and detailed images on the distribution of hydrocarbons, which are important aspects for numerical modeling and predictive analyses, drainage strategies, and the understanding of flow [47, 48].

In the later years, PRM systems of the major fields Johan Castberg and Johan Sverdrup have also been implemented, which are significant factors for Equinor's high recovery strategies on the NCS, of 60% and 70% respectively. Equinor's two fields were the first in the world to install PRM in advance of production start, with efficiency and economic benefits in mind. The accurate seismic data provided by such a network of sensors on the seabed creates high quality 4D seismic monitoring of changes in the subsurface and aids the placement of templates and wells The PRM system at Johan Sverdrup was designed for utilizing active reservoir management and covers a total area of approximately 125 km^2 illustrated in Figure 3.13 [4, 48-51].

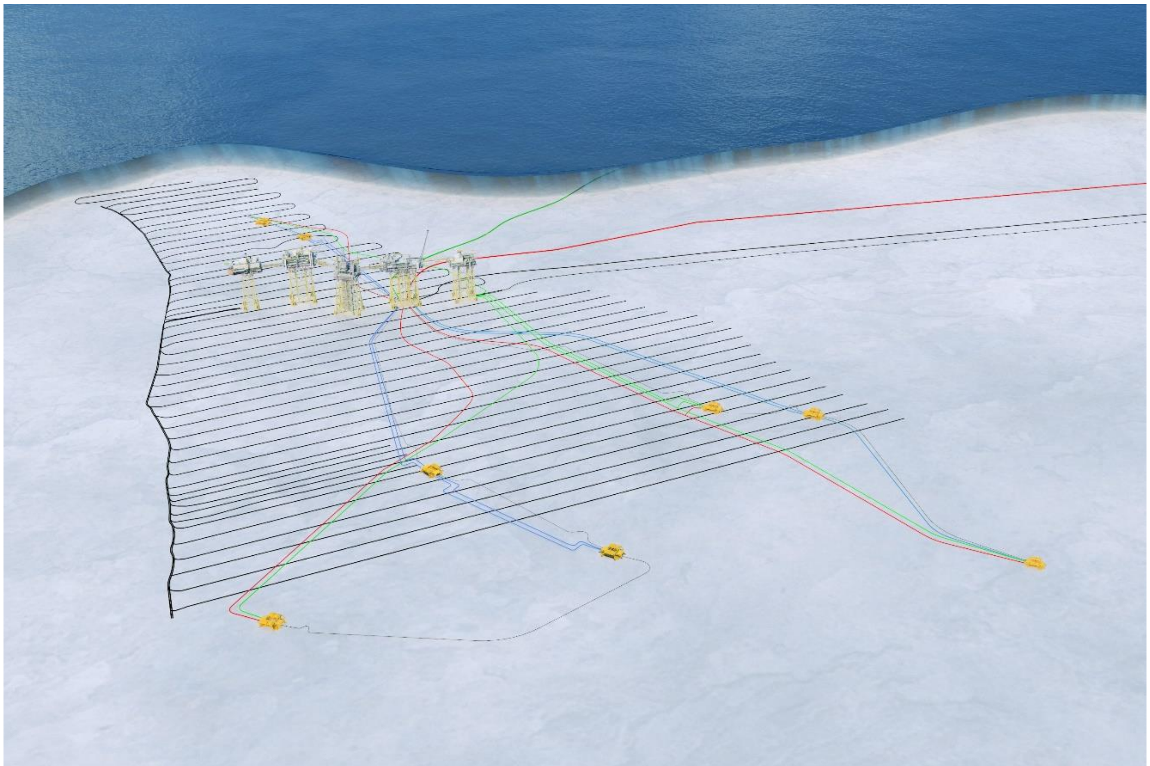

Figure 3.13: Map illustrating the PRM seismic cables over the Johan Sverdrup field [36].

In-well PRM

For collecting even more data from a producing field, the Johan Sverdrup licenses introduced the first in-well PRM system on the NCS in 2020, collecting live data in the form of temperatures and acoustics. A processing system and server onshore stream 5 GB of data every second, which delivers unique insight on installed equipment and well performance. By placing fiber optics along the entire well path, it is possible to track fluid flow through valves and ICD sand screens, and monitor well integrity simultaneously. Distributed sensing leads to optimization of production and gas lifts, and helps to reduce energy consumption and deliver lower carbon emissions [25, 26].

The first production well with fiber optics in the reservoir section was at Johan Sverdrup, installed in Phase 1 at the end of 2020. DAS and DTS measurements were collected, giving the onshore data acquisition system live imaging of flow through standalone screens in the lower completion, and opening/closing of valves in the upper completion. By placing a fiber optic cable along the entire well, a little over 4000 meters long, acoustics and temperature could be recorded for every meter. From an operational point of view, being able to "listen" to downhole equipment functioning, cuts down time spent on i.e. testing equipment. For the production in the screen section, which was designed entirely for the Johan Sverdrup producers, acoustics provide information of in-flow for every screen. As the production of this well is relatively new, a detailed presentation of this case could unfortunately not be obtained for this thesis [40, 52].

In-flow Monitoring – SPE 180465-MS

One of the key factors for production optimization is being able to create an inflow profile of the fluids. From knowledge on distributed measurements individually, DAS and DTS, Bukhamsin and Horne [53] looked at co-interpretation of the two. The objective of combining data from DAS and DTS to obtain information on multiphase flow leads to accurate determination of three-phase flow fractions. Individually DAS and DTS measurements can be used for analyzing one- and two-phase flow but is not adequate for solving a three-phase flow issue as there one variable too many [53].

From DAS an estimate of fluid flow velocity was obtained, by combining acoustics and inflow control valves in an oil producing well. When gas is dominating the flow, DAS measurements are not sensitive enough with regard to gas fractions. Thus, integrating DTS measurements with DAS measurements, was helpful in a system containing gas, oil, and water. Although it was concluded that production logging tools gave similar results of flow properties, the advantage of DAS is the continuous data, providing valuable information on changes during production [53].

Well-Integrity Monitoring

Well integrity is defined in the NORSOK standard as “the application of technical, operational and organizational solutions to reduce the risk of uncontrolled release of formation fluids throughout the entire life cycle of the well and of course safety aspects” [54]. An important part of well integrity is how well the casing string is cemented. The cement itself is the outermost layer towards the formation, temperature, and pressure changes which occur frequently in both oil and gas wells, and in geothermal wells [54].

Raab et. al [55] investigated the use of real-time monitoring of well integrity by fiber optics, in a geothermal well In Iceland. Both DTS and DAS were used to monitor changes throughout the operation of cementing the casing. From monitoring temperature changes for the arrival and setting of cement along the casing string, the depth interval of thermal gradients in the well could be identified. Throughout several well operations, such as cementing, drilling, and injection, monitoring of axial strain through DAS data provided information on the cement integrity. By comparison to conventional cementation tools, in this case, cement bond logging, measurements from the fiber optic cable along the casing correlate to both signal amplitudes and temperatures. It was concluded that real-time monitoring can give several advantages when implemented in well operations. DTS and DAS monitoring can be a better option than conventional tools for i.e. low-density foam cement investigations, and long-term conditions for the wellbore's mechanical integrity. Although, limitations when it comes to exposure of the fiber optic cable in harsh environments are present. Hence, the design of a fiber optic downhole cable in oil and gas wells is critical for its lifetime [55].

Well intervention

Coiled tubing can be used in drilling, completion, logging, clean out, or well interventions. In a drilling context, it is defined as "A long, continuous length of pipe wound on a spool." [56]. When running the pipe into a wellbore, it is straightened beforehand, and coiled back onto a spooling unit afterward. Coiled tubing can vary in length, within a range of 2000 to 15000, depending on the diameter and size of the spooling unit. When used in well interventions throughout a well's lifetime, it allows for safe interventions in a live well by utilizing a continuous string. The advantage of well interventions on coiled tubing is that pumping of fluids is not dependent on neither position nor direction of travel. Hence, fluids can be pumped at any given time [56, 57].

Along with the several applications for coiled tubing, fiber optics and downhole monitoring have provided another field of application. By implementing fiber optic measurements, trough point sensors, DTS, and DAS, real-time data of the conditions in the well are always available. Other areas for optimization, presented at SPE France Section in 2020 by Pierre Ramondenc [57], are monitoring of downhole assemblies. An overview of load, torque, and accelerations provides an overall performance of downhole tools. Thus, real-time measurements during coiled tubing interventions result in "faster, safer, and more efficient operations while maximizing return on investment." [57].

Steam Assisted Gravity Drainage – SPE-49184

As early as the 90's field implementation of fiber optics took place, and Saputelli et al. [58] investigated how the technology could improve oil recovery in wells with steam flooding in 1998. Improved oil recovery is often mentioned as tertiary recovery, and it is when natural energy can no longer be used to produce the hydrocarbons left in the reservoirs. There are several different methods that can be applied as enhanced oil recovery, and they are often a replacement of primary or secondary recovery methods when these are no longer feasible. Such processes involve miscible gases, chemicals, or thermal energy to displace hydrocarbons. The process presented in this paper is steam-assisted gravity drainage (SAGD) [6, 58].

With a philosophy of a "smart reservoir", using downhole instrumentation to interact with upper platforms, real-time data could be analyzed and put directly into production strategies. The philosophy is a concept consisting of using monitoring and the right tools to create a rock-fluid model, making it possible to create strategies and decisions in an integrated system, and have control over operations. The model was based on automation of processes, by integration of the above concepts in decision systems, such as numerical reservoir simulators, and project and reservoir management environments [58].

A better understanding of fluid flow is crucial for improved oil recovery, and Saputelli et al.'s paper addresses the use of fiber optic cables in horizontal SAGD wells in Venezuela, to obtain a distributed temperature profile of the reservoir. A comparison of the temperature profile and resistivity logs was done, providing information on which parts of the reservoir had been contacted by steam. From correlating information, a prediction of which parts of the reservoir would be swept by the displacing fluid could be made. They concluded that the practice was beneficial to planning the injection profile such that an improved spatial and microscopic sweep efficiency could be obtained. Fiber optic cables in the wells gave good results, and the data collected is a good representation of thermal fluid conditions. Permanent DTS was concluded to be beneficial for steam flood performance, and such monitoring of flow can lead to increasing the recovery factor and project's lifetime [58].

Drilling and well placement with acoustics

For drilling and well placement there are a few logs that are needed for acquiring information on the formation and reservoir, and the ability to run logs simultaneously can lead to a reduction in rig time and costs. A vertical seismic profile (VSP) is defined as "A class of borehole seismic measurements used for correlation with surface seismic data, for obtaining images of higher resolution than surface seismic images and for looking ahead of the drill bit." [56]. A VSP is made by using geophones, providing very detailed surveys by placing the geophones close to each other [56].

Martinez et. al [59] conducted a case study of using fiber optics in seismic applications, for optimizing drilling efficiency and well placement. A hybrid wireline cable, optical-electrical, was used to combine VSP and DAS data during an exploration well. The hybrid cable was developed to acquire seismic when carrying out wireline interventions, "from intermediate drilling section evaluations through well integrity and production" [59].

With the optical fiber part of the hybrid cable as a sensing element, the VSP could be obtained in a timeframe of minutes compared to hours or even days. For drilling efficiency, it was concluded that implementation of the hybrid wireline cable could save rig time by eliminating the seismic run, operational risks were decreased, and the seismic information was gathered in economically. There was an optimization of gathering seismic data, by combining conventional tools and fiber optics to take measurements simultaneously, along with quality assurance [59].

4. Results and Discussion

Results and brief discussion on findings in the in-house experiments, a discussion of the field application, and case studies will be presented in the following chapter.

4.1. Results from the experimental part

4.1.1. In-house splicing

RMS readings

With no attenuator, the light from the RIH box was too strong, resulting in very high amplitude peaks for both ports A and B. The peaks are higher than 25 000 for both pressure and temperature and are presented in Figure 4.1 and Figure 4.2. The plot presenting the amplitude vs index contains a total of 4 peaks. From the left-hand side the first peak is the pressure reading, and next to it the temperature reading, a clearer reference is shown in Figure 4.3. The two peaks on the right-hand side of the plot, are reference peaks for each of the sensing elements. Figure 4.5, a bar chart plotting amplitude vs wavelength, gave zero readings because of the blinding. In the latter figure the amplitude is given in ADC units which have 16-bit resolution and a range of [-32768, +32767], and the wavelength in x10 femtometer which equals x10^{-6} nm.

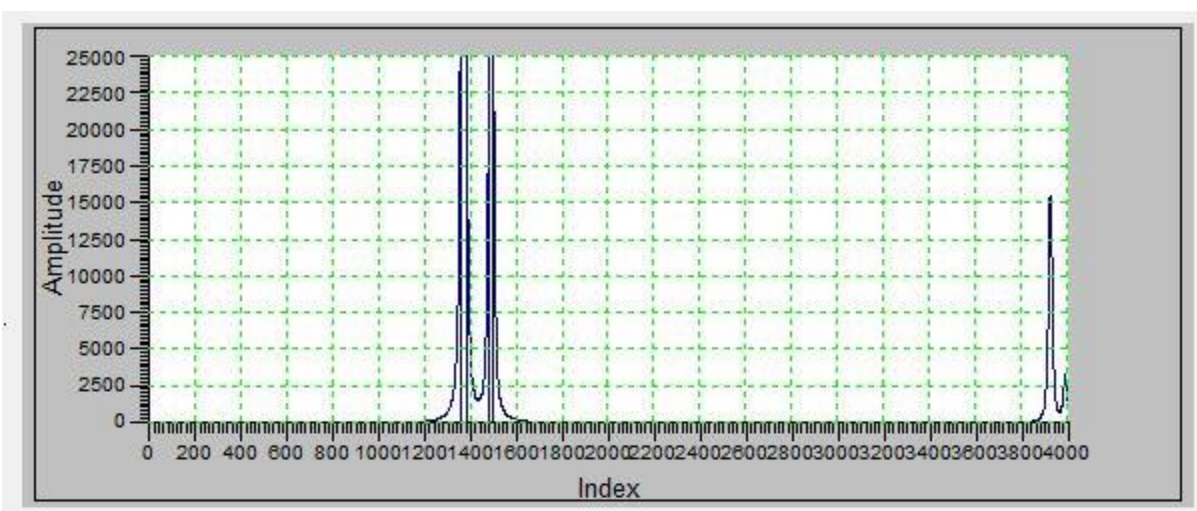

Figure 4.1: Amplitude vs index for SM1, port A, no attenuation.

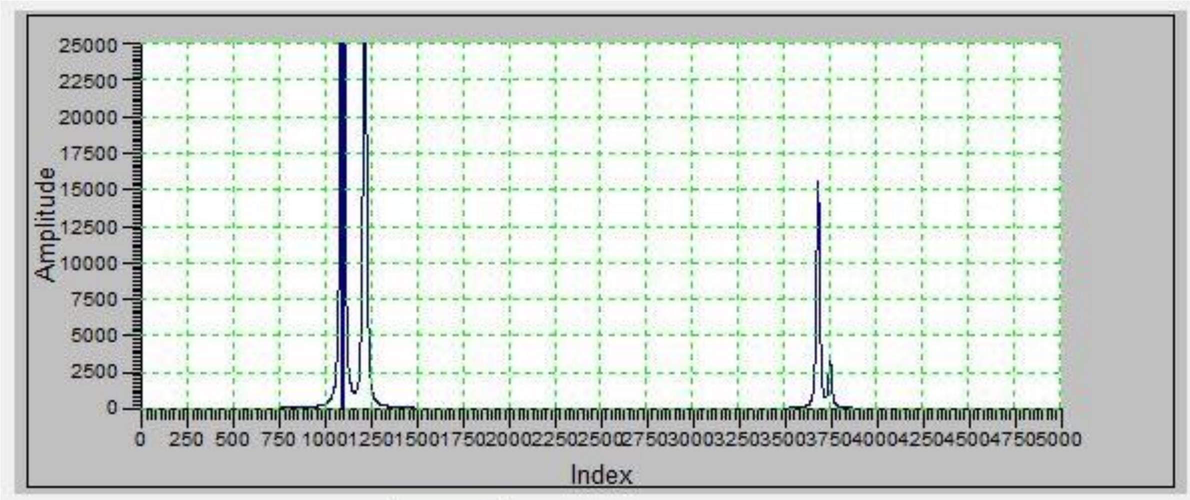

Figure 4.2: Amplitude vs index for SM1, port B, no attenuation.

An attenuator of 2 dB gave amplitude vs. index peak readings of just below 20 000 for pressure, and 12 000 for temperature in port A at a given time, Figure 4.3. Port B gave amplitude vs. index peak readings of 15 000 and approximately 9 000 for pressure and temperature respectively at a given time, presented in Figure 4.4. The bar chart in Figure 4.6 and Figure 4.7 is plotted from Bragg grating interrogation with amplitude vs. wavelengths. The average amplitude and wavelength plotted from data in Experimental Data is presented in Table 4.1. Port A gave an average amplitude of 20 272 and an average wavelength of 1 534 nm for the pressure reading, and an average amplitude of 12 211, and an average wavelength of 1 536 nm for temperature. Port B gave an average amplitude of 14 844 and an average wavelength of 1 534 nm for pressure, together with an average amplitude of 8 980 and an average wavelength of 1 536 nm for the temperature. Average values were calculated from data collected in a time interval of approximately 20 seconds.

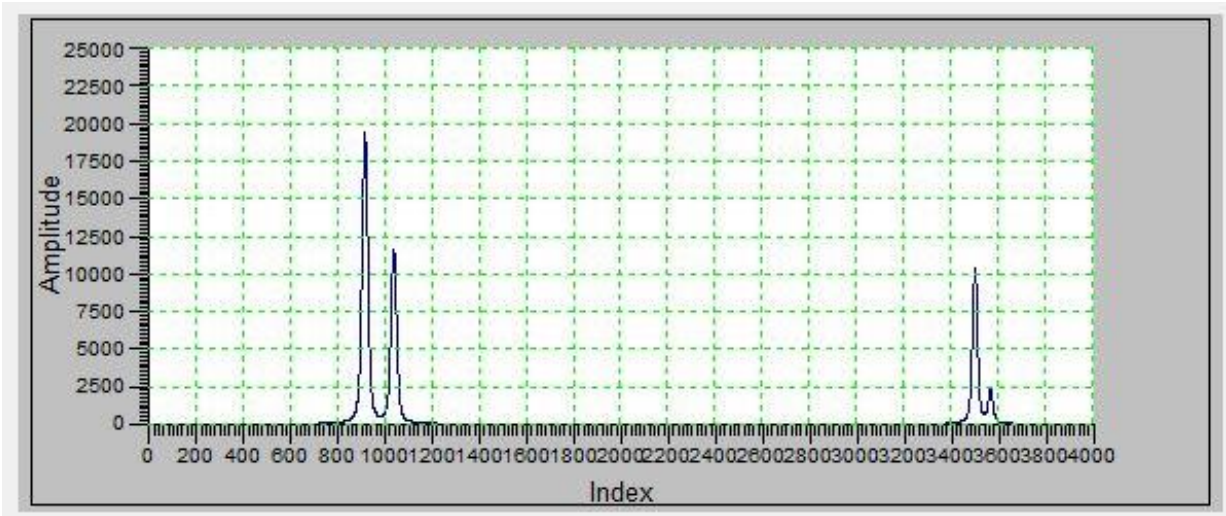

Figure 4.3: Amplitude vs index for SM1, port A, 2 dB attenuation.

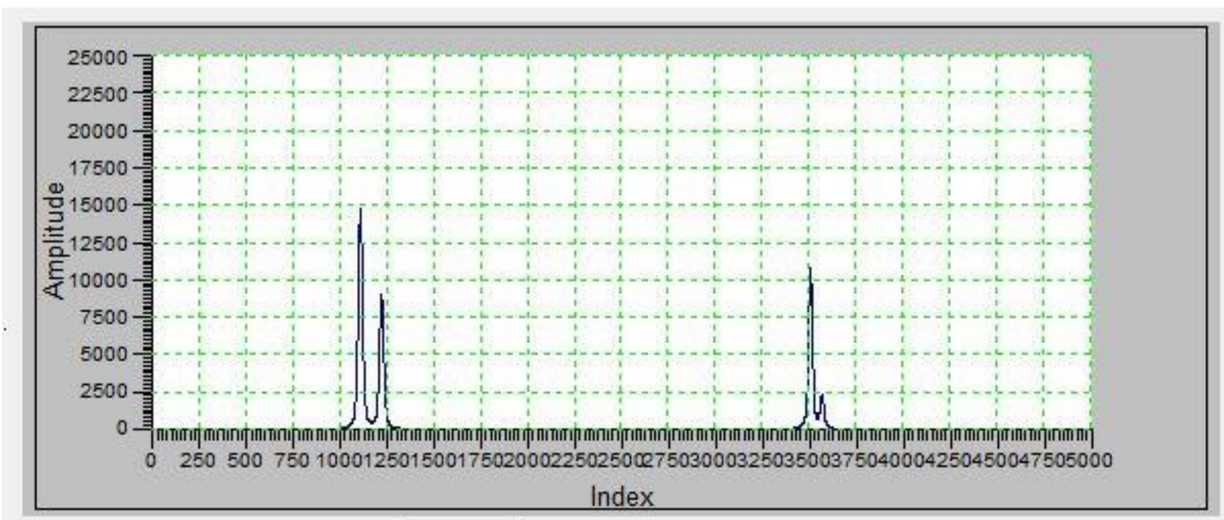

Figure 4.4: Amplitude vs index for SM1, port B, 2 dB attenuation.

Table 4.1: Average values from port A & B with 2 dB attenuation

Port	Sensing element	Avg. Amplitude	Avg. Wavelength [nm]
A	Pressure	20272	1534
A	Temperature	12211	1536
B	Pressure	14844	1534
B	Temperature	8980	1536

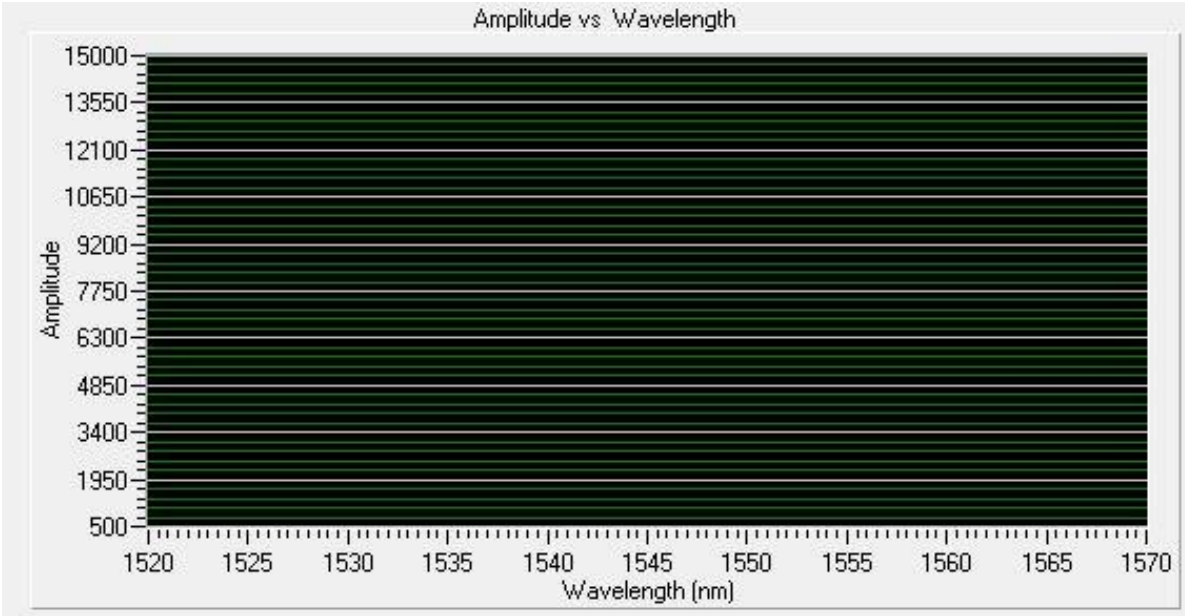

Figure 4.5: Amplitude vs wavelength for SM1, port A, no attenuation.

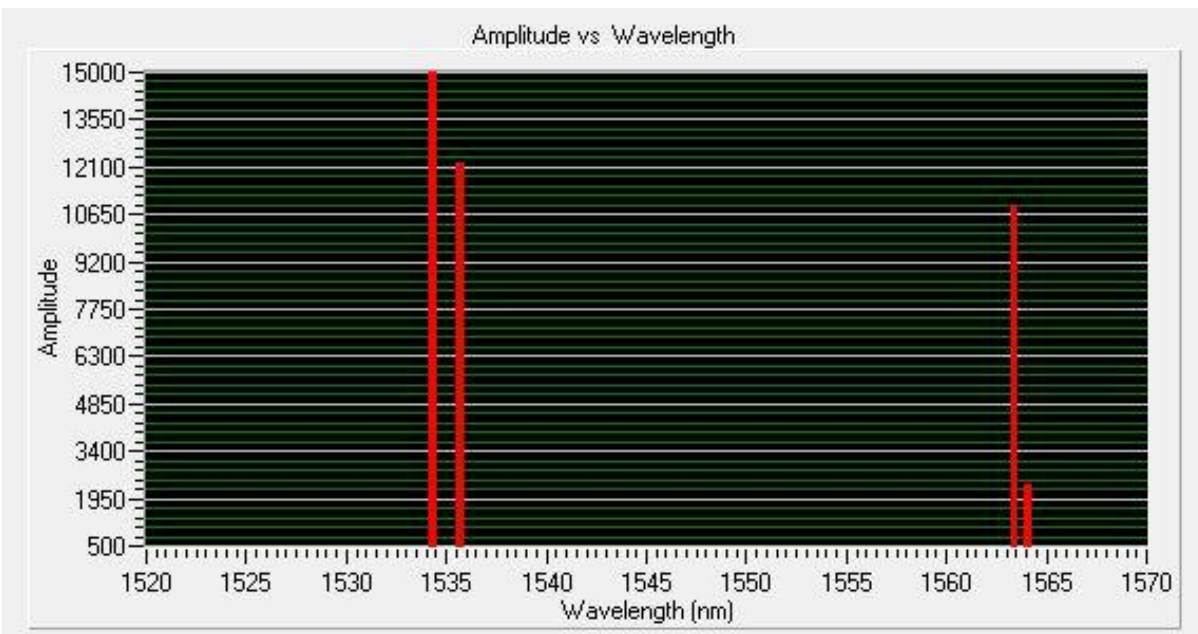

Figure 4.6: Amplitude vs wavelength for SM1, port A, 2 dB attenuation.

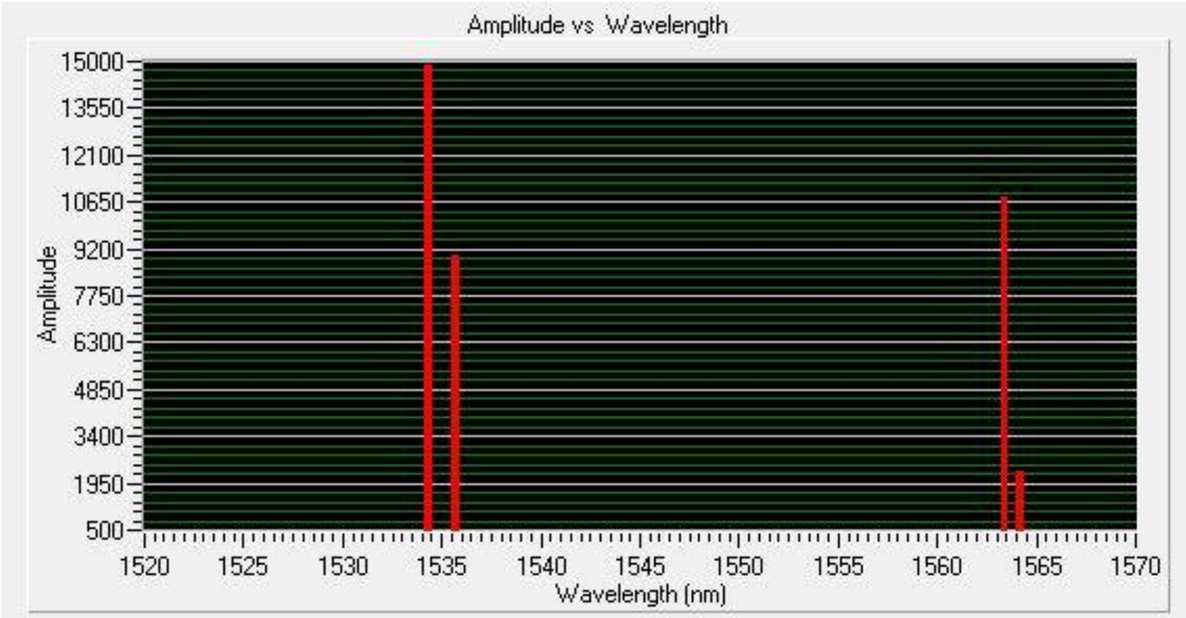

Figure 4.7: Amplitude vs wavelength for SM1, port B, 2 dB attenuation.

RMS was used to read SM1, as the processing software reads sensing elements. In this experiment, the sensing element was the PT gauge, which is a point sensing element connected to the SM1 fiber. SM2 had no sensing element connected to it. Thus, RMS could not be set up to read this fiber.

OTDR Traces

OTDR traces of 30 seconds were recorded at 10 ns, 50 ns, and 100 ns pulse width, with 1310 nm and 1550 nm wavelengths. For investigation of attenuation at a specific length and with the most details, the presented traces below are at pulse width 10 ns and wavelength 1550 nm. The OTDR instrument was of the brand Anritsu, which also has trace viewer software to study the recordings on a computer.

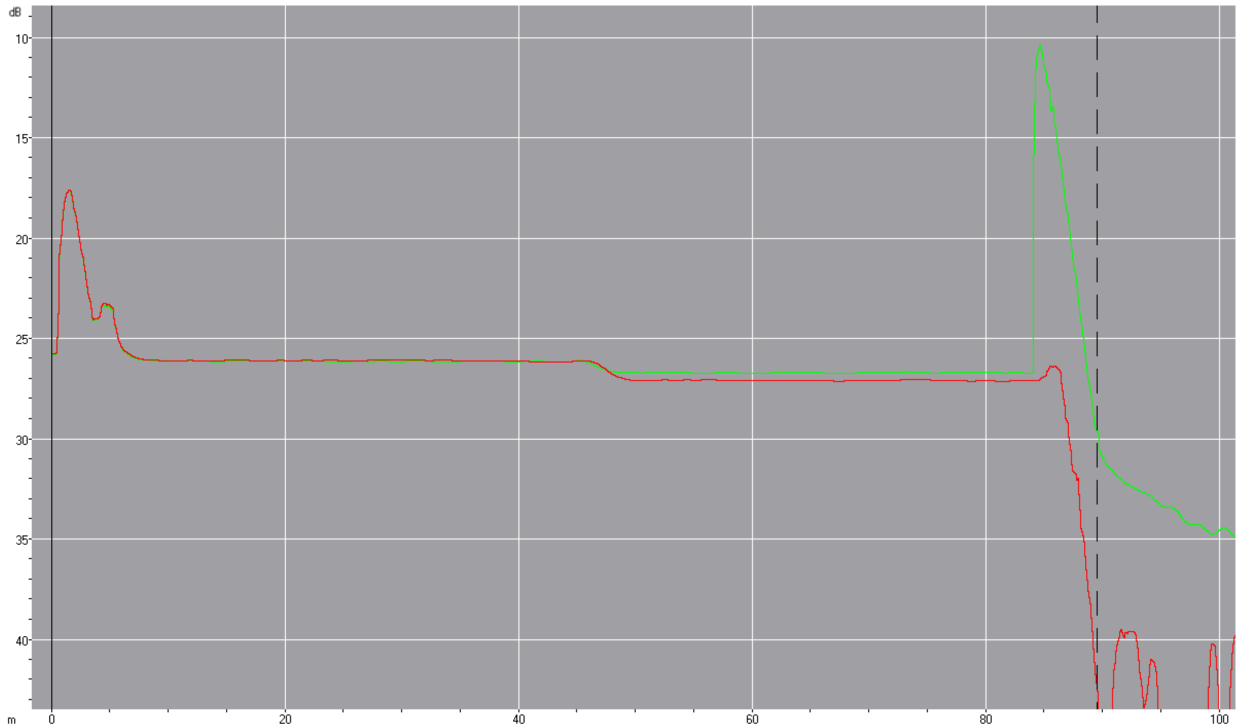

Figure 4.8: OTDR traces at 1550 nm of SM1 (green) and SM2 (red) of entire cable length.

Figure 4.8 presents a trace of the entire fiber cable length, with SM1 in green and SM2 in red. The peak left to the dotted black line illustrates where the PT gauge is located, and to the left of the same line is the end of the fibers. A 40 m patch cable was used to gain some length on the traces and make it clear where the splices were located. The x-axis measures distance [m] and the y-axis measure attenuation and reflection [dB]. The y-axis's value is a quantification the power entering the fiber compared to the power returned to the OTDR, as in equation 2-7. Peaks illustrate reflection, and the slope illustrates the attenuation coefficient as a function of distance over the entire length.

To locate the splices performed on the two fibers, length interval 40-65 m was investigated. An enlargement of the interval is presented in Figure 4.9. Attenuation over the interval was measured for each fiber. SM1 had a loss of 0.540 dB and SM2 a loss of 0.961 dB. The higher loss of SM2 is clearly illustrated in Figure 4.9 by the green line being approximately 0.4 dB higher than the red line at 50 m.

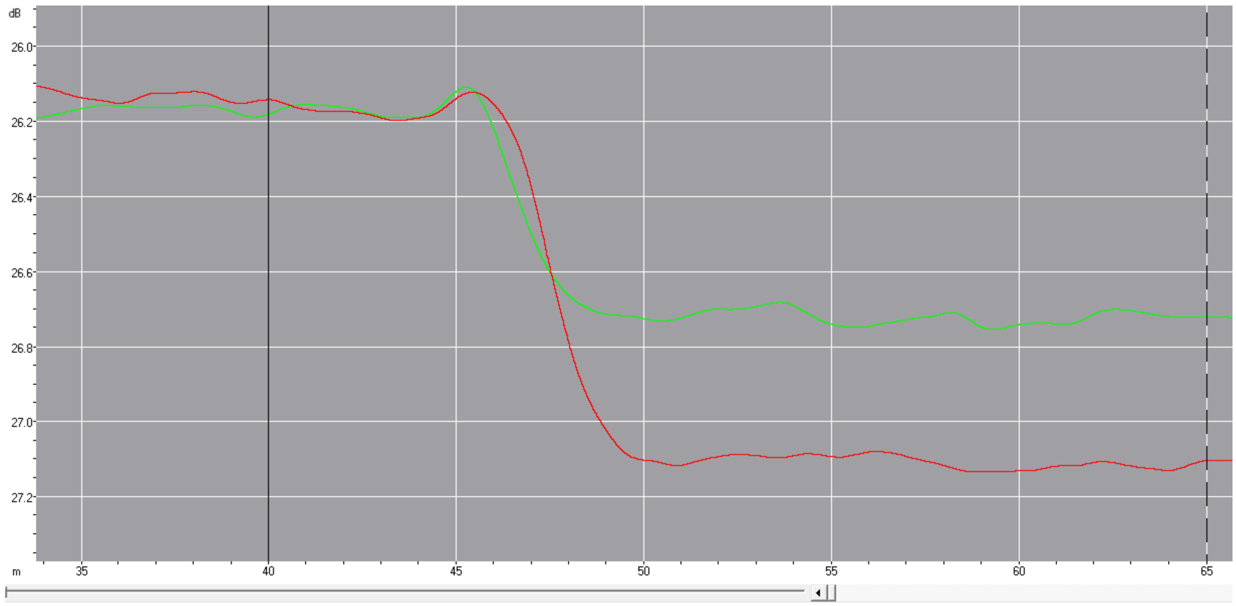

Figure 4.9: OTDR traces at 1550 nm of SM1 (green) and SM2 (red) at length 40-65 m.

The 2 splices on each fiber, according to the configuration in Figure 3.2 and Figure 3.3 in the previous chapter, were located between 40 m and 46 m. Figure 4.10 below, shows an enlargement of the given interval. An optical loss and some reflection in the given interval could be observed, indicating an event i.e. a fiber optic connector or splice. Traceview reported a negative loss of -0.009 dB (reflection) for SM1 between the whole and dotted line in Figure 4.10, and a loss of 0.022 dB for SM2 for the same interval. The attenuation recorded for the interval including the splices are presented in Table 4.2 below.

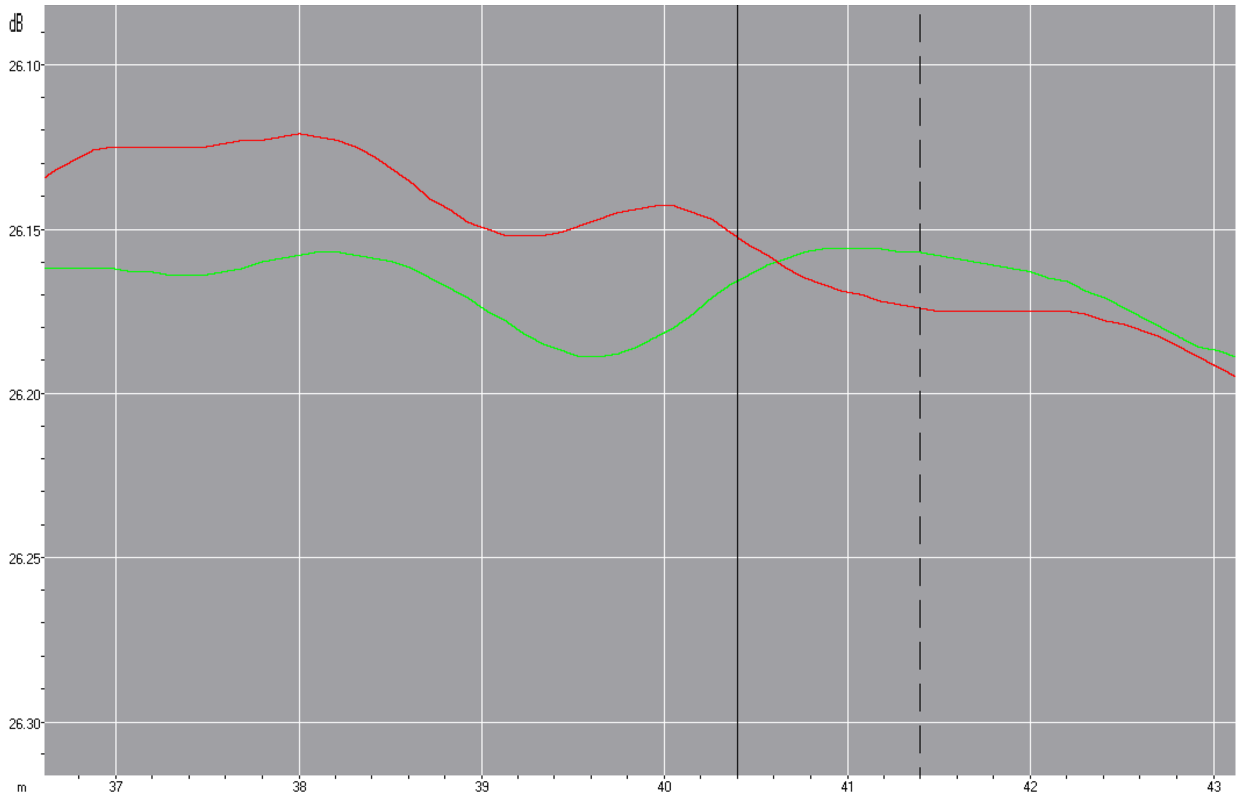

Figure 4.10: OTDR traces at 1550 nm of SM1 (green) and SM2 (red) at length 40-46 m.

Table 4.2: Attenuation over different intervals for SM1 and SM2 at pulse width 10ns.

SM1/SM2	Wavelength [nm]	Position on fiber [m]	Attenuation [dB]
SM1	1310	40-65	0.499
SM2	1310	40-65	1.177
SM1	1550	40-65	0.540
SM2	1550	40-65	0.961
SM1	1310	40.2-41.2	-0.019
SM2	1310	40.2-41.2	-0.025
SM1	1550	40.2-41.2	-0.009
SM2	1550	40.2-41.2	0.022

4.1.2. Bragg grating

RMS data were recorded for 15-30 seconds. The calibration files used for the ATS sensors has a narrow wavelength spectrum of 2.00 nm specified for each sensor, corresponding to a linear temperature gradient. The expected wavelength spectrum to be recorded for the ATS sensor in the splice block was 1538 – 1540 nm, Table 4.3, corresponding to a temperature gradient of 0.00 – 175.00 ºC.

Table 4.3: Recorded wavelengths from ATS sensors in splice block, with serial number and calibration file, expected wavelengths, and actual wavelengths.

ATS location	Serial number	Calibration file	Expected wavelength spectrum [nm]	Actual wavelength spectrum [nm]
In splice block	20184-03	20015285-16	1538 – 1540	No recorded wavelength.

When the RIH box first was set up with 2 dB attenuation, a high amplitude could be observed in RMS, presented in Figure 4.11. The plot illustrates an amplitude reading of 20 000 or more in the left-hand peak, along with two reference peaks on the right-hand side. When looking at the bar chart in Figure 4.12 plotting amplitude vs wavelength, no readings could be observed. Hence, no temperature could be recorded in RMS. The RMS software's response read "Unable to read wavelength for sensor 20184-03.".

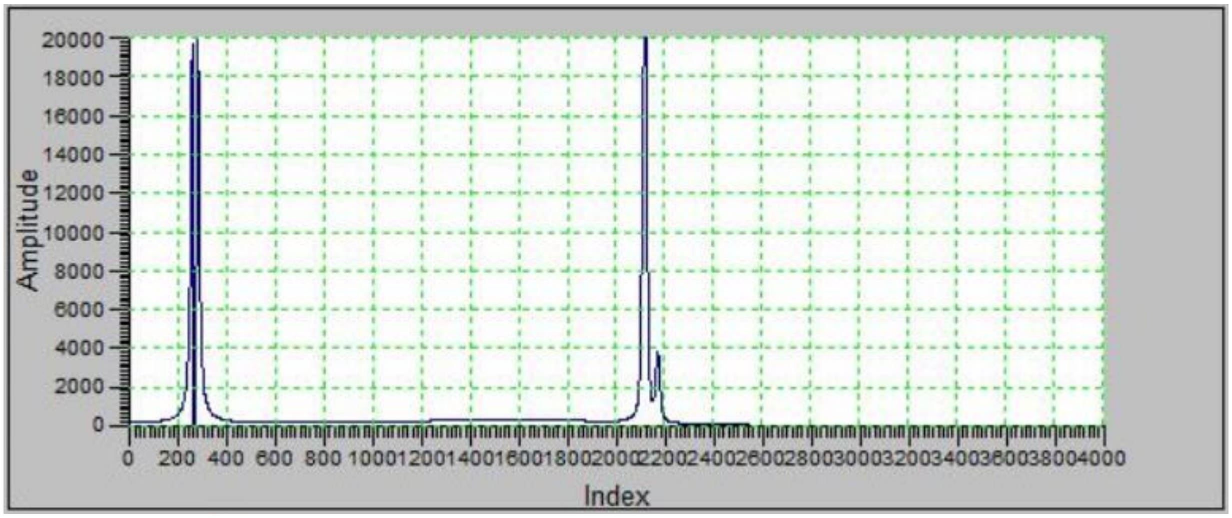

Figure 4.11: Amplitude vs index for ATS sensor in splice block, port A, 2 dB attenuation.

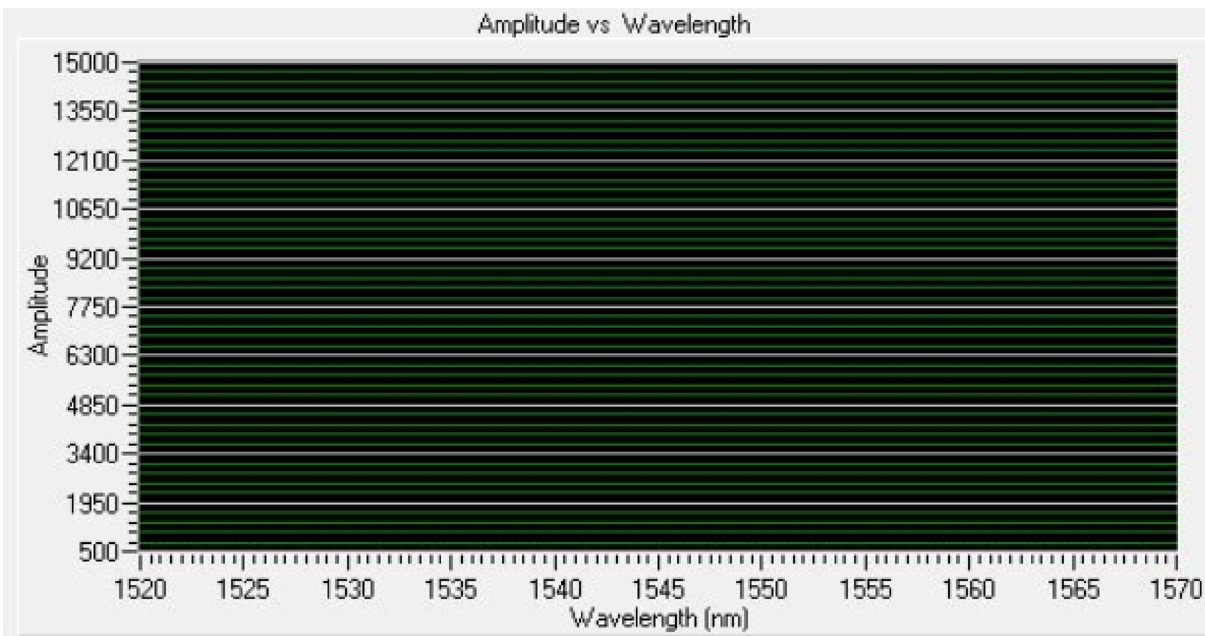

Figure 4.12: Amplitude vs wavelength for ATS sensor in splice block, port A, 2 dB attenuation.

To decrease the high amplitude in Figure 4.11 suspecting that the RIH box was blinding itself, 6 dB attenuation was added to the RIH box. New readings were recorded in RMS. The reference peak moved towards the right-hand side of the plot, and the ATS reading gave no reading due to the too low amplitude, Figure 4.13. The bar chart in Figure 4.14 shows an amplitude and wavelength reading of the reference peaks. No wavelength or temperature was recorded for the ATS sensor with 6 dB attenuation. RMS gave the same response as for 2 dB attenuation "Unable to read wavelength for sensor 20184-03.".

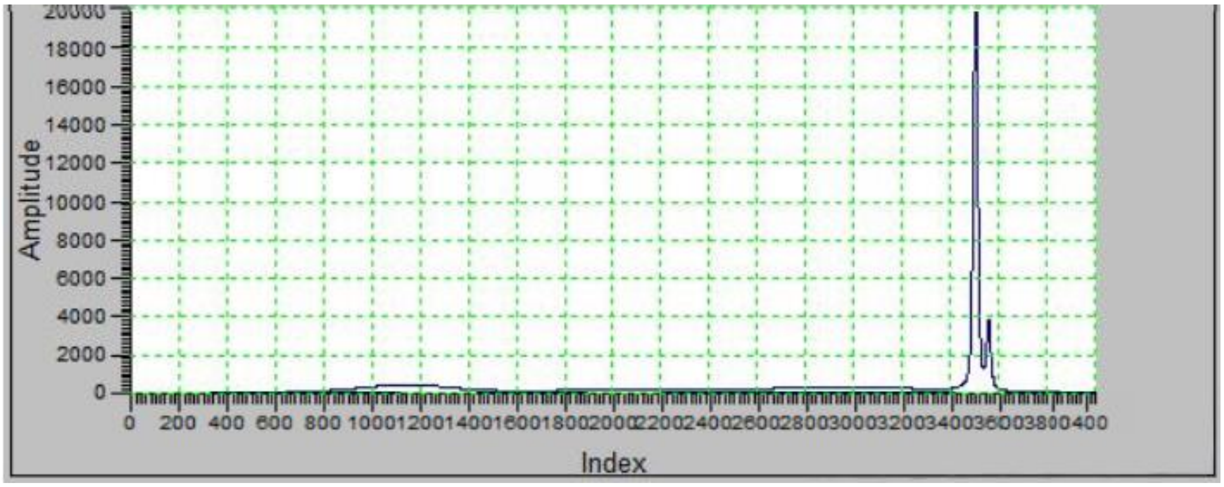

Figure 4.13: Amplitude vs index for ATS sensor in splice block, port A, 6 dB attenuation.

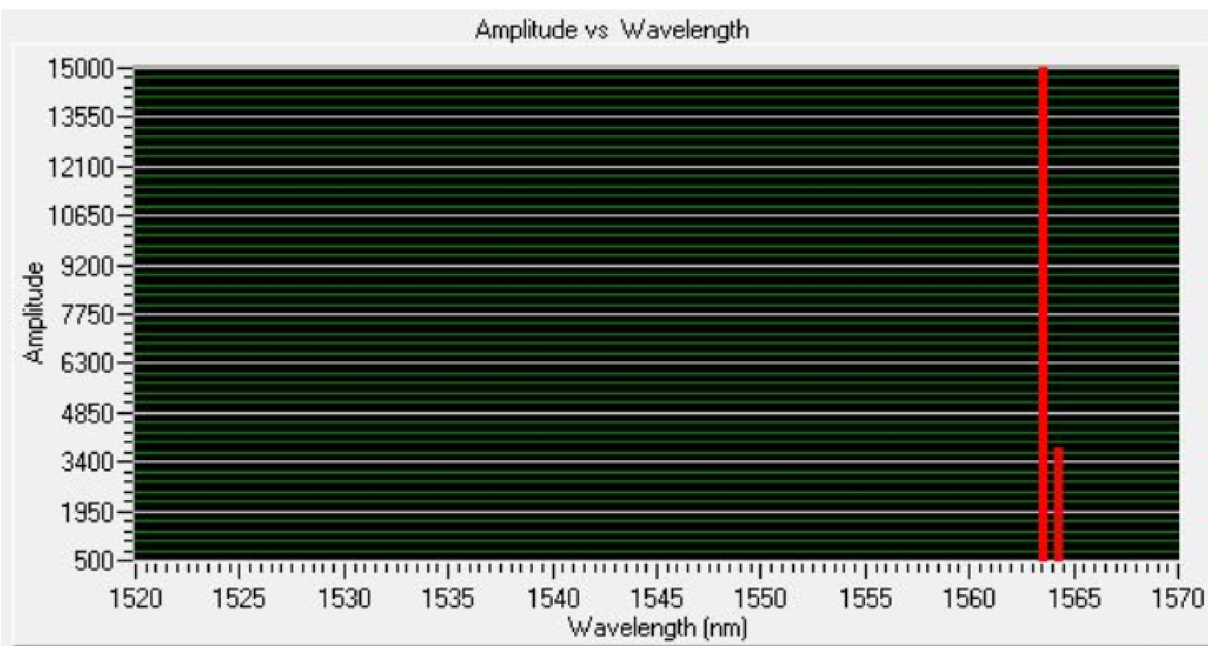

Figure 4.14: Amplitude vs wavelength for ATS sensor in splice block, port A, 6 dB attenuation.

Data extracted from RMS, in Table 4.4, for 2 dB attenuation gave no data, while 6 dB attenuation gave the reference wavelengths and amplitudes observed in Figure 4.14.

Table 4.4: Data extracted from RMS for the ATS sensor, with 6 dB attenuation.

Port	Attenuation	Ref. wavelength (left/right) [nm]	Ref. amplitude (left/right)	Recorded wavelength [nm]	Recorded amplitude
A	2 dB	No data	No data	No data	No data
A	6 dB	1563/1564	22246/3790	No data	No data

4.1.3. SIT

Simulations of a SIT was performed according to Weatherford's procedure. From the OTDR traces, actual attenuation was noted, for each element of the measurement system. The total attenuation over splices, connectors, and optical sensing elements was recorded and making up the first part of the optical budget for the measurement system. The total attenuation over the measurement system is presented in Table 4.5. With regards to the optical traces, no major attenuation or reflection was observed.

Table 4.5: Total attenuation over primary and backup measurement systems.

System	Total attenuation over system [dB]
Primary	2.091
Backup	1.453

Readings from RMS from the two PT gauges gave good readings for the primary gauge, but not for the backup gauge. The primary gauge read temperature and pressure from the workshop, and had good signal strength with a 2 dB attenuator added to Port A, Figure 4.15. The readings for the primary gauge are presented in Figure 4.16, showing a pressure of 0.70 bar and a temperature of 22.51 ^{o}C. To be able to read wavelengths off a PT gauge, a calibration file for the specific PT gauge had to be added to RMS software beforehand. When trying to read wavelengths off the backup PT gauge, no wavelengths could be recorded. The readings were outside the specified wavelength spectrum from the calibration file, indicating a calibration file error and not a functionality error. Thus, the calibration file had to be adjusted for which wavelengths the PT gauge was reading at.

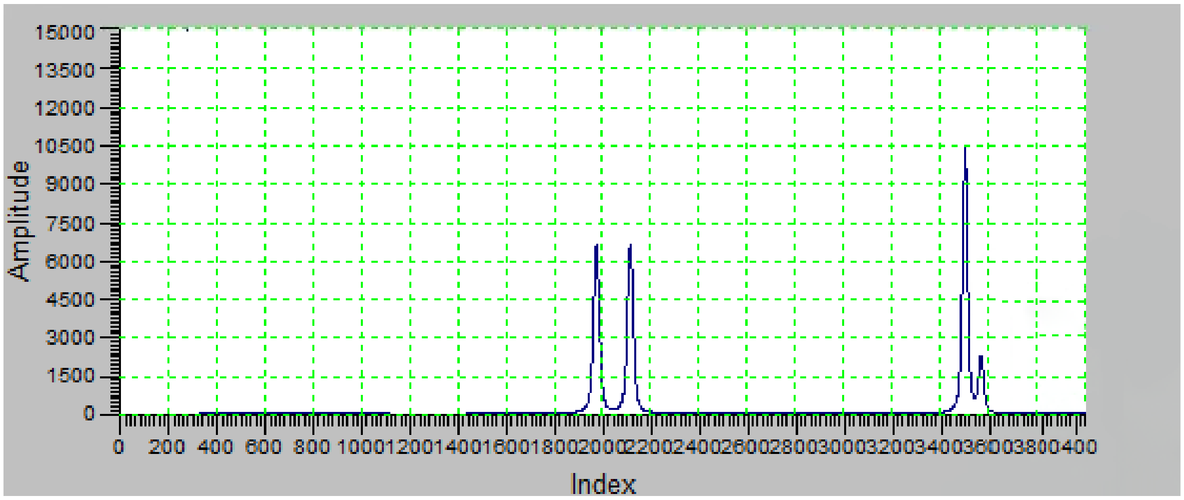

Figure 4.15: Amplitude vs. index for PT gauge in SIT.

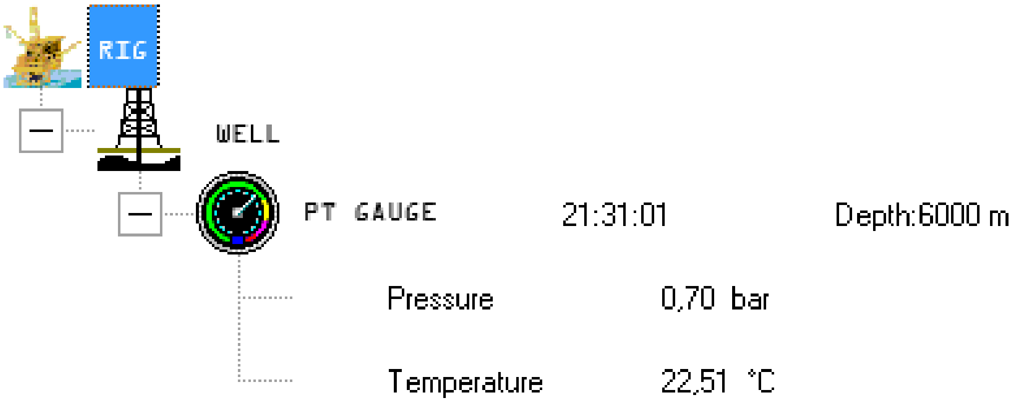

Figure 4.16: PT reading in RMS.

4.2. Discussion (in-house)

To carry out experiments on fiber optics, can be challenging on available equipment. An important factor to have in mind is also the length of the fiber optic cable. To best present a measurement system with a source, processing, conditioning, and presentation element, a similar setup to a i.e. completion measurement system is required. Thus, the challenging part when investigating attenuation and sensing elements individually, is to have enough length on the fiber optic cable and the right environment for measurements. The following section brings forth the in-house experiments, and the results obtained.

4.2.1. Splicing & SIT

When looking at the optical traces recorded in 3.1.1 and 3.1.3 shows the importance of an optical measurement system's integrity with regards to splices and connections. Fiber optic cables are fragile and easy to contaminate or damage if caution and experience are not applied. Sensing elements provide accurate measurements and are strongly dependent on the system integrity, to provide values of interest.

The splicing in 3.1.1 was performed by me and took a few attempts before obtaining the desired results. Carrying out poor preparation of the fiber ends was easy, both for cleaning and cutting the correct cleave angles. Using an old solvent for cleaning, or not cleaning the fibers enough, lead to the fusion splicer not accepting the fiber ends for splicing. Figure 4.17 below shows how the fusion splicer examines the fiber ends, with one clean end on the left-hand side and one dirty end on the right-hand side, not being accepted by the apparatus. Poor cleaning and handling of the cleaver lead to bad cleave angles, where the fusion splicer would not accept the fiber ends, providing a warning of a too high cleave angles leading to too much fiber optic loss.

Figure 4.17: Contaminated fiber end (left) aligned with clean fiber end (right).

After a few attempts, an approved splice was obtained on the SM1 fiber, according to Weatherford criteria and procedure, while the SM2 fiber had a bad cleave angle resulting in the desired bad splice. The SM1 fiber was prooftested with 85 kPsi and withstood the applied strain for 5 seconds. The prooftest is presented in Figure 4.18, holding both sides of the fiber splice. The 85 kPsi were applied to the splice when a leaver arm was freed, and a spring applied strain between the two holding points.

By looking at the attenuations for SM1 and SM2 fibers in Table 4.2, the good and the bad splice are emphasized. A splice of poor quality, with a high loss, results in less light through the splice. Thus, less optical energy will reach i.e. the gauge at the end, resulting in even less optical energy back to the receiver. A reflection or loss can propagate and does not necessarily have to be at the exact location of the splice itself.

It was difficult to manipulate the fusion splicer and provoke the bad splice, as there is a type of fail-safe system in the apparatus. The precision required for the fusion splicers to fuse two fiber ends together, as they are extremely sensitive and thorough, emphasizes the experience needed for such work.

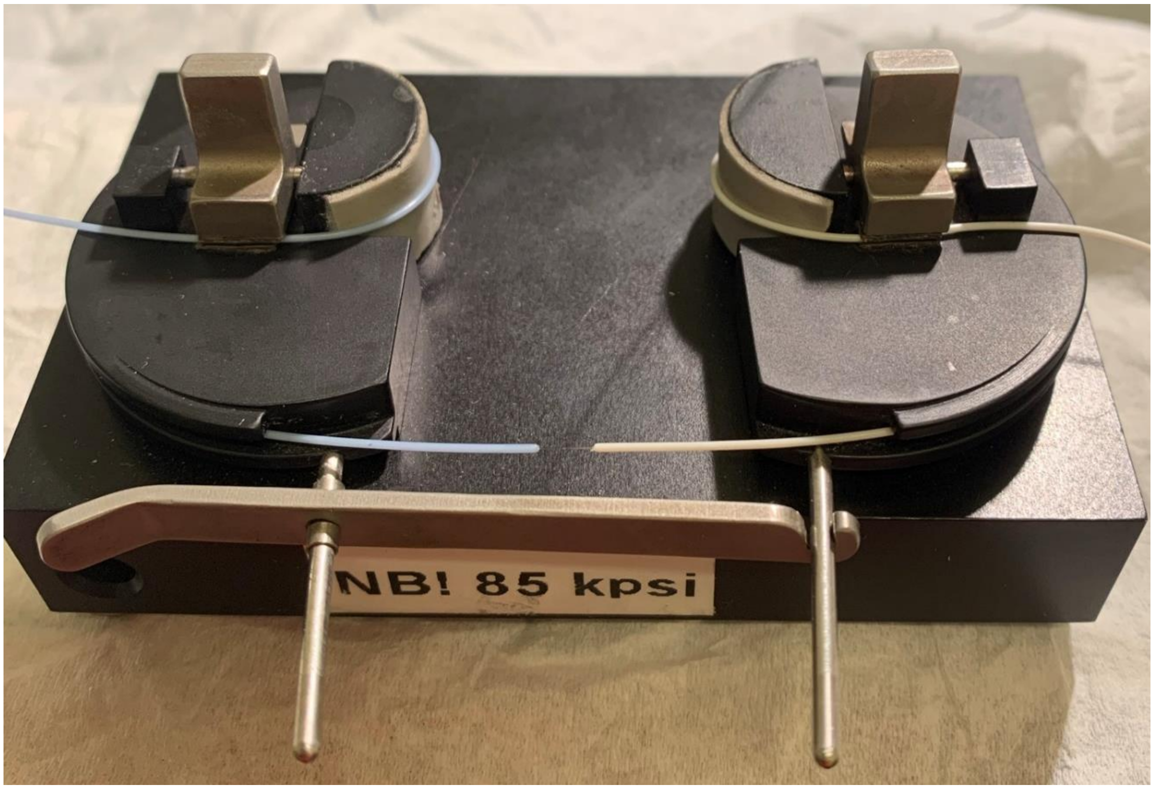

Figure 4.18: Prooftest of splice on SM1 fiber.

Imagine how this precise and sensitive work can be carried out on an offshore drilling platform, with the surrounding weather conditions and dirty surfaces. For controlling the humidity and temperature conditions, an over-pressured tent can be set up on the drill floor. This provides a controlled environment, and fewer surrounding conditions to hinder fusion splicing. Another factor to be kept in mind in offshore operations is the fact that you do not have several attempts on creating splices on the fibers. This is due to one end of the fiber being installed on the already installed downhole equipment, often several hundred or thousands of meters in the ground, and there is always a maximum length of fiber optic cable available for one installation. Thus, the planning and execution of installing fiber optics are crucial.

Going through the cleaning and cleaving processes is a time-consuming process itself. Everything happening on rig-time, meaning well operations are waiting to be carried out, generates pressure with regards to time spent on the fiber optic equipment. Operators have a time budget to maintain and preferably would not like to wait longer than necessary. Acknowledging the time it takes to prepare, splice, and implement fiber optics in downhole equipment, might look bad on a time critical budget, but the resulting data acquired speaks for itself. One could say it is a long-term investment in both time and equipment.

For the more critical work carried out in 3.1.3, a highly experienced workshop technician performed the fusion splices in the measurement systems. When equipment is to i.e. be used offshore, one does not want to perform poor work. Unnecessary splicing will lead to a waste of fiber lengths and is not optimal for readings or traces. Thus, I did not participate in the splicing. The pressure tests were performed by qualified personnel, and the rest of the SIT was carried out with supervision.

Encountering problems such as a calibration file error, cannot be fixed in a matter of minutes and needs addressing by personnel with the proper expertise. Thus, is an operational point of view, the time before mobilization would be a decisive factor for whether a new system would have to be set up and tested, or if the issue could be resolved in time. After the equipment has been installed in a well, the calibration of topside instrumentation can be carried out separately. A topside interrogation system is rarely planned for only one well, which means several connections on the surface will be made up when wells are drilled, and the completion installed. In this phase of the installation of the measurement system, calibration files can be updated, and the processing and presenting parameters adjusted.

4.2.2. ATS

The readings observed in RMS from the ATS sensor in the splice block, and the lack of temperature data obtained, it is quick to suspect that there was an issue with the ATS sensor. Although, with regards to the effect of strain on the ATS sensor, this was most likely not the issue for this case. Figure 4.11 contains two peaks as expected, the amplitude of the peaks appearing at the higher end is also a good indication of reflected wavelengths for this ATS sensor. When looking at Figure 4.12 there are neither wavelength nor reference bars, which is due to RMS not being able to record any data.

As the amplitude in Figure 4.11 was high, more attenuation was applied in case the missing data was due to blinding of the RIH box. When applying 6 dB attenuation, the signal strength went to zero for the ATS sensor peak while the reference peak remained at a high amplitude slightly shifted to the left on the index axis, Figure 4.13. RMS was recording the reference peaks, shown in the amplitude vs. wavelength plot in Figure 4.14. Data extracted from RMS verified that only reference peaks were recorded, Table 4.4.

When comparing the change in signal strength from 2 dB to 6 dB attenuation, in Figure 4.11 and Figure 4.13, the loss appeared to be very high and much higher than expected. A suspected reason for this could either be due to the attenuator being too strong, or that the connection between the RIH box and ATS sensor being too poor. From Table 2.1 the trending values below the black line indicate that the amount of transmitted light was close to zero for 6 dB attenuation. A new connection will have to be attempted to retrieve new data, with a 3-4 dB attenuator. By having a limited access to the ATS sensor in the splice block, as it was placed at a third party's workshop, no further investigation on this matter could be pursued at the time of this thesis.

4.3. Results from the field application

4.3.1. Johan Sverdrup

As previously mentioned, production numbers and results have yet to be released for Johan Sverdrup. What has been presented so far though, by Senior Reservoir Engineers in Equinor Håkon Sunde Bakka and Jonas Sørbel [31], is very high production and injection rates. Already 6 days after production starts when the third well was started up, they were producing at over 20 000 Sm^3/day, which was the largest producer on the NCS at the time. Although the field is a green field the production was stable at these high rates, with 75 000 Sm^3/day and 80 000 Sm^3/day for production and injection respectively. Thus, the injectivity was as good as the productivity [31].

An illustration of the stacked well production from November 2019 to July 2020 is presented in Figure 4.19 below. From November 2020 to March 2020 there was production from their 8 first pre-drilled production wells, and from there on a total of 11 wells are shown. The production cut in June 2020 was a government mandated cut because of the ongoing pandemic [31].

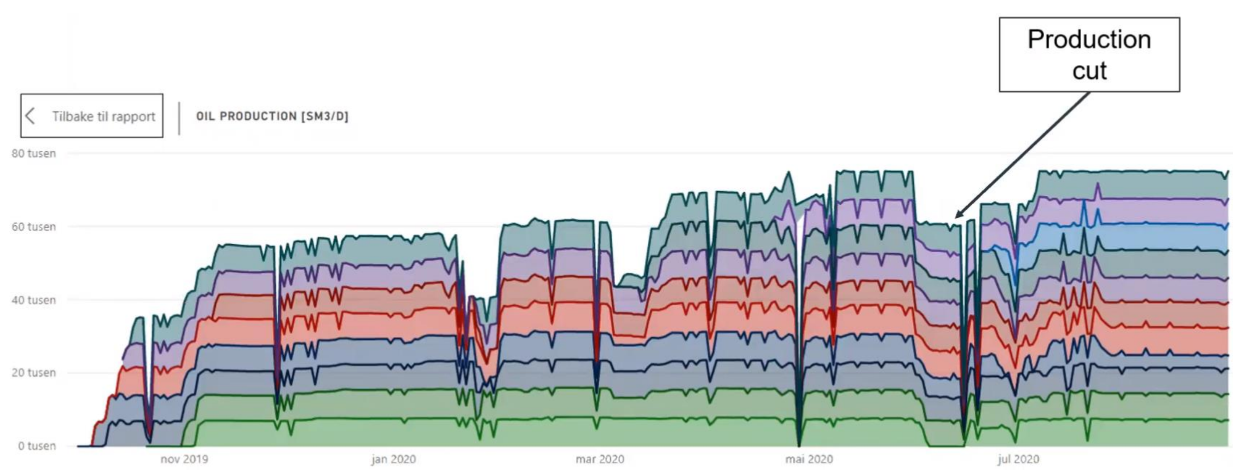

Figure 4.19: Stacked well production from Johan Sverdrup wells 2019-2020 [31].

The in-well fiber optics are placed from the surface to the top of the reservoirs along with the tubing, providing a sensing element of temperatures and acoustics along the wellbore. The interrogators on the surface which are connected to the downhole fibers are crucial for the processing of data from all wells with fiber optics. The major investments at Johan Sverdrup include fiber optics and the largest PRM system in the world. The long-term target, of the advanced monitoring system, is to be able to increase the lifetime of well components with less down-time due to failures and a reduction in operational costs. By being able to monitor the completion, especially the lower completion in the reservoir section, the performance of chosen well design can be understood and evaluated constantly. Thus, improvements can be made and implemented for i.e. the next placement of a well, or reservoir management [31].

Explicit examples of the utilization of DAS and DTS measurements presented by Håkon Sunde Bakka [31] was an observation of an unintentional gas lift, as production was ramped up on a production well, by DAS measurements showing noise where gas was flowing in through a valve. The DTS measurements, which are easier to interpret, showed fluid interfaces during displacement of brine with gas, by temperature changes at the interface [31].

The digitalization of the giant field has been said to have increased the profits by more than 2 billion NOK during its first year of production. The profits are due to automated production optimization and sustaining such high production rates, more accurate data and information on the reservoir, and efficiency in daily operations [31, 36, 40].

Lars Vinje – Equinor

With several licenses and partners included, official results and information has not yet been made available for the public eye. At a later time this year, there will be presented an official report on the Johan Sverdrup development and use of fiber optics, at the Society of Petroleum Engineers Offshore Conference 2021. Although, one of the engineers working towards the reservoir monitoring projects in Equinor, has shared some feedback from the Johan Sverdrup installations [60].

"One of the major contributions of the Johan Sverdrup installations has been the data streaming solution of DAS, which has been shared on a collaboration platform called Github. The streaming solution makes it possible to stream several interrogators in parallel, and it works. Suppliers can pick frequency band energy data from Github and use it as desired. There is a large number of signals received by these measurements, and the challenge is to set a value to such information.

Potential for the technology could i.e. be to replace the conventional production logging tools (PLT), but a verification of this solution is still needed. It would require a fiber optic cable installed in the reservoir section, which is a technical challenge, and also an expensive one. To be able to evaluate such a valuable element for technology, all factors need to be taken into account and opposed to how many times it is believed that PLT will be run in a well. If one could say that fiber optic measurements could replace PLT, one could also give this a value. When it comes to well integrity, the fiber optics undoubtedly provide very good observations on changes along the wellbore. Although, setting a value to the information can be challenging." [60].

4.3.2. PRM

For PRM systems the quality and precision of the received data is a major factor for mapping reservoirs and the subsurface. In the Jubarte field in Brazil with the first deep-water optical PRM system, Petrobas and PGS [47] were able to validate the accuracy of the optical PRM system to be less than 3 %, in detecting very small 4D elastic changes in the reservoir. For the heterogeneous reservoir it was crucial to have a PRM system that gathered data with high quality and high signal-to-noise ratio. For the 4D Bayesian Inversion geological model the result was high quality images using fiber optic technology, where the model was updated with an improved flow pattern understanding. The system could deliver information from areas where well control was limited, and link together the subsurface disciplines for field production statistics [47].

Equinor operated fields Johan Castberg and Johan Sverdrup are great investments on the NCS for using fiber optic technology as one of the methods for improving hydrocarbon recovery. The investments include optical PRM systems for having high quality images of the reservoirs, leading to a better understanding of the changes taking place in the sub surface. Real-time measurements provide more frequent updates for reservoir models, which are helpful in decisions needed to be made. By implementing this technology Equinor can set an ambition for high recoveries, because the measures for enhanced oil recovery are present before wells and templates are placed, and production has started [50].

4.3.3. Well Monitoring

For monitoring wells by in-well PRM, the results from Johan Sverdrup mentioned in Chapter 4.3.1 have not been published yet. The in-well monitoring with DAS and DTS provide valuable information on production and injection rates. Together with the ICD screens and zone division in the reservoir, reservoir changes around individual wells can be observed [31].

The amount of fluids passing through valves can be determined with continuous DAS measurements, but by using DAS and DTS data together, fluid phase profiling of 2- and 3-phase flow could be established, as proved by Bukhamsin and Horne [53]. During displacement of fluids DTS can give real-time data of fluid fronts as they move, which was has been used in an injector at Johan Sverdrup and for SAGD wells in Venezuela [31, 58].

Fiber optic measurement systems can be used in many of the phases in the lifetime of well. Well integrity, which is an important factor for making sure formation fluids are not released to the surroundings of a reservoir, DAS and DTS measurements proved to be useful for the harsh environment present by Raab et. al [55], during cementing of a geothermal well. Cementing is also done for production and injection wells within petroleum. Hence, fiber optics could be an option for monitoring well-integrity in such wells. As in-well fiber optics provide real-time data along the entire wellbore, the changes can be observed continuously. Although, one of the challenges with real-time data mentioned by Lars Vinje [60], is to interpret the enormous amounts and give the unknowns a value [55, 60].

5. Conclusion

There are many fields of application for fiber optic measuring systems, especially within reservoir monitoring. Sensing elements in the form of point sensors or distributed sensing with the entire fiber optic cable as the sensing element, can be implemented in wellbores from the reservoir section and up to the surface. Fiber optic PT gauges has been used in wellbores for many years and can be implemented in a well completion design. The more advanced optical measurement system would be the distributed sensing, DAS and DTS. With the amount of data gathered from a single well installed with a fiber optic cable, the required capacity for the receiving and processing element is very high. What has been done at the Johan Sverdrup field with DAS and DTS measurements and streaming several interrogators simultaneously, has been a great success. Although, it is important to bring forth the challenge of giving the great amount of data a value for all scenarios. With time and experience from this type of application, the resulting value of continuous real-time data from the reservoir and wells will be beneficial in active reservoir management and automated processes in hydrocarbon production [12, 31, 60].

Advantages of fiber optic sensors are their ability to endure the harsh environments encountered in oil and gas reservoirs, with high pressures, temperatures, and flow rates. With flexibility in solutions of implementation, and great reliability of the measurements systems, risks and costs are reduced throughout the lifetime of a well. The possibilities of gathering information during drilling and completion operations, and during well intervention, provide great advantages to the decisions to be made in time-critical processes. For PRM fiber optic measurement systems are the optimal choice [35, 57].

Challenges to keep in mind is the sensitivity of the fragile optical fibers during installation. Great care and expertise during splicing and installation in general is important, as well as the fiber optic cable needs the proper protection during RIH and throughout the lifetime of the well. This highlights the importance of proper equipment housing the optical sensing elements. The longer a fiber optic cable is, the more attenuation will be present. Thus, the optical budget is limited, and optical couplers and splices cannot have to high losses.

References

1. Ficocelli, P., et al. *Accuracy and Reliability of a New-Generation Optical PT Gauge in a SAGD Field Trial*. in *SPE Canada Heavy Oil Technical Conference*. 2016.
2. Kragas, T.K., B.A. Williams, and G.A. Myers. *The Optic Oil Field: Deployment and Application of Permanent In-well Fiber Optic Sensing Systems for Production and Reservoir Monitoring*. in *SPE Annual Technical Conference and Exhibition*. 2001.
3. Directorate, N.P. *Plenty of oil and gas left on the Norwegian shelf*. 2021 19.02.2021; Available from: https://www.npd.no/en/facts/news/general-news/2021/plenty-of-oil-and-gas-left-on-the-norwegian-shelf/.
4. Directorate, N.P., *Resource Report Discoveries and Fields 2019*. 2019, Norwegian Petroleum Directorate.
5. Bentley, J.P., *Principles of measurement systems*. 4th ed. ed. 2005, Harlow: Pearson/Prentice Hall.
6. Kverme, S.T., *An investigation of alkaline flooding and comparison to Smart Water injection*. 2018, University of Stavanger.
7. Günther Mahlke, P.G., *Fiber Optic Cables*. 1987: Siemens Aktiengesellschaft, Berlin and München; John Wiley & Sons Ltd.
8. Hecht, J., *City of Light : The Story of Fiber Optics*. 1999, New York, UNITED STATES: Oxford University Press, Incorporated.
9. Serway, R.A., J.W. Jewett, and V. Peroomian, *Physics for scientists and engineers*. 9th ed., International ed. ed. 2014, S.l.: Brooks/Cole, Cengage learning.
10. Times, T.E. *Definition of 'Electromagnetic Waves'*. 2021 13.02.2021 13.02.2021]; Available from: https://economictimes.indiatimes.com/definition/electromagnetic-waves#:~:text=Definition%3A%20Electromagnetic%20waves%20or%20EM,oscillating%20magnetic%20and%20electric%20fields.&text=They%20are%20also%20perpendicular%20to%20the%20direction%20of%20the%20EM%20wave.
11. Britannica, E., *Electromagnetic waves*. 2021.
12. Weatherford, *Lecture notes*. 2021.
13. Inc., F. *Total Internal Reflection*. n.d.; Available from: https://www.fiberlabs.com/glossary/total-internal-reflection/.

14. Dragic, P.D., M. Cavillon, and J. Ballato, *Materials for optical fiber lasers: A review*. Applied Physics Reviews, 2018. **5**(4): p. 041301.

15. Viva. *Difference Between Step Index Fiber And Graded Index Fiber (With Comparison Chart)*. 2019 2020 16.03.2021]; Available from: https://vivadifferences.com/difference-between-step-index-fiber-and-graded-index-fiber/.

16. Bunge, C.-A., M. Beckers, and T. Gries, *Polymer Optical Fibres : Fibre Types, Materials, Fabrication, Characterisation and Applications*. 2016, Cambridge, UNITED KINGDOM: Elsevier Science & Technology.

17. Bjorlykke, K., *Petroleum Geoscience: From Sedimentary Environments to Rock Physics*. 2010, Berlin, Heidelberg: Berlin, Heidelberg: Springer Berlin / Heidelberg.

18. Mark Curran, B.S. *Basics of Fiber Optics*. 2019.

19. Krohn, D.A., T. MacDougall, and A. Mendez, *Fiber optic sensors: fundamentals and applications*. 2014: Spie Press Bellingham, WA.

20. Culshaw, B. and A. Kersey, *Fiber-Optic Sensing: A Historical Perspective.* Journal of lightwave technology, 2008. **26**(9): p. 1064-1078.

21. Fang, Z., et al., *Fundamentals of Optical Fiber Sensors*. 2012, New York, UNITED STATES: John Wiley & Sons, Incorporated.

22. Balkanski, M., *SEMICONDUCTOR PHYSICS | Light Scattering*, in *Encyclopedia of Modern Optics*, R.D. Guenther, Editor. 2005, Elsevier: Oxford. p. 460-465.

23. Nave, C.R. *HyperPhysics*. 2017 2017; Available from: http://hyperphysics.phy-astr.gsu.edu/hbase/atmos/blusky.html.

24. Jacob, L.J. and H.-P. Deigner, *Chapter 10 - Nanoparticles and Nanosized Structures in Diagnostics and Therapy*, in *Precision Medicine*, H.-P. Deigner and M. Kohl, Editors. 2018, Academic Press. p. 229-252.

25. Lohumi, S., et al., *Raman imaging from microscopy to macroscopy: Quality and safety control of biological materials.* TrAC Trends in Analytical Chemistry, 2017. **93**.

26. Kersey, A.D., J.R. Dunphy, and A.D. Hay. *Optical Reservoir Instrumentation System*. in *Offshore Technology Conference*. 1998.

27. Jderu, A., et al., *Liquid Flow Meter by Fiber-Optic Sensing of Heat Propagation.* Sensors (Basel, Switzerland), 2021. **21**(2).

28. Lipták, B. *The Incredible Fiber-Optic Flowmeter*. 2014 02.05.2014; Available from: https://www.controlglobal.com/articles/2014/the-incredible-fiber-optic-flowmeter/.
29. Arnaout, I., et al. *Optimizing Production in Maximum Reservoir Contact Wells with Intelligent Completions and Optical Downhole Flowmeters*. in *Abu Dhabi International Petroleum Exhibition and Conference*. 2008.
30. Silixa.com, W.i.d.s.n.d. *What is distributed sensing?* n.d. * 21.04.2021]; Available from: https://silixa.com/resources/what-is-distributed-sensing/.
31. Veraas, T.J., *Johan Sverdrup - An excellent first year*, J.S. Håkon Sunde Bakka, Editor. 2021, Tor Jørgen Veraas: SPE Stavanger Section.
32. Meng, Z., et al., *Recent Progress in Fiber-Optic Hydrophones.* Photonic Sensors, 2021. **11**(1): p. 109-122.
33. Weatherford. *Weatherford*. 2021; Available from: https://www.weatherford.com/en/.
34. Larsen, P.F., et al. *Johan Sverdrup: The Digital Flagship*. in *Offshore Technology Conference*. 2020.
35. Langhammer, J., et al. *Fiber-Optic Sensing is the Technology of Choice for Permanent Reservoir Monitoring Applications*. in *Offshore Technology Conference*. 2013.
36. Equinor. *Digital technologies boosted earnings by over two billion NOK in the first year at Johan Sverdrup*. 2020 05.10.2020 19.01.2021]; Available from: https://www.equinor.com/en/news/20201005-johan-sverdrup-first-year.html.
37. NPD, F. *Utsira FM, Nordland Group, Johan Sverdrup Field*. 2021 18.01.2021 18.01.2021]; Available from: https://factpages.npd.no/en/strat/pageview/litho/formations/183, https://factpages.npd.no/en/strat/pageview/litho/groups/113, https://factpages.npd.no/no/field/pageview/producing/26376286, https://www.norskpetroleum.no/en/facts/field/johan-sverdrup/.
38. Feder, J., *Recovering More Than 70% From the Johan Sverdrup Field.* Journal of Petroleum Technology, 2020. **72**(09): p. 62-63.
39. Meling, T.S., et al. *Johan Sverdrup: Lessons-Learned from the Field-Development of a North Sea Giant*. in *Offshore Technology Conference*. 2020.
40. Equinor. *Johan Sverdrup - What we do*. 2020 26.01.2021]; What we do - page]. Available from: https://www.equinor.com/en/what-we-do/johan-sverdrup.html.

41. Olsen, H., N.A. Briedis, and D. Renshaw, *Sedimentological analysis and reservoir characterization of a multi-darcy, billion barrel oil field – The Upper Jurassic shallow marine sandstones of the Johan Sverdrup field, North Sea, Norway.* Marine and Petroleum Geology, 2017. **84**: p. 102-134.
42. Devold, H., T. Graven, and S.O. Halvorsrød. *Digitalization of Oil and Gas Facilities Reduce Cost and Improve Maintenance Operations*. in *Offshore Technology Conference*. 2017.
43. Weatherford International, I.H. *Weatherford International, Inc. History*. n.d.; Available from: http://www.fundinguniverse.com/company-histories/weatherford-international-inc-history/.
44. Bloomberg. *EVI Completes Weatherford Merger*. 1998 27.05.1998; Available from: https://www.bloomberg.com/press-releases/1998-05-27/evi-completes-weatherford-merger.
45. Rao, V. and R. Knight, *Chapter 1 - Background*, in *Sustainable Shale Oil and Gas*, V. Rao and R. Knight, Editors. 2017, Elsevier. p. 1-7.
46. Fleming, N., M. Karunakaran, and S. Hireche, *Qualification and Implementation of Oil-Based Mud as a Cost-Effective and Low-Damaging Perforation Fluid for High-Pressure/High-Temperature Fields: Gudrun Case History.* SPE Production & Operations, 2018. **34**(03): p. 429-445.
47. Yermek Balabekov, M.S., Ruan Couto, Paula Dariva, Wilson Lisboa, Cyrille Reiser, Paulo Johann, *Permanent Reservoir Monitoring - 4D Quantitative Interpretation*, in *15th International Congress of the Brazilian Geophysical Society*. 2017: Rio de Janeiro, Brazil.
48. Bertrand, A., et al., *Ekofisk PRM Seismic Operations*, in *Second EAGE Workshop on Permanent Reservoir Monitoring 2013 - Current and Future Trends*. 2013, EAGE Publications BV, Netherlands: Stavanger, Norway.
49. Castberg, C.f.i.r.a.J. *Contract for improved recovery at Johan Castberg*. 2018 24.08.2018; Available from: https://www.equinor.com/en/news/23aug-contract-for-improved-recovery-at-johan-castberg.html.

50. field, P.h.t.i.r.f.t.J.C. *PRM helping to improve recovery from the Johan Castberg field*. 2018 24.08.2018; Available from: https://energyindustryreview.com/oil-gas/prm-helping-to-improve-recovery-from-the-johan-castberg-field/.
51. Fayemendy, C., et al. *Designing a Permanent Reservoir Monitoring system for the Johan Sverdrup field*. in *2017 SEG International Exposition and Annual Meeting*. 2017.
52. change, C.e. *Collaboration equals change*. n.d. n.d.; Available from: https://www.loop.equinor.com/en/stories/digital-subsurface.html.
53. Bukhamsin, A. and R. Horne. *Cointerpretation of Distributed Acoustic and Temperature Sensing for Improved Smart Well Inflow Profiling*. in *SPE Western Regional Meeting*. 2016.
54. NORSOK, *Well integrity in drilling and well operations*. 2004, Standard Norge.
55. Raab, T., et al., *Real-Time Well-Integrity Monitoring Using Fiber-Optic Distributed Acoustic Sensing.* SPE Journal, 2019. **24**(05): p. 1997-2009.
56. Schlumberger, *The Schlumberger Oilfield Glossary*, in *Oilfield Glossary*, Schlumberger, Editor. 2021.
57. Ramondenc, P., *Coiled Tubing Real-Time Monitoring: A New Era of Well Intervention & Workover Optimization*, in *SPE France Section*. 2020: TechnipFMC, tour Adria – La Défense.
58. Saputelli, L., et al., *Monitoring Steamflood Performance through Fiber Optic Temperature Sensing.* SPE Reprint Series, 1998. **SPE 49184**.
59. Martinez, A., M. Useche, and R. Guerra. *Use of Fiber Optic Acoustics to Improve Drilling Efficiency and Well Placement*. in *Offshore Technology Conference*. 2020.
60. Vinje, L., *Fiber Optics in reservoir monitoring*, S.T. Kverme, Editor. 2021.
61. Khalifeh, M. and A. Saasen, *General Principles of Well Barriers*. 2020. p. 11-69.
62. Bellarby, J., *Well Completion Design*. 2009, Oxford, NETHERLANDS, THE: Elsevier Science & Technology.
63. Olav Skjæveland, *Well Barrier Schematic*, Siren T. Kverme, Editor. 2020.

Appendices

Elements in a well's construction and the main aspects within a well's completion is presented here. The data collected from RMS for the in-house splicing and ATS experiments are presented in tables.

I. The Well

a. Construction and barriers

Before oil or gas can be produced from a reservoir, a well is drilled and constructed in several sections. During these processes well integrity is crucial for well control, when creating a pathway to the subsurface where pressures and temperatures are higher than at the surface. Well integrity is defined by the Norsok Standard D-010[54] as "the application of technical, operational and organizational solutions to reduce the risk of uncontrolled release of formation fluids throughout the entire life cycle of the well and of course safety aspects". For maintaining well control, there are five main barriers in a well. These include casing, cement, completion, wellhead, and Christmas tree [54].

Firstly, the wellbore is drilled, and the is casing placed inside. As one gets further down towards the reservoir, the dimensions of the casing decrease. When the final casing size has been set in place, cement is pumped down through the steel pipes, and up between casing and wellbore. The cement keeps everything in place, and functions as a protection for the surroundings of the well, i.e. groundwater, oil, or gas. Throughout this construction the well must go through pressure and integrity tests, to make sure everything functions as it is supposed to. Such tests are also performed in intervals during the lifetime of the well [54, 61].

Figure 0.1 received from Completion Engineer in Equinor, Olav Skjæveland, shows a schematic of a well barrier system consisting of primary (blue) and secondary (red) elements in a well, along with the dimensions and completion components. Well barrier element criteria vary with operating companies but has one general rule "at least two tested independent barriers between hydrocarbons in the reservoir and the environment at all times." [62]. The primary barrier elements prevent hydrocarbons from escaping, and the secondary elements are backup in case primary elements fail [54, 61-63].

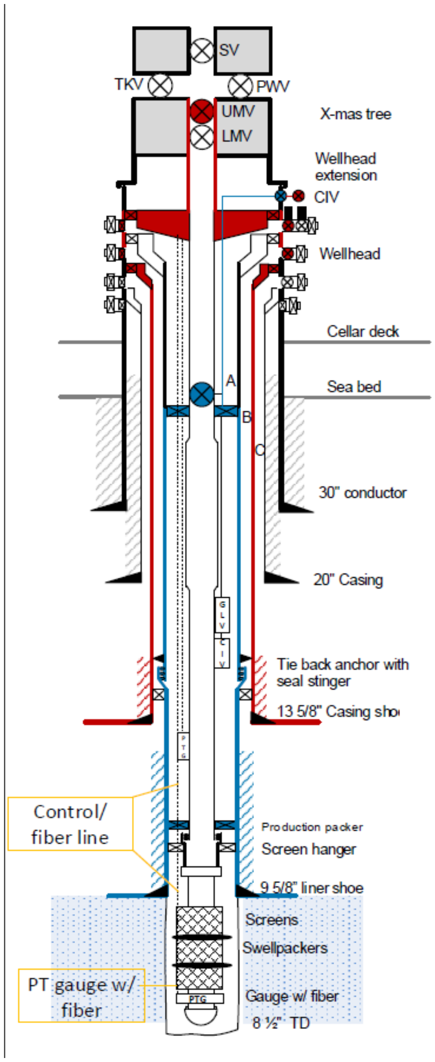

Figure 0.1: Well Barrier Schematic with primary (blue) and secondary (red) barrier elements [63].

b. Completion

Whether a well is a producer or injector, in an open or cased hole, the completion is a barrier separating the reservoir from the surface production. Completion in a drilling context is defined by The Schlumberger Oilfield Glossary [56] as “the hardware used to optimize the production of hydrocarbons from the well”. It can include filtering elements, packers, and measurement systems, which are present to improve production efficiency, safety, and economics. Measurements systems designed for production optimization and do not require human intervention are known as intelligent completions [56].

Designing a well takes hands-on experience, and the completion segment has many essentials elements with regards to safety, efficiency, and cost. A major aspect is the effect the oil and gas industry have on the environment. When the planning, designing, and operational phases of completion are well accomplished, it can protect our environment in many ways. A very important issue of today’s society is for instance how much energy is consumed, and how large emissions are when hydrocarbons are produced. With regards to cost and production of waste materials, completions can achieve good control of water or gas production. Besides this, a well completion can also be designed to reinject gas, water, and other fluids. In other words, a completion is important throughout a well’s lifetime [62].

Completions can be divided into a reservoir or lower completion which is where i.e. sand control screens are placed, and an upper completion containing i.e. a production packer, downhole-safety valves, wellhead, and Christmas tree. The reservoir section is the interface between the wellbore and reservoir rock and can be an open hole or a cased hole completion. The upper completion is the last section of the wellbore before production or injection can start and can consist of elements providing well control and monitoring of flow [62].

The production packer is one of the primary well barrier elements and can be installed with different completion elements i.e. as a screen hanger or dividing zones in a lower completion, but mainly it is for “isolating the annulus and anchor or secure the bottom of the production tubing string” [56].

Another primary well barrier element and one of the most important elements is the downhole safety valve. Its function is to isolate the pressure and fluids in a well in emergencies where there is a loss of well control or failure of surface equipment. To install a downhole safety valve is mostly a legislative requirement for wells today [33, 56].

The wellhead in a completion is the termination of the completion string to the surface. As defined by Khalifeh and Saasen [61] "primary functions of the surface wellhead include pressure isolation, pressure containment, casing and tubing weight suspension, and the Christmas tree housing.". As a pressure-containing element, wellhead outlets are critical with regards to safety and well integrity. A wellhead outlet is where the control lines are fed through, i.e. hydraulic lines or fiber optic cables, safely exiting from the well [2, 56, 61].

On top of the wellhead system, there is "a controllable interface between the well and production facility" [61] called the Christmas tree. The flow of reservoir fluids is controlled through the Christmas tree, and intervention on downhole equipment would also be accessible through it. Figure 0.1 shows the Christmas tree as one of the secondary well barrier elements at the very top of the well [61].

II. Experimental Data

a. Port A

Table 0.1: RMS data for Port A from in-house splice of SM1 fiber.

DATE	TIME	P REF WL	P REF AMP	P WL	P AMP	T WL	T AMP	T REF WL	T REF AMP
2021-04-13	17:13:41.623	156347435	10900	153435187	20275	153577450	12207	156418743	2361
2021-04-13	17:13:41.783	156347425	10901	153435173	20283	153577446	12216	156418775	2365
2021-04-13	17:13:41.943	156347425	10901	153435173	20283	153577446	12216	156418775	2365
2021-04-13	17:13:42.104	156347435	10891	153435180	20272	153577457	12209	156418760	2359
2021-04-13	17:13:42.264	156347435	10901	153435177	20270	153577455	12207	156418767	2361
2021-04-13	17:13:42.426	156347435	10901	153435177	20270	153577455	12207	156418767	2361
2021-04-13	17:13:42.586	156347435	10910	153435163	20280	153577424	12220	156418768	2365
2021-04-13	17:13:42.746	156347425	10895	153435180	20263	153577455	12211	156418772	2358
2021-04-13	17:13:42.906	156347435	10907	153435155	20276	153577456	12216	156418798	2366
2021-04-13	17:13:43.066	156347435	10907	153435155	20276	153577456	12216	156418798	2366
2021-04-13	17:13:43.226	156347435	10895	153435192	20272	153577469	12215	156418767	2361
2021-04-13	17:13:43.386	156347435	10900	153435162	20273	153577451	12215	156418791	2360
2021-04-13	17:13:43.547	156347435	10900	153435162	20273	153577451	12215	156418791	2360
2021-04-13	17:13:43.707	156347435	10892	153435161	20282	153577428	12217	156418761	2365
2021-04-13	17:13:43.868	156347435	10904	153435166	20270	153577451	12209	156418770	2361
2021-04-13	17:13:44.028	156347435	10903	153435160	20277	153577448	12213	156418770	2362
2021-04-13	17:13:44.188	156347435	10903	153435160	20277	153577448	12213	156418770	2362
2021-04-13	17:13:44.348	156347435	10900	153435171	20272	153577461	12212	156418809	2365

2021-04-13	17:13:44.508	*156347435*	*10903*	153435170	20266	153577451	12207	*156418796*	*2362*
2021-04-13	17:13:44.669	*156347435*	*10903*	153435170	20266	153577451	12207	*156418796*	*2362*
2021-04-13	17:13:44.830	*156347435*	*10907*	153435164	20271	153577456	12209	*156418807*	*2361*
2021-04-13	17:13:44.990	*156347435*	*10902*	153435171	20284	153577464	12218	*156418770*	*2366*
2021-04-13	17:13:45.150	*156347435*	*10898*	153435190	20273	153577452	12209	*156418780*	*2359*
2021-04-13	17:13:45.310	*156347435*	*10898*	153435190	20273	153577452	12209	*156418780*	*2359*
2021-04-13	17:13:45.470	*156347435*	*10896*	153435175	20266	153577441	12208	*156418789*	*2360*
2021-04-13	17:13:45.630	*156347435*	*10903*	153435173	20276	153577434	12212	*156418734*	*2365*
2021-04-13	17:13:45.790	*156347435*	*10903*	153435173	20276	153577434	12212	*156418734*	*2365*
2021-04-13	17:13:45.950	*156347435*	*10898*	153435182	20270	153577452	12213	*156418751*	*2361*
2021-04-13	17:13:46.110	*156347435*	*10904*	153435161	20277	153577432	12216	*156418792*	*2366*
2021-04-13	17:13:46.270	*156347435*	*10898*	153435171	20279	153577458	12214	*156418757*	*2361*
2021-04-13	17:13:46.431	*156347435*	*10898*	153435171	20279	153577458	12214	*156418757*	*2361*
2021-04-13	17:13:46.591	*156347435*	*10905*	153435166	20269	153577453	12207	*156418798*	*2361*
2021-04-13	17:13:46.751	*156347435*	*10901*	153435145	20273	153577466	12209	*156418804*	*2367*
2021-04-13	17:13:46.912	*156347435*	*10901*	153435145	20273	153577466	12209	*156418804*	*2367*
2021-04-13	17:13:47.072	*156347435*	*10897*	153435168	20268	153577461	12207	*156418801*	*2361*
2021-04-13	17:13:47.232	*156347435*	*10907*	153435157	20272	153577443	12206	*156418782*	*2362*
2021-04-13	17:13:47.392	*156347435*	*10906*	153435166	20280	153577430	12212	*156418780*	*2366*
2021-04-13	17:13:47.552	*156347435*	*10906*	153435166	20280	153577430	12212	*156418780*	*2366*
2021-04-13	17:13:47.712	*156347435*	*10896*	153435161	20277	153577437	12211	*156418760*	*2361*
2021-04-13	17:13:47.872	*156347435*	*10903*	153435168	20267	153577428	12208	*156418771*	*2362*
2021-04-13	17:13:48.032	*156347435*	*10903*	153435168	20267	153577428	12208	*156418771*	*2362*

2021-04-13	17:13:48.192	*156347435*	*10910*	153435165	20258	153577455	12206	*156418763*	*2366*
2021-04-13	17:13:48.352	*156347435*	*10903*	153435162	20261	153577438	12210	*156418784*	*2360*
2021-04-13	17:13:48.512	*156347435*	*10901*	153435162	20277	153577437	12216	*156418767*	*2366*
2021-04-13	17:13:48.672	*156347435*	*10901*	153435162	20277	153577437	12216	*156418767*	*2366*
2021-04-13	17:13:48.832	*156347435*	*10889*	153435163	20270	153577442	12213	*156418775*	*2360*
2021-04-13	17:13:48.992	*156347445*	*10902*	153435170	20276	153577458	12209	*156418790*	*2361*
2021-04-13	17:13:49.152	*156347445*	*10902*	153435170	20276	153577458	12209	*156418790*	*2361*
2021-04-13	17:13:49.312	*156347445*	*10904*	153435183	20277	153577464	12216	*156418803*	*2367*
2021-04-13	17:13:49.472	*156347445*	*10893*	153435173	20272	153577450	12215	*156418784*	*2361*
2021-04-13	17:13:49.632	*156347435*	*10902*	153435153	20271	153577426	12209	*156418755*	*2361*
2021-04-13	17:13:49.792	*156347435*	*10902*	153435153	20271	153577426	12209	*156418755*	*2361*
2021-04-13	17:13:49.953	*156347445*	*10904*	153435167	20275	153577451	12214	*156418784*	*2367*
2021-04-13	17:13:50.113	*156347445*	*10901*	153435153	20257	153577419	12206	*156418757*	*2362*
2021-04-13	17:13:50.273	*156347445*	*10901*	153435153	20257	153577419	12206	*156418757*	*2362*
2021-04-13	17:13:50.433	*156347445*	*10909*	153435182	20267	153577468	12217	*156418831*	*2365*
2021-04-13	17:13:50.593	*156347445*	*10897*	153435165	20265	153577462	12207	*156418805*	*2361*
2021-04-13	17:13:50.753	*156347445*	*10904*	153435161	20272	153577442	12207	*156418785*	*2361*
2021-04-13	17:13:50.913	*156347445*	*10904*	153435161	20272	153577442	12207	*156418785*	*2361*
2021-04-13	17:13:51.073	*156347445*	*10908*	153435182	20272	153577459	12216	*156418791*	*2366*
2021-04-13	17:13:51.234	*156347445*	*10893*	153435169	20277	153577445	12213	*156418788*	*2359*
2021-04-13	17:13:51.394	*156347445*	*10893*	153435169	20277	153577445	12213	*156418788*	*2359*
2021-04-13	17:13:51.554	*156347445*	*10898*	153435153	20268	153577427	12211	*156418803*	*2362*
2021-04-13	17:13:51.714	*156347445*	*10898*	153435164	20286	153577445	12219	*156418771*	*2364*

2021-04-13	17:13:51.874	*156347455*	*10908*	153435163	20259	153577441	12209	*156418771*	*2362*
2021-04-13	17:13:52.034	*156347455*	*10908*	153435163	20259	153577441	12209	*156418771*	*2362*
2021-04-13	17:13:52.194	*156347455*	*10905*	153435155	20262	153577430	12205	*156418776*	*2361*
2021-04-13	17:13:52.354	*156347445*	*10906*	153435134	20272	153577417	12211	*156418768*	*2367*
2021-04-13	17:13:52.514	*156347445*	*10906*	153435134	20272	153577417	12211	*156418768*	*2367*
2021-04-13	17:13:52.674	*156347445*	*10907*	153435159	20272	153577426	12208	*156418791*	*2362*
2021-04-13	17:13:52.834	*156347445*	*10910*	153435153	20274	153577434	12214	*156418770*	*2367*
2021-04-13	17:13:52.994	*156347445*	*10891*	153435165	20270	153577446	12208	*156418777*	*2360*
2021-04-13	17:13:53.154	*156347445*	*10891*	153435165	20270	153577446	12208	*156418777*	*2360*
2021-04-13	17:13:53.314	*156347445*	*10903*	153435171	20247	153577455	12201	*156418790*	*2362*
2021-04-13	17:13:53.474	*156347445*	*10903*	153435161	20273	153577443	12212	*156418813*	*2366*
2021-04-13	17:13:53.635	*156347445*	*10903*	153435161	20273	153577443	12212	*156418813*	*2366*
2021-04-13	17:13:53.795	*156347445*	*10903*	153435144	20260	153577455	12205	*156418797*	*2362*
2021-04-13	17:13:53.955	*156347445*	*10908*	153435165	20268	153577441	12211	*156418794*	*2368*
2021-04-13	17:13:54.115	*156347445*	*10906*	153435146	20275	153577448	12210	*156418788*	*2361*
2021-04-13	17:13:54.275	*156347445*	*10906*	153435146	20275	153577448	12210	*156418788*	*2361*
2021-04-13	17:13:54.435	*156347445*	*10902*	153435156	20272	153577442	12210	*156418794*	*2361*
2021-04-13	17:13:54.595	*156347455*	*10910*	153435165	20269	153577449	12209	*156418805*	*2367*
2021-04-13	17:13:54.755	*156347455*	*10910*	153435165	20269	153577449	12209	*156418805*	*2367*
2021-04-13	17:13:54.916	*156347455*	*10894*	153435173	20273	153577464	12207	*156418794*	*2360*
2021-04-13	17:13:55.076	*156347455*	*10900*	153435162	20277	153577458	12212	*156418804*	*2361*
2021-04-13	17:13:55.236	*156347445*	*10909*	153435138	20272	153577435	12213	*156418774*	*2367*
2021-04-13	17:13:55.396	*156347445*	*10909*	153435138	20272	153577435	12213	*156418774*	*2367*

2021-04-13	17:13:55.556	*156347455*	*10897*	153435193	20268	153577479	12214	*156418810*	*2361*
2021-04-13	17:13:55.716	*156347445*	*10897*	153435157	20270	153577431	12212	*156418782*	*2366*
2021-04-13	17:13:55.876	*156347445*	*10897*	153435157	20270	153577431	12212	*156418782*	*2366*
2021-04-13	17:13:56.036	*156347455*	*10891*	153435172	20278	153577451	12215	*156418810*	*2359*
2021-04-13	17:13:56.196	*156347455*	*10903*	153435156	20272	153577438	12212	*156418809*	*2361*
2021-04-13	17:13:56.356	*156347455*	*10898*	153435161	20271	153577426	12213	*156418781*	*2366*
2021-04-13	17:13:56.516	*156347455*	*10898*	153435161	20271	153577426	12213	*156418781*	*2366*
2021-04-13	17:13:56.681	*156347455*	*10904*	153435169	20267	153577431	12208	*156418801*	*2362*
2021-04-13	17:13:56.852	*156347455*	*10900*	153435172	20259	153577437	12205	*156418796*	*2362*
2021-04-13	17:13:57.012	*156347455*	*10900*	153435172	20259	153577437	12205	*156418796*	*2362*
2021-04-13	17:13:57.172	*156347455*	*10908*	153435159	20275	153577417	12216	*156418775*	*2366*
2021-04-13	17:13:57.332	*156347455*	*10897*	153435174	20273	153577433	12208	*156418780*	*2360*
2021-04-13	17:13:57.492	*156347455*	*10908*	153435161	20286	153577448	12213	*156418770*	*2366*
2021-04-13	17:13:57.652	*156347455*	*10908*	153435161	20286	153577448	12213	*156418770*	*2366*
2021-04-13	17:13:57.812	*156347455*	*10900*	153435145	20269	153577418	12204	*156418808*	*2362*
2021-04-13	17:13:57.972	*156347455*	*10897*	153435162	20262	153577420	12202	*156418791*	*2361*
2021-04-13	17:13:58.133	*156347455*	*10897*	153435162	20262	153577420	12202	*156418791*	*2361*
2021-04-13	17:13:58.293	*156347455*	*10904*	153435145	20266	153577431	12210	*156418794*	*2365*
2021-04-13	17:13:58.453	*156347455*	*10907*	153435148	20270	153577430	12211	*156418801*	*2361*
2021-04-13	17:13:58.613	*156347455*	*10905*	153435138	20278	153577444	12210	*156418796*	*2362*
2021-04-13	17:13:58.773	*156347455*	*10905*	153435138	20278	153577444	12210	*156418796*	*2362*
2021-04-13	17:13:58.933	*156347455*	*10903*	153435129	20275	153577436	12211	*156418794*	*2366*
2021-04-13	17:13:59.093	*156347455*	*10898*	153435165	20266	153577454	12209	*156418767*	*2361*

2021-04-13	17:13:59.253	*156347455*	*10898*	153435165	20266	153577454	12209	*156418767*	*2361*
2021-04-13	17:13:59.414	*156347455*	*10889*	153435154	20270	153577435	12212	*156418786*	*2360*
2021-04-13	17:13:59.574	*156347455*	*10905*	153435165	20271	153577457	12212	*156418822*	*2366*
2021-04-13	17:13:59.734	*156347455*	*10893*	153435159	20274	153577441	12213	*156418798*	*2359*
2021-04-13	17:13:59.894	*156347455*	*10893*	153435159	20274	153577441	12213	*156418798*	*2359*
2021-04-13	17:14:00.055	*156347455*	*10907*	153435133	20276	153577425	12215	*156418773*	*2367*
2021-04-13	17:14:00.215	*156347455*	*10907*	153435133	20276	153577425	12215	*156418773*	*2367*
2021-04-13	17:14:00.375	*156347455*	*10907*	153435133	20276	153577425	12215	*156418773*	*2367*
2021-04-13	17:14:00.536	*156347455*	*10907*	153435133	20276	153577425	12215	*156418773*	*2367*
2021-04-13	17:14:00.696	*156347455*	*10907*	153435133	20276	153577425	12215	*156418773*	*2367*
2021-04-13	17:14:00.856	*156347455*	*10907*	153435133	20276	153577425	12215	*156418773*	*2367*

b. Port B

Table 0.2: RMS data for Port B from in-house splice of SM1 fiber.

DATE	TIME	P REF WL	P REF AMP	P WL	P AMP	T WL	T AMP	T REF WL	T REF AMP
2021-04-13	18:23:43.260	156349632	10760	153435217	14818	153577497	8956	156420996	2306
2021-04-13	18:23:43.421	156349642	10788	153435217	14829	153577507	8958	156420998	2318
2021-04-13	18:23:43.582	156349642	10789	153435216	14826	153577499	8970	156420993	2325
2021-04-13	18:23:43.743	156349642	10798	153435219	14835	153577524	8968	156421010	2324
2021-04-13	18:23:43.903	156349642	10786	153435205	14833	153577485	8967	156420983	2325
2021-04-13	18:23:44.065	156349642	10786	153435205	14833	153577485	8967	156420983	2325
2021-04-13	18:23:44.226	156349642	10796	153435204	14840	153577487	8966	156420990	2325
2021-04-13	18:23:44.387	156349642	10791	153435205	14827	153577459	8971	156420965	2325
2021-04-13	18:23:44.548	156349642	10791	153435205	14827	153577459	8971	156420965	2325
2021-04-13	18:23:44.709	156349642	10792	153435219	14827	153577491	8971	156420982	2326
2021-04-13	18:23:44.870	156349642	10800	153435223	14836	153577520	8965	156420976	2324
2021-04-13	18:23:45.031	156349642	10801	153435210	14841	153577494	8969	156421009	2323
2021-04-13	18:23:45.192	156349642	10801	153435210	14841	153577494	8969	156421009	2323
2021-04-13	18:23:45.353	156349642	10788	153435207	14840	153577506	8969	156420962	2327
2021-04-13	18:23:45.514	156349642	10801	153435224	14829	153577507	8972	156420974	2325
2021-04-13	18:23:45.674	156349642	10809	153435202	14830	153577504	8979	156420981	2329
2021-04-13	18:23:45.835	156349642	10809	153435202	14830	153577504	8979	156420981	2329
2021-04-13	18:23:45.996	156349642	10804	153435217	14836	153577494	8976	156420981	2330
2021-04-13	18:23:46.156	156349642	10807	153435205	14843	153577477	8971	156420970	2331

2021-04-13	18:23:46.321	*156349642*	*10807*	153435205	14843	153577477	8971	*156420970*	*2331*
2021-04-13	18:23:46.489	*156349642*	*10812*	153435215	14836	153577476	8973	*156420979*	*2329*
2021-04-13	18:23:46.657	*156349642*	*10809*	153435215	14836	153577496	8972	*156420966*	*2329*
2021-04-13	18:23:46.820	*156349642*	*10805*	153435222	14844	153577496	8973	*156420968*	*2330*
2021-04-13	18:23:46.989	*156349642*	*10805*	153435222	14844	153577496	8973	*156420968*	*2330*
2021-04-13	18:23:47.159	*156349642*	*10807*	153435201	14838	153577505	8971	*156421015*	*2330*
2021-04-13	18:23:47.327	*156349642*	*10805*	153435214	14834	153577500	8968	*156420998*	*2331*
2021-04-13	18:23:47.496	*156349642*	*10807*	153435221	14836	153577489	8972	*156420953*	*2330*
2021-04-13	18:23:47.664	*156349642*	*10807*	153435221	14836	153577489	8972	*156420953*	*2330*
2021-04-13	18:23:47.833	*156349642*	*10805*	153435216	14840	153577490	8971	*156421011*	*2332*
2021-04-13	18:23:48.001	*156349642*	*10806*	153435205	14838	153577481	8973	*156420978*	*2330*
2021-04-13	18:23:48.169	*156349642*	*10808*	153435202	14833	153577495	8976	*156420956*	*2330*
2021-04-13	18:23:48.339	*156349642*	*10808*	153435202	14833	153577495	8976	*156420956*	*2330*
2021-04-13	18:23:48.508	*156349642*	*10806*	153435211	14842	153577511	8971	*156420994*	*2331*
2021-04-13	18:23:48.676	*156349642*	*10815*	153435202	14835	153577493	8986	*156420986*	*2335*
2021-04-13	18:23:48.839	*156349642*	*10808*	153435224	14840	153577496	8986	*156420969*	*2337*
2021-04-13	18:23:49.007	*156349642*	*10808*	153435224	14840	153577496	8986	*156420969*	*2337*
2021-04-13	18:23:49.176	*156349642*	*10814*	153435212	14838	153577483	8983	*156420973*	*2335*
2021-04-13	18:23:49.344	*156349642*	*10803*	153435205	14844	153577472	8982	*156420964*	*2337*
2021-04-13	18:23:49.513	*156349642*	*10802*	153435217	14832	153577495	8982	*156420981*	*2338*
2021-04-13	18:23:49.683	*156349642*	*10802*	153435217	14832	153577495	8982	*156420981*	*2338*
2021-04-13	18:23:49.853	*156349642*	*10806*	153435208	14835	153577502	8983	*156420995*	*2336*
2021-04-13	18:23:50.021	*156349642*	*10808*	153435220	14847	153577491	8975	*156420982*	*2336*

2021-04-13	18:23:50.190	*156349642*	*10812*	153435226	14848	153577501	8978	*156420974*	*2335*
2021-04-13	18:23:50.352	*156349642*	*10812*	153435226	14848	153577501	8978	*156420974*	*2335*
2021-04-13	18:23:50.514	*156349642*	*10807*	153435186	14839	153577460	8981	*156420962*	*2337*
2021-04-13	18:23:50.682	*156349642*	*10808*	153435208	14835	153577494	8981	*156420981*	*2337*
2021-04-13	18:23:50.851	*156349652*	*10804*	153435217	14846	153577516	8971	*156421015*	*2337*
2021-04-13	18:23:51.022	*156349652*	*10804*	153435217	14846	153577516	8971	*156421015*	*2337*
2021-04-13	18:23:51.191	*156349642*	*10811*	153435183	14850	153577486	8977	*156420977*	*2336*
2021-04-13	18:23:51.361	*156349642*	*10799*	153435175	14851	153577475	8974	*156420977*	*2337*
2021-04-13	18:23:51.529	*156349642*	*10802*	153435203	14849	153577494	8975	*156420985*	*2337*
2021-04-13	18:23:51.698	*156349642*	*10802*	153435203	14849	153577494	8975	*156420985*	*2337*
2021-04-13	18:23:51.866	*156349652*	*10814*	153435224	14836	153577513	8984	*156421019*	*2336*
2021-04-13	18:23:52.035	*156349652*	*10819*	153435188	14848	153577479	8979	*156420982*	*2336*
2021-04-13	18:23:52.203	*156349642*	*10814*	153435204	14841	153577477	8981	*156420975*	*2337*
2021-04-13	18:23:52.367	*156349642*	*10814*	153435204	14841	153577477	8981	*156420975*	*2337*
2021-04-13	18:23:52.530	*156349642*	*10800*	153435216	14846	153577484	8983	*156420980*	*2337*
2021-04-13	18:23:52.695	*156349642*	*10804*	153435193	14845	153577478	8978	*156420961*	*2337*
2021-04-13	18:23:52.864	*156349642*	*10820*	153435189	14854	153577477	8981	*156420954*	*2340*
2021-04-13	18:23:53.033	*156349642*	*10820*	153435189	14854	153577477	8981	*156420954*	*2340*
2021-04-13	18:23:53.201	*156349652*	*10814*	153435222	14848	153577462	8984	*156420987*	*2342*
2021-04-13	18:23:53.370	*156349642*	*10811*	153435207	14851	153577487	8987	*156420960*	*2342*
2021-04-13	18:23:53.538	*156349642*	*10819*	153435207	14853	153577466	8984	*156421011*	*2340*
2021-04-13	18:23:53.707	*156349642*	*10819*	153435207	14853	153577466	8984	*156421011*	*2340*
2021-04-13	18:23:53.877	*156349642*	*10819*	153435216	14852	153577472	8986	*156420983*	*2341*

2021-04-13	18:23:54.046	*156349652*	*10821*	153435193	14859	153577496	8978	*156420963*	*2342*
2021-04-13	18:23:54.214	*156349652*	*10817*	153435190	14859	153577494	8980	*156420950*	*2342*
2021-04-13	18:23:54.383	*156349652*	*10817*	153435190	14859	153577494	8980	*156420950*	*2342*
2021-04-13	18:23:54.551	*156349642*	*10810*	153435217	14849	153577499	8988	*156420991*	*2343*
2021-04-13	18:23:54.719	*156349642*	*10824*	153435186	14844	153577476	8991	*156421001*	*2340*
2021-04-13	18:23:54.888	*156349652*	*10818*	153435229	14847	153577505	8989	*156420995*	*2342*
2021-04-13	18:23:55.058	*156349652*	*10818*	153435229	14847	153577505	8989	*156420995*	*2342*
2021-04-13	18:23:55.229	*156349652*	*10826*	153435217	14845	153577495	8987	*156420987*	*2342*
2021-04-13	18:23:55.392	*156349652*	*10810*	153435189	14855	153577461	8980	*156420982*	*2344*
2021-04-13	18:23:55.562	*156349652*	*10815*	153435217	14853	153577497	8983	*156420997*	*2342*
2021-04-13	18:23:55.724	*156349652*	*10815*	153435217	14853	153577497	8983	*156420997*	*2342*
2021-04-13	18:23:55.893	*156349652*	*10814*	153435213	14854	153577512	8983	*156420985*	*2343*
2021-04-13	18:23:56.066	*156349652*	*10813*	153435198	14853	153577469	8987	*156420972*	*2343*
2021-04-13	18:23:56.228	*156349652*	*10827*	153435218	14854	153577510	8982	*156420978*	*2343*
2021-04-13	18:23:56.397	*156349652*	*10827*	153435218	14854	153577510	8982	*156420978*	*2343*
2021-04-13	18:23:56.559	*156349652*	*10821*	153435219	14850	153577467	8982	*156420956*	*2340*
2021-04-13	18:23:56.726	*156349652*	*10819*	153435198	14846	153577467	8985	*156420966*	*2342*
2021-04-13	18:23:56.895	*156349652*	*10819*	153435198	14846	153577467	8985	*156420966*	*2342*
2021-04-13	18:23:57.064	*156349642*	*10811*	153435213	14848	153577478	8989	*156421013*	*2343*
2021-04-13	18:23:57.234	*156349642*	*10819*	153435200	14849	153577485	8988	*156420972*	*2342*
2021-04-13	18:23:57.402	*156349642*	*10825*	153435197	14852	153577490	8984	*156420957*	*2341*
2021-04-13	18:23:57.571	*156349652*	*10820*	153435222	14854	153577496	8982	*156420977*	*2341*
2021-04-13	18:23:57.740	*156349652*	*10820*	153435222	14854	153577496	8982	*156420977*	*2341*

2021-04-13	18:23:57.909	156349642	10819	153435205	14851	153577524	8987	156420998	2343
2021-04-13	18:23:58.077	156349642	10821	153435211	14854	153577476	8982	156420969	2342
2021-04-13	18:23:58.245	156349642	10823	153435229	14848	153577482	8987	156420983	2342
2021-04-13	18:23:58.414	156349642	10823	153435229	14848	153577482	8987	156420983	2342
2021-04-13	18:23:58.582	156349642	10821	153435218	14846	153577471	8990	156420965	2342
2021-04-13	18:23:58.751	156349642	10820	153435203	14843	153577501	8988	156420970	2342
2021-04-13	18:23:58.919	156349642	10825	153435227	14854	153577502	8988	156420979	2341
2021-04-13	18:23:59.088	156349642	10825	153435227	14854	153577502	8988	156420979	2341
2021-04-13	18:23:59.257	156349642	10815	153435205	14842	153577492	8991	156420989	2343
2021-04-13	18:23:59.426	156349642	10813	153435204	14852	153577470	8990	156420983	2344
2021-04-13	18:23:59.588	156349642	10822	153435212	14851	153577490	8981	156420971	2342
2021-04-13	18:23:59.757	156349642	10822	153435212	14851	153577490	8981	156420971	2342
2021-04-13	18:23:59.927	156349652	10826	153435224	14837	153577514	8993	156421022	2341
2021-04-13	18:24:00.095	156349652	10824	153435195	14851	153577487	8987	156420966	2343
2021-04-13	18:24:00.264	156349642	10823	153435206	14839	153577481	8989	156420980	2340
2021-04-13	18:24:00.433	156349642	10823	153435206	14839	153577481	8989	156420980	2340
2021-04-13	18:24:00.602	156349642	10822	153435226	14843	153577494	8991	156420960	2341
2021-04-13	18:24:00.772	156349642	10818	153435226	14848	153577494	8987	156420972	2343
2021-04-13	18:24:00.941	156349642	10826	153435198	14845	153577471	8990	156420949	2341
2021-04-13	18:24:01.110	156349642	10826	153435198	14845	153577471	8990	156420949	2341
2021-04-13	18:24:01.278	156349652	10825	153435196	14851	153577494	8989	156420994	2341
2021-04-13	18:24:01.444	156349652	10824	153435203	14846	153577477	8985	156420953	2342
2021-04-13	18:24:01.615	156349642	10827	153435200	14840	153577487	8991	156420998	2343

2021-04-13	18:24:01.784	*156349642*	*10827*	153435200	14840	153577487	8991	*156420998*	*2343*
2021-04-13	18:24:01.952	*156349652*	*10822*	153435212	14844	153577510	8991	*156421012*	*2342*
2021-04-13	18:24:02.122	*156349642*	*10821*	153435199	14855	153577484	8980	*156420957*	*2343*
2021-04-13	18:24:02.284	*156349642*	*10826*	153435195	14855	153577489	8984	*156420976*	*2341*
2021-04-13	18:24:02.454	*156349642*	*10826*	153435195	14855	153577489	8984	*156420976*	*2341*
2021-04-13	18:24:02.623	*156349652*	*10825*	153435215	14861	153577501	8985	*156420989*	*2347*
2021-04-13	18:24:02.792	*156349642*	*10826*	153435194	14854	153577485	8982	*156421006*	*2341*
2021-04-13	18:24:02.961	*156349652*	*10827*	153435215	14852	153577506	8993	*156420969*	*2347*
2021-04-13	18:24:03.129	*156349652*	*10827*	153435215	14852	153577506	8993	*156420969*	*2347*
2021-04-13	18:24:03.297	*156349652*	*10825*	153435204	14859	153577466	8990	*156420969*	*2347*

c. ATS

Table 0.3: RMS data for ATS sensor in splice-block.

DATA	*TIME*	*T REF1 WL*	*T REF1 AMP*	*T REF2 WL*	*T REF2 AMP*
2021-05-28	13:01:11.512	*156360596*	*22246*	*156432297*	*3790*
2021-05-28	13:01:11.605	*156360596*	*22246*	*156432297*	*3790*
2021-05-28	13:01:11.699	*156360596*	*22265*	*156432299*	*3793*
2021-05-28	13:01:11.793	*156360596*	*22265*	*156432299*	*3793*
2021-05-28	13:01:11.886	*156360596*	*22252*	*156432298*	*3780*
2021-05-28	13:01:11.980	*156360596*	*22252*	*156432298*	*3780*
2021-05-28	13:01:12.073	*156360598*	*22258*	*156432326*	*3790*
2021-05-28	13:01:12.167	*156360598*	*22258*	*156432326*	*3790*
2021-05-28	13:01:12.261	*156360598*	*22259*	*156432303*	*3793*
2021-05-28	13:01:12.354	*156360598*	*22245*	*156432307*	*3790*
2021-05-28	13:01:12.448	*156360598*	*22245*	*156432307*	*3790*
2021-05-28	13:01:12.541	*156360598*	*22247*	*156432310*	*3791*
2021-05-28	13:01:12.635	*156360598*	*22247*	*156432310*	*3791*
2021-05-28	13:01:12.729	*156360598*	*22253*	*156432294*	*3792*
2021-05-28	13:01:12.822	*156360598*	*22253*	*156432294*	*3792*
2021-05-28	13:01:12.916	*156360598*	*22251*	*156432296*	*3792*
2021-05-28	13:01:13.009	*156360598*	*22251*	*156432296*	*3792*
2021-05-28	13:01:13.103	*156360598*	*22240*	*156432309*	*3781*
2021-05-28	13:01:13.197	*156360598*	*22240*	*156432309*	*3781*
2021-05-28	13:01:13.290	*156360598*	*22251*	*156432289*	*3789*
2021-05-28	13:01:13.384	*156360598*	*22251*	*156432289*	*3789*
2021-05-28	13:01:13.477	*156360598*	*22261*	*156432320*	*3791*
2021-05-28	13:01:13.571	*156360598*	*22261*	*156432320*	*3791*
2021-05-28	13:01:13.665	*156360598*	*22260*	*156432314*	*3788*
2021-05-28	13:01:13.758	*156360598*	*22260*	*156432314*	*3788*
2021-05-28	13:01:13.852	*156360598*	*22264*	*156432317*	*3790*
2021-05-28	13:01:13.945	*156360598*	*22257*	*156432290*	*3791*
2021-05-28	13:01:14.039	*156360598*	*22257*	*156432290*	*3791*
2021-05-28	13:01:14.133	*156360598*	*22262*	*156432299*	*3793*
2021-05-28	13:01:14.226	*156360598*	*22262*	*156432299*	*3793*
2021-05-28	13:01:14.320	*156360598*	*22238*	*156432298*	*3782*
2021-05-28	13:01:14.413	*156360598*	*22238*	*156432298*	*3782*
2021-05-28	13:01:14.507	*156360598*	*22226*	*156432333*	*3791*
2021-05-28	13:01:14.601	*156360598*	*22226*	*156432333*	*3791*
2021-05-28	13:01:14.694	*156360598*	*22245*	*156432278*	*3793*
2021-05-28	13:01:14.788	*156360598*	*22245*	*156432278*	*3793*
2021-05-28	13:01:14.881	*156360598*	*22253*	*156432324*	*3794*

2021-05-28	13:01:14.975	*156360598*	*22253*	*156432324*	*3794*
2021-05-28	13:01:15.069	*156360598*	*22265*	*156432334*	*3790*
2021-05-28	13:01:15.162	*156360598*	*22265*	*156432334*	*3790*
2021-05-28	13:01:15.256	*156360598*	*22257*	*156432319*	*3793*
2021-05-28	13:01:15.349	*156360598*	*22271*	*156432298*	*3792*
2021-05-28	13:01:15.443	*156360598*	*22271*	*156432298*	*3792*
2021-05-28	13:01:15.537	*156360598*	*22242*	*156432313*	*3783*
2021-05-28	13:01:15.630	*156360598*	*22242*	*156432313*	*3783*
2021-05-28	13:01:15.724	*156360598*	*22256*	*156432314*	*3787*
2021-05-28	13:01:15.817	*156360598*	*22256*	*156432314*	*3787*
2021-05-28	13:01:15.911	*156360598*	*22250*	*156432295*	*3792*
2021-05-28	13:01:16.005	*156360598*	*22250*	*156432295*	*3792*
2021-05-28	13:01:16.098	*156360598*	*22258*	*156432326*	*3790*
2021-05-28	13:01:16.192	*156360598*	*22258*	*156432326*	*3790*
2021-05-28	13:01:16.285	*156360598*	*22240*	*156432311*	*3793*
2021-05-28	13:01:16.379	*156360598*	*22240*	*156432311*	*3793*
2021-05-28	13:01:16.473	*156360598*	*22258*	*156432318*	*3790*
2021-05-28	13:01:16.566	*156360598*	*22258*	*156432318*	*3790*
2021-05-28	13:01:16.660	*156360598*	*22242*	*156432347*	*3790*
2021-05-28	13:01:16.753	*156360598*	*22243*	*156432316*	*3779*
2021-05-28	13:01:16.847	*156360598*	*22243*	*156432316*	*3779*
2021-05-28	13:01:16.941	*156360598*	*22243*	*156432316*	*3779*
2021-05-28	13:01:17.034	*156360598*	*22243*	*156432316*	*3779*
2021-05-28	13:01:17.128	*156360598*	*22243*	*156432316*	*3779*
2021-05-28	13:01:17.221	*156360598*	*22243*	*156432316*	*3779*